

UNCLASSIFIED

AD NUMBER
AD240432
NEW LIMITATION CHANGE
TO Approved for public release, distribution unlimited
FROM Distribution authorized to U.S. Gov't. agencies and their contractors; Administrative/Operational Use; Jun 1959. Other requests shall be referred to the Department of the Air Force, Attn: Public Affairs Office, Washington, DC 20330.
AUTHORITY
USAF Rand Project Office ltr, 28 Jun 1967

THIS PAGE IS UNCLASSIFIED

UNCLASSIFIED

AD

240 432

Reproduced

Armed Services Technical Information Agency

ARLINGTON HALL STATION; ARLINGTON 12 VIRGINIA

NOTICE: WHEN GOVERNMENT OR OTHER DRAWINGS, SPECIFICATIONS OR OTHER DATA ARE USED FOR ANY PURPOSE OTHER THAN IN CONNECTION WITH A DEFINITELY RELATED GOVERNMENT PROCUREMENT OPERATION, THE U. S. GOVERNMENT THEREBY INCURS NO RESPONSIBILITY, NOR ANY OBLIGATION WHATSOEVER; AND THE FACT THAT THE GOVERNMENT MAY HAVE FORMULATED; FURNISHED, OR IN ANY WAY SUPPLIED THE SAID DRAWINGS, SPECIFICATIONS, OR OTHER DATA IS NOT TO BE REGARDED BY IMPLICATION OR OTHERWISE AS IN ANY MANNER LICENSING THE HOLDER OR ANY OTHER PERSON OR CORPORATION, OR CONVEYING ANY RIGHTS OR PERMISSION TO MANUFACTURE, USE OR SELL ANY PATENTED INVENTION THAT MAY IN ANY WAY BE RELATED THERETO.

UNCLASSIFIED

AD No: **248432**
ASTIA FILE COPY

U.S. AIR FORCE
Project **RAND**
RESEARCH MEMORANDUM

This is a working paper. It may be expanded, modified, or withdrawn at any time. The views, conclusions, and recommendations expressed herein do not necessarily reflect the official views or policies of the United States Air Force.

FILE COPY

Return to

ASTIA

ARLINGTON HALL STATION

ARLINGTON 12, VIRGINIA

Attn: TISS



— The **RAND** Corporation —
SANTA MONICA • CALIFORNIA

PAGES _____
ARE
MISSING
IN
ORIGINAL
DOCUMENT

RAND RESEARCH MEMORANDUM
A REVIEW OF BINARY BOUNDARY LAYER CHARACTERISTICS

J. F. Gross
J. P. Hartnett

D. J. Masson
C. Gazley, Jr.

RM-2516

June 18, 1959

in brief

For several years RAND has investigated means of applying principles of mass-transfer and ablation cooling to problems of atmospheric re-entry and to the design of efficient hypersonic flight vehicles. In connection with ablation cooling, this research memorandum examines the binary boundary-layer problem. The study should make possible more rapid and reliable estimates of surface-cooling methods for use with hypersonic vehicles, such as intercontinental ballistic missile nose cones.

A binary boundary layer is one in which some foreign substance has been injected to alter the properties of the flow, notably its heat-transfer characteristics. Several methods available for accomplishing this injection, or mass transfer, are the transpiration of gas through slots, and the ablation or sloughing away of surface particles.

The mechanism of laminar binary boundary layer flow is discussed in mathematical terms, and five different analyses involving a variety of injected substances are reviewed. Generalized expressions are then developed for predicting heat-transfer and skin-friction performance in the presence of mass-transfer cooling for laminar flow over a flat plate. The results indicate that different foreign materials (for example, hydrogen, carbon dioxide, and iodine vapor) injected into the boundary-layer stream reduce heat-transfer and skin-friction coefficients by an amount which depends on the molecular weight of the injected material. In conclusion, mass-transfer cooling in a turbulent boundary layer and sublimation cooling are considered.

U. S. AIR FORCE
PROJECT RAND
RESEARCH MEMORANDUM

A REVIEW OF BINARY BOUNDARY LAYER CHARACTERISTICS

J. F. Gross
J. P. Hartnett
D. J. Masson
Carl Gazley, Jr.

RM-2516

June 18, 1959

Assigned to. _____

This is a working paper. It may be expanded, modified, or withdrawn at any time. The views, conclusions, and recommendations expressed herein do not necessarily reflect the official views or policies of the United States Air Force.

The **RAND** Corporation

1700 MAIN ST. • SANTA MONICA • CALIFORNIA

SUMMARY

The purpose of this report is to examine the several theoretical analyses of laminar and turbulent binary boundary layers. A generalization of the different theories leads to simplified expressions for the heat transfer and friction in both laminar and turbulent binary boundary layers. The results indicate that the effects of different foreign materials are primarily dependent on their relative molecular weights.

The importance of the injection of foreign materials to the stability characteristics of the flow is discussed and experimental results seem to show non-transitional flow for moderate injection rates even with light gases.

Sublimation cooling is treated and typical numerical results are presented for three materials: ice, carbon dioxide, and ferrous chloride.

CONTENTS

SUMMARY	iii
LIST OF FIGURES	vi
SYMBOLS	ix
Section	
I. INTRODUCTION.	1
II. BINARY LAMINAR BOUNDARY LAYER THEORY.	7
III. REVIEW OF AVAILABLE BINARY LAMINAR BOUNDARY LAYER ANALYSES.	11
Constant Property Analysis.	11
Analysis of Baron	22
Analysis of Eckert and Co-workers	28
Analysis of Sziklas and Banas	31
Analysis of Gross	33
IV. GENERALIZED PRESENTATION OF LAMINAR FLAT PLATE BINARY BOUNDARY LAYER RESULTS	37
V. EFFECT OF PRESSURE GRADIENT ON LAMINAR MASS-TRANSFER COOLING	49
VI. STABILITY OF THE LAMINAR BINARY BOUNDARY LAYER.	55
Theoretical Studies	55
Experimental Studies.	62
VII. MASS-TRANSFER COOLING IN A TURBULENT BOUNDARY LAYER .	65
VIII. SUBLIMATION COOLING	75
Appendix	
A. ADDITIONAL VERIFICATION OF THE DIMENSIONLESS PRESENTATIONS	81
B. RELATION BETWEEN WALL CONCENTRATION AND MASS-TRANSFER PARAMETER	89
C. ON THE USE OF MASS-TRANSFER RESULTS FOR PREDICTION OF HEAT TRANSFER.	95
REFERENCES.	97

LIST OF FIGURES

1. Various cooling methods.....	3
2. Flat plate, solid wall, no mass transfer.....	12
3. Flat plate, mass transfer.....	13
4. Effect of air injection on velocity profile.....	17
5. Effect of air injection on local skin friction.....	18
6. Effect of air injection on local Nusselt number.....	19
7. Effect of air injection on recovery factor.....	21
8. Effect of mass transfer on modified Reynolds analogy.....	23
9. Helium results of Baron.....	27
10. Effect of light gas injection on laminar velocity profiles....	29
11. Effect of light gas injection on skin friction.....	30
12. Effect of hydrogen injection on laminar heat transfer.....	32
13. Variation of laminar heat transfer with helium injection.....	34
14. Friction coefficient as a function of the blowing parameter...	35
15. Effect of mass transfer on skin friction; hydrogen-air.....	38
16. Effect of mass transfer on skin friction; helium-air.....	39
17. Effect of mass transfer on skin friction; summary.....	41
18. Effect of mass transfer on Stanton number.....	42
19. Effect of mass transfer on recovery factor.....	43
20. Effect of mass transfer on heat transfer; hydrogen-air.....	44
21. Effect of mass transfer on heat transfer; helium-air.....	45
22. Effect of mass transfer on heat transfer; summary.....	46
23. Dimensionless mass-transfer parameter versus molecular weight of coolant gas.....	48
24. Effect of air injection on heat transfer and skin-friction coefficient.....	50

25. Effect of pressure gradient on mass-transfer cooling.....	52
26. Effect of pressure gradient on mass-transfer cooling.....	53
27. Effect of mass transfer on the minimum critical Reynolds number.....	57
28. Effect of helium injection on cooling required for complete boundary layer stability.....	60
29. Effect of mass transfer on boundary layer transition.....	61
30. Effect of mass transfer on heat transfer, turbulent flow.....	67
31. Predicted and measured skin friction for air injection into a turbulent boundary layer on a flat plate.....	68
32. Recovery factor for air injection into turbulent boundary layer on a flat plate.....	70
33. Prediction of skin friction for foreign gas injection into a turbulent air boundary layer on a flat plate.....	71
34. Effect of mass transfer on heat transfer, turbulent flow.....	72
35. Turbulent mass-transfer parameter versus molecular weight of coolant gas.....	74
36. Subliming systems: wall temperature versus mass-transfer parameter.....	78
37. Effect of mass transfer on skin friction.....	82
38. Effect of mass transfer on heat transfer.....	83
39. Effect of mass transfer on Stanton number.....	84
40. Effect of mass transfer on Stanton number.....	85
41. Effect of mass transfer on recovery factor.....	86
42. Effect of mass transfer on recovery factor.....	87
43. Wall mass fraction versus dimensionless mass transfer.....	90
44. Wall mass fraction versus dimensionless mass transfer.....	91
45. Wall mass fraction versus dimensionless mass transfer.....	92
46. Wall mass fraction versus dimensionless mass transfer; summary.....	93
47. Effect of mass-transfer rate on the mass-transfer Stanton number.....	96

SYMBOLS

C	Chapman-Rubesin parameter defined in Eq. (17)
C_f	local skin friction coefficient
C_{f_o}	local skin friction evaluated for solid wall exposed to some free stream conditions and held at same temperature as the actual wall
C_H	local heat-transfer Stanton number, $q/\rho_e u_e C_{p_e} (T_r - T_w)$
C_{H_o}	local Stanton number evaluated for solid wall exposed to same free stream conditions and held at same temperature as the actual wall
C_M	mass-transfer Stanton number, $\dot{m}/\rho_e u_e Y_w$
c_p	specific heat at constant pressure
c_v	specific heat at constant volume
D_{12}	ordinary diffusion coefficient
f	dimensionless stream function
g_o	gravitational constant, $32.2 \text{ lb}_m \text{ ft}/\text{lb}_f \text{ sec}^2$
H	enthalpy associated with change of phase
h	heat-transfer coefficient, Eq. (19)
k	thermal conductivity
m	refers to wedge flows, where free stream velocity, u_∞ , varies as x^m
m_1	molecule weight of coolant gas
m_2	molecule weight of pure air
\bar{m}	ratio of molecule weights, m_1/m_2
\dot{m}_x	mass flow rate of coolant gas at position x along the surface
p	pressure
p_1	partial pressure of coolant gas
q	local heat-transfer rate per unit area, $k_w (\partial T/\partial y)_w$

q_o	local heat-transfer rate per unit area evaluated for solid wall exposed to same free stream conditions and held at same temperature as actual wall
R	universal gas constant
r	recovery factor
T	temperature
T_r	recovery temperature, defined as the wall temperature where $k_w(\partial T/\partial y)_w = 0$
T^*	reference temperature defined in Eq. (9)
u	component of velocity parallel to surface
u_1	defined in Eq. (23)
v	component of velocity normal to surface
x	coordinates along the body
Y	mass fraction of coolant gas
y	coordinates normal to the body

Greek Symbols

α	condensation coefficient
γ	ratio of specific heats
δ^*	displacement thickness, Eq. (22)
η	transformed coordinate defined in text
θ	dimensionless temperature
λ	defined in Eq. (17)
μ	dynamic viscosity
ν	kinematic viscosity
ρ	density
ϕ	dimension mass fraction
ψ	stream function

Dimensionless Numbers

M Mach number, ratio of local speed to local speed of sound

Pr Prandtl number, μ_c/κ

$\left[Re_{min_{cr}} \right]_{\delta^*}$ minimum critical Reynolds number based on δ^* , $u_e \delta^*/\nu_e$

Re_x local Reynolds number, $u_e x/\nu_e$

Sc Schmidt number, ν/D_{12}

Subscripts

1 refers to pure coolant

2 refers to pure air

e evaluated at outer edge of the boundary layer

r refers to recovery conditions, i.e., where $k(\partial T/\partial y)_w = 0$

w evaluated at wall conditions

x refers to local conditions

y_1 evaluated at y_1 as defined in Eq. (23)

Superscript

* evaluated at the reference temperature, Eq. (9)

I. INTRODUCTION

Recently, the alleviation of the high heating rates encountered by surfaces of hypersonic vehicles has been recognized as an important problem. One of the cooling methods that appears to have great ultimate promise is mass-transfer cooling, wherein a "foreign" material is transferred from the surface into the boundary layer. This has a two-fold advantage in alleviation of the heat-transfer problem. The transferred coolant may absorb heat from the boundary layer through a phase change (sublimation, evaporation, melting, etc.) and/or by acting as a dispersed heat sink. It will be advantageous, therefore, to employ coolants with high heats of sublimation (or evaporation, melting, etc.) as well as high thermal heat capacities. In addition, it has been shown that the introduction of a material (with its normal velocity component) at the surface acts to decelerate the flow and consequently, to reduce the skin friction. This also implies a reduction in heat transfer at the wall.

The usual boundary layer equations are complicated by the appearance of (a) an equation defining the conservation of the species at any point in the boundary layer, and (b) transport terms which result from thermodynamic coupling coefficients such as the thermal diffusion coefficient.

There are a number of methods for effecting the injection of a foreign material into the boundary layer, and the following descriptions have been advanced to describe specific mass-transfer cooling schemes:

1. Transpiration cooling
2. Film cooling
 - a) using liquid as a coolant

b) using gas as a coolant

3. Ablation

a) sublimation

b) other ablation phenomena, such as melting, erosion, fusion, etc.

These schemes are diagrammatically shown in Fig. 1.^{(1)*} With the exception of film cooling with a gas, these methods all involve the same mechanism in the gaseous phase of the boundary layer. However, there is a difference in the boundary conditions at the wall which distinguishes the three methods from a thermodynamic as well as a mechanical viewpoint. Transpiration cooling involves the introduction of a coolant gas through a porous surface. Consequently, the rate of fluid injection through the surface and into the boundary layer may be arbitrarily adjusted by purely mechanical means and the temperature at the surface may thereby be regulated depending upon the injection rate and storage temperature of the coolant gas. It should be noted that a transpiration-cooling system requires pumps, storage tanks, pressure regulators, and accessory plumbing. In addition, the fabrication and maintenance of porous surfaces represent a difficult engineering problem.

A film-cooling system involves pumping a liquid or gas onto the surface through an inlet slot configuration such that a thin film of the material covers the surface. This acts as an insulating coating and, in the case of a liquid, absorbs heat in its vaporization. These systems are usually limited by such characteristics as the stability of the

*Figures in parentheses refer to references presented at the end of the text.

Various cooling methods

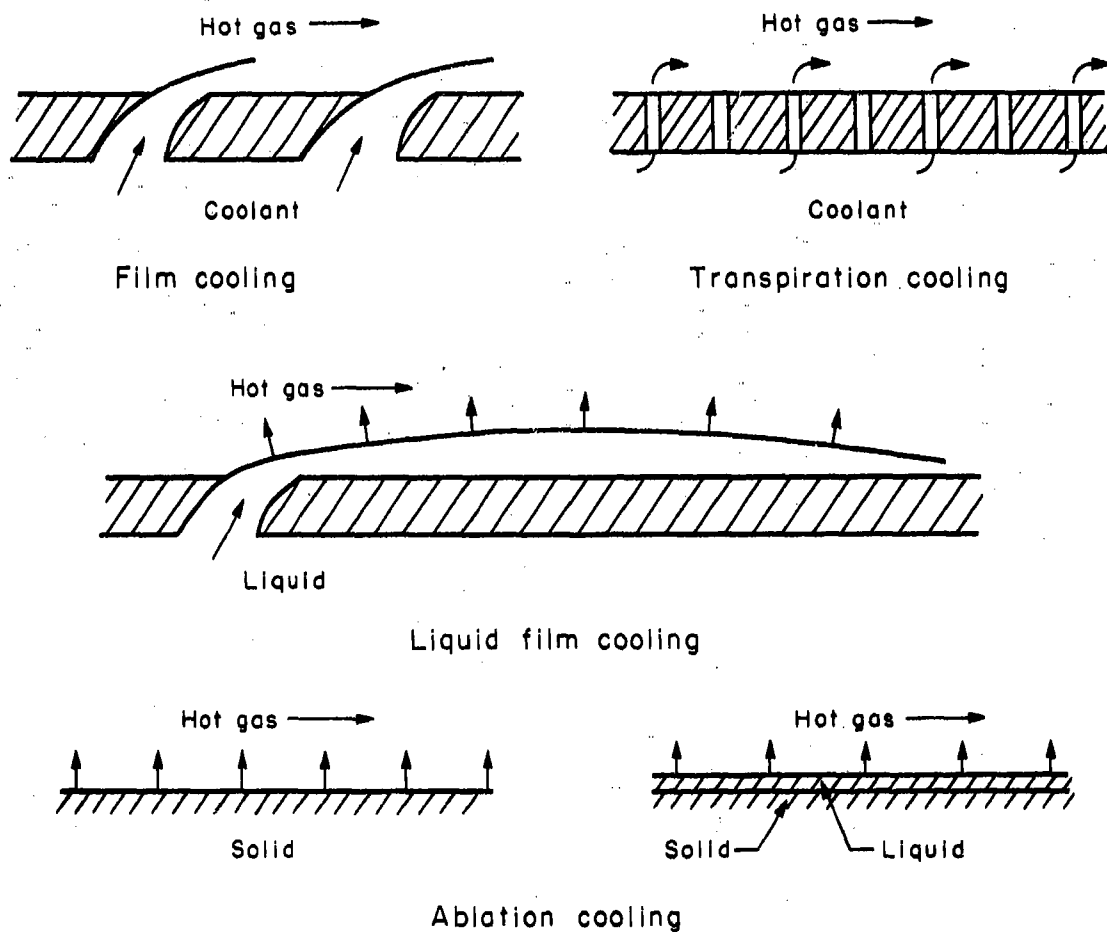


Fig. 1 — Various cooling methods

liquid film and the pumping power available. Film-cooling systems require essentially all the plumbing and control equipment of a transpiration-cooled operation; however, the surface construction is mechanically simpler.

A sublimation-cooling system is self-controlled through the relation between the vapor pressure and surface temperature of a solid, the Clausius-Clapeyron equation:

$$\ln p_1 = \frac{-\Delta H_s}{RT} + B \quad (1)$$

where

p_1 = vapor pressure of subliming material

R = universal gas constant

H_s = heat of sublimation per mole

B = constant of integration

Heat is absorbed by the material as it sublimes. Thus, the heat transfer into the interior is reduced in two ways: (a) direct absorption in the form of heat of sublimation, and (b) reduction of heat transfer because of the movement of the sublimed mass away from the surface. The mass release at the surface depends upon the heat of sublimation and the temperature of the surface. Furthermore, the surface temperature can no longer be arbitrarily controlled and, in fact, will always find "its own level" depending upon the heat load, heat of sublimation, and the external flow situation. It should be noted that film cooling with a liquid is essentially a sublimation process provided that the surface is

completely covered by a liquid layer.

In addition to sublimation, more complex ablation cooling schemes may be visualized. Depending upon the surface material and the flight conditions, it is possible to have such phenomena as fusion of the surface material, mechanical erosion, dissociation of both air and surface material, ionization, and chemical reactions between the components in the boundary layer. The obvious complications involved in an analysis of these complex ablating systems have prevented any really accurate description of the mechanism.

There is another method of classifying these systems which may be helpful conceptually; i.e., by specifying the method of controlling the rate of injection. In the case of transpiration cooling, as we have seen, the rate is arbitrarily controlled depending upon certain mechanical requirements such as the porous surface and pumping power available. This may be considered an arbitrarily controlled system. For a subliming or ablating surface, however, the rate of injection is determined by the heat of sublimation and the surface temperature. For a set of flight conditions and a surface material, the steady-state injection is fixed thermodynamically. We may call this a self-controlled system. Film cooling may be considered a mixed system, with the rate of mass transfer into the boundary layer being self-controlled, but the flow rate of liquid or gas over the surface remaining arbitrary.

II. BINARY LAMINAR BOUNDARY LAYER THEORY

Baron,^(2,3) Eckert, et al.,^(4,5,6) Sziklas and Banas,⁽⁷⁾ and Gross⁽⁸⁾ have investigated theoretically the problem of mass-transfer cooling in the laminar boundary layer on a flat plate. The introduction of a species conservation equation as well as the appearance of thermodynamic coupling terms in both the species and energy equations complicates the mathematical analysis of the boundary layer.

The equations have been derived by Hall⁽⁹⁾ who first treats the multicomponent fluid system and then from an order-of-magnitude argument obtains the boundary layer equations for a binary boundary layer. The final binary boundary layer equations for flow over a flat plate, neglecting the effects of thermal diffusion may be reproduced as follows:

$$\text{Continuity:} \quad \frac{\partial}{\partial x} (\rho u) + \frac{\partial}{\partial y} (\rho v) = 0 \quad (2)$$

$$\text{Momentum:} \quad \rho u \frac{\partial u}{\partial x} + \rho v \frac{\partial u}{\partial y} = \frac{\partial}{\partial y} \left(\mu \frac{\partial u}{\partial y} \right) \quad (3)$$

$$\begin{aligned} \text{Energy:} \quad \rho c_p u \frac{\partial T}{\partial x} + \rho c_p v \frac{\partial T}{\partial y} &= \frac{\partial}{\partial y} \left(k \frac{\partial T}{\partial y} \right) \\ &+ \mu \left(\frac{\partial u}{\partial y} \right)^2 + \rho D_{12} (c_{p1} - c_{p2}) \frac{\partial T}{\partial y} \frac{\partial Y}{\partial y} \end{aligned} \quad (4)$$

$$\text{Species:} \quad \rho u \frac{\partial Y}{\partial x} + \rho v \frac{\partial Y}{\partial y} = \frac{\partial}{\partial y} \left[\rho D_{12} \frac{\partial Y}{\partial y} \right] \quad (5)$$

The boundary conditions for this system of equations follow from physical considerations:

$$\left. \begin{array}{l} u = 0 \\ T = T_w \\ Y = Y_w \end{array} \right\} \quad \text{at } y = 0 \quad (6)$$

$$\left. \begin{array}{l} u = u_e \\ T = T_e \\ Y = 0 \end{array} \right\} \quad \text{at } y \rightarrow \infty \quad (7)$$

Since we are concerned with a seventh-order system of equations, another boundary condition must be specified. This condition may be obtained by noting that the mass velocity of the air molecules disappears at the surface of the plate; that is to say, there is no net mass transfer of the boundary layer air into the plate surface. Therefore, the mass flow of air by convection away from the surface must be equal and opposite to the diffusive flow of air toward the surface. This consideration yields the following boundary condition:

$$v = - \frac{\rho D_{12}}{1 - Y} \frac{\partial Y}{\partial y} \quad \text{at } y = 0 \quad (8)$$

This system of Eqs. (2) - (8), forms the starting point for the various investigators cited above. In all cases, a transformation of the coordinates is next introduced with the result that the system of partial differential equations is changed into a new set of interdependent ordinary differential equations. This system of equations is still difficult to solve since, in general, all of the physical properties are

functions of the local temperature and concentration of the particular gas mixtures being investigated. To obtain a representative number of solutions in a reasonable time requires the use of high-speed electronic computers. Although the same basic system of differential equations was used by the various investigators (Eqs. (2) - (8)), somewhat different assumptions were imposed to obtain the final solution. A brief review of the available analyses is given below.

III. REVIEW OF AVAILABLE BINARY LAMINAR BOUNDARY LAYER ANALYSES

CONSTANT PROPERTY ANALYSIS⁽¹⁰⁾

Considerable insight into the mass-transfer cooling process is obtained if it is assumed that the injected coolant has physical properties not markedly different from those of the main stream, thereby permitting the assumption of constant physical properties. The advantage of such a constant property solution is that the dimensionless heat-transfer and skin-friction results are dependent on a minimum number of parameters. This is indicated in Figs. 2 and 3 which compare the dimensionless quantities which are of importance for the solid-wall, heat-transfer case and those arising in the presence of mass transfer. For the solid wall, it has been demonstrated^(11, 12) that the constant property solutions for dimensionless skin friction, Nusselt numbers, and recovery factors have additional value in that they may be used even when large variations in physical properties are encountered (including dissociation), provided the properties are evaluated at a so-called reference temperature, T^* , which may be given explicitly in terms of the surface, the free stream, and the recovery temperatures:

$$T^* = T_e + 0.5 (T_w - T_e) + 0.22 (T_r - T_e) \quad (9)$$

It will be demonstrated that this temperature, T^* , will also prove of value in correlating the mass-transfer results.

It should be noted from Fig. 3 that the heat transfer, q , is defined in terms of the temperature gradient at the wall. This definition is

$$q = -k_w \left(\frac{\partial T}{\partial y} \right)_w$$

FOR GIVEN FREE STREAM CONDITIONS

$$T_w = T_r \text{ WHEN } -k_w \left(\frac{\partial T}{\partial y} \right)_w = 0$$

$$T_r = T_r (Me, Te)$$

DEFINITION OF HEAT-TRANSFER COEFFICIENT, h

$$q = h (T_w - T_r)$$

$$Nu = \frac{hx}{k}$$

$$\frac{Nu_x}{\sqrt{Re_x}} = f (Me, Te, Tw)$$

$$\text{CONSTANT PROPERTIES, } \frac{Nu_x}{\sqrt{Re_x}} = f (Pr)$$

$$T_r = T_r (Pr)$$

Fig. 2—Flat plate, solid wall, no mass transfer

$$q = -k_w \left(\frac{\partial T}{\partial y} \right)_w$$

FOR GIVEN FREE STREAM CONDITIONS

$$T_w = T_r \text{ WHEN } -k_w \left(\frac{\partial T}{\partial y} \right)_w = 0$$

$$T_r = T_r \left(M_e, T_e, \frac{\rho_w v_w}{\rho_e u_e} \sqrt{Re_x}, \text{INJECTED GAS} \right)$$

DEFINITION OF HEAT-TRANSFER COEFFICIENT, h

$$q = h (T_w - T_r)$$

$$Nu = \frac{hx}{k}$$

$$\frac{Nu_x}{\sqrt{Re_x}} = f \left(M_e, T_e, T_w, \frac{\rho_w v_w}{\rho_e u_e} \sqrt{Re_x}, \text{INJECTED GAS} \right)$$

$$\text{CONSTANT PROPERTIES, } \frac{Nu}{\sqrt{Re_x}} = f \left(\frac{\rho_w v_w}{\rho_e u_e} \sqrt{Re_x}, Pr \right)$$

$$T_r = T_r \left(\frac{\rho_w v_w}{\rho_e u_e} \sqrt{Re_x}, Pr \right)$$

Fig. 3 — Flat plate, mass transfer

convenient in that this quantity, q , represents the convective heat transferred to the surface from the boundary layer, and in this sense the boundary layer heat transfer is considered separately from the enthalpy carried across the surface by the coolant. To be consistent with this point of view, the recovery temperature, T_r , is defined as that temperature where the wall-temperature gradient vanishes; in this case there still exists a transport of enthalpy across the surface, by virtue of the coolant flow, but there is no convective heat transferred to the wall from the boundary layer.

Returning to the solutions of Eqs. (2) - (8) it is obvious that the energy equation is linear and consequently, the general solution of the complete equation may be obtained from the addition of (a) a general solution of the homogeneous equation (that is, neglecting the dissipation term) and (b) a particular solution of the complete equation. The particular solution results in the specification of the recovery factor, a direct measure of the temperature assumed by the surface if it is allowed to come to equilibrium with the surroundings by convection alone. We need, therefore, only to direct our attention to the general solution of the homogeneous equation. To accomplish this solution, a stream function, ψ , is first introduced to satisfy the continuity equation, and a new independent variable, η , and the new dependent variables defined below are substituted into the original equations:

$$\text{Stream function:} \quad u = \frac{\partial \psi}{\partial y}, \quad v = \frac{\partial \psi}{\partial x} \quad (10)$$

$$\left. \begin{aligned} f &= \psi / \sqrt{\nu u_e x} \\ \eta &= (y/x) \sqrt{u_e x/\nu} \\ \theta &= (T - T_w)/(T_e - T_w) \\ \phi &= (Y_w - Y)/Y_w \end{aligned} \right\} \quad (11)$$

The following equations result:

$$\text{Momentum:} \quad \frac{d^3 f}{d\eta^3} - \frac{1}{2} f \frac{d^2 f}{d\eta^2} = 0 \quad (12)$$

$$\text{Energy:} \quad \frac{d^2 \theta}{d\eta^2} + \frac{1}{2} \text{Pr} f \frac{d\theta}{d\eta} = 0 \quad (13)$$

$$\text{Diffusion:} \quad \frac{d^2 \phi}{d\eta^2} + \frac{1}{2} \text{Sc} f \frac{d\phi}{d\eta} = 0 \quad (14)$$

Boundary conditions:

$$\left. \begin{aligned} \frac{df}{d\eta} &= 0 \\ \theta &= 0 \\ \phi &= 0 \\ f_w &= -2(v_w/u_e) \sqrt{u_e x/\nu} \end{aligned} \right\} \quad \text{at } \eta = 0 \quad (15)$$

$$\left. \begin{aligned} \frac{df}{d\eta} &= 1 \\ \theta &= 1 \\ \phi &= 1 \end{aligned} \right\} \text{ at } \eta \rightarrow \infty \quad (16)$$

An important observation common to all flat-plate binary laminar boundary layer solutions is that the mass transfer into the boundary layer must vary as $1/\sqrt{x}$ if we are to arrive at a system of ordinary differential equations. Further, we have assumed an isothermal surface and it will be shown that this is completely compatible with the imposed mass-transfer distribution.

The velocity profiles for the constant property mass-transfer system are shown in Fig. 4 for several different injection rates. Inspection of these profiles brings out the following conclusions:

1. The effect of mass addition is to thicken the velocity boundary layer.
2. The velocity profile becomes S-shaped with mass addition, and since this is known to be an unstable type of profile, it may be concluded that mass transfer is destabilizing.
3. The boundary layer "lifts off" the wall at a relatively low value of mass transfer; i.e., at $(\rho_w v_w / \rho_e u_e) \cdot \sqrt{u_e x / \nu} = 0.619$. Apparently the boundary layer equations fail to describe the flow field at this mass-transfer condition.

The skin friction coefficient and Nusselt number, presented in Figs. 5 and 6, are seen to decrease with increasing mass transfer, both going to zero at the limiting value where the boundary layer "leaves"

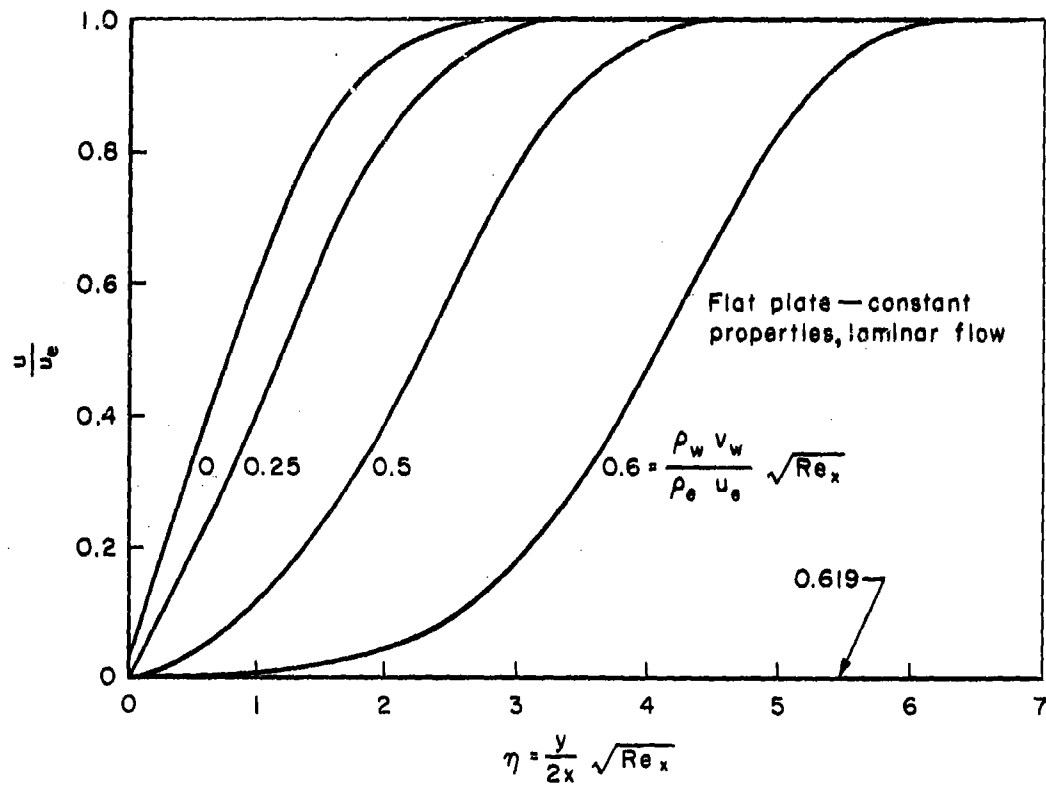


Fig.4—Effect of air injection on velocity profile

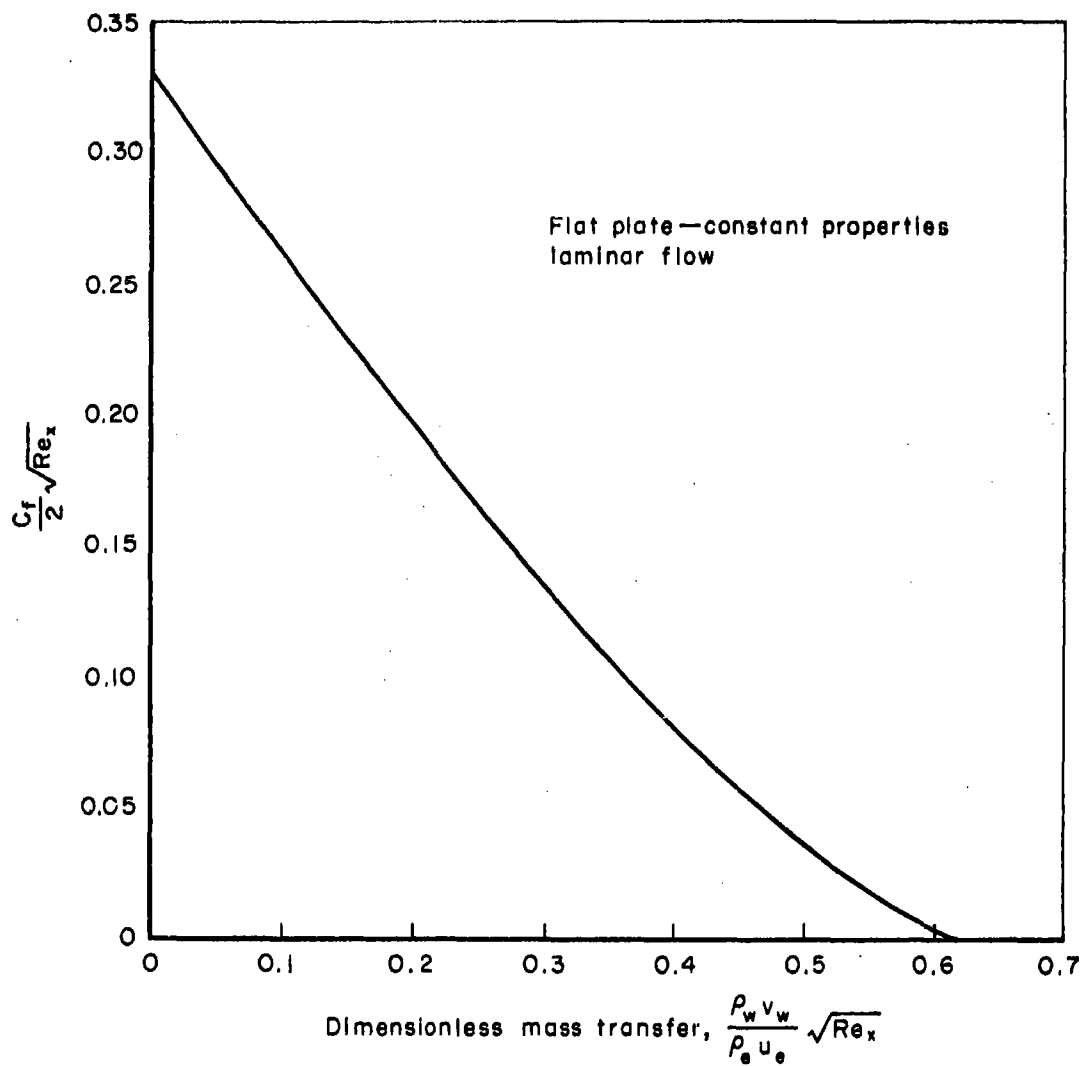


Fig.5—Effect of air injection on local skin friction

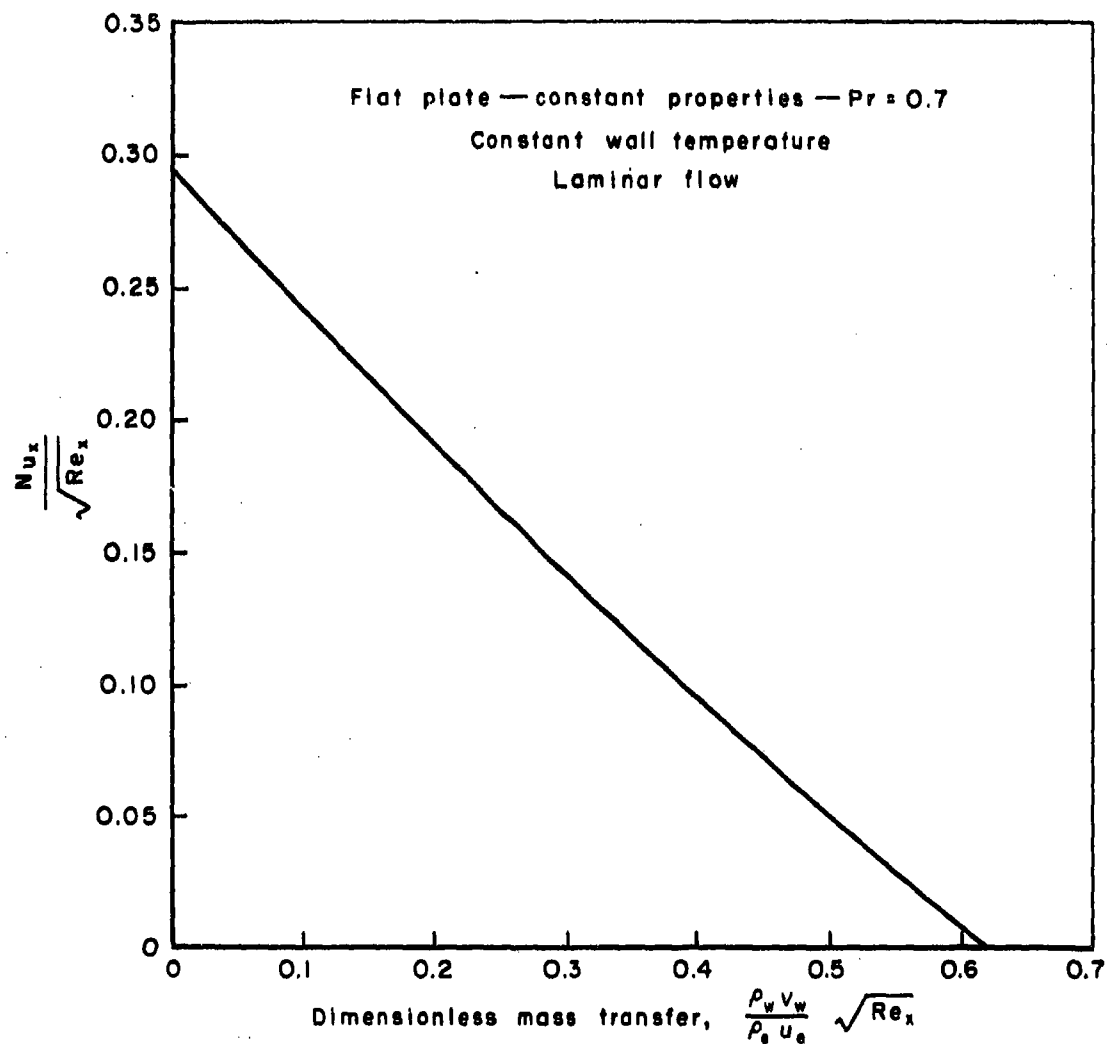
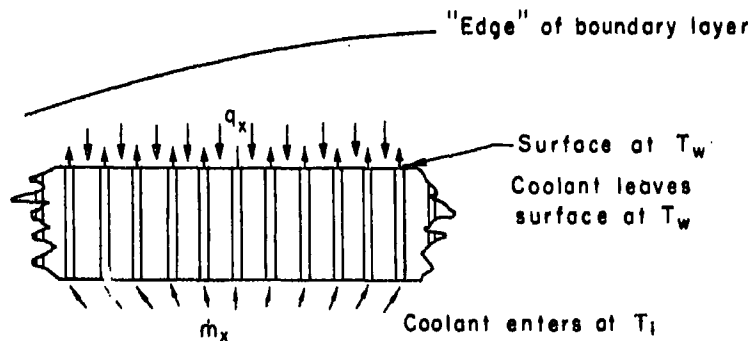


Fig. 6 — Effect of air injection on local Nusselt number

the wall. The recovery factor, shown in Fig. 7, is somewhat reduced by mass transfer but not as markedly as the Nusselt values. At hypersonic velocities the actual heat transfer to the surface is proportional to the product of the Nusselt number and the recovery temperature, and we conclude that a considerable reduction in heat transfer is obtainable with modest amounts of coolant. This is the feature which has drawn attention to this cooling scheme.

It may be noted that the heat-transfer solutions reveal that the local heat rate, q_x , is proportional to $1/\sqrt{x}$, which is precisely the distribution of the injected coolant. A simple heat balance on a sublimation or transpiration system yields the following expression:

$$\dot{m}_x [\Delta H + c_{p_1} (T_w - T_1)] = q_x$$



where

\dot{m}_x = mass flow rate of coolant

ΔH = change in enthalpy due to phase change

c_{p_1} = specific heat of the pure coolant

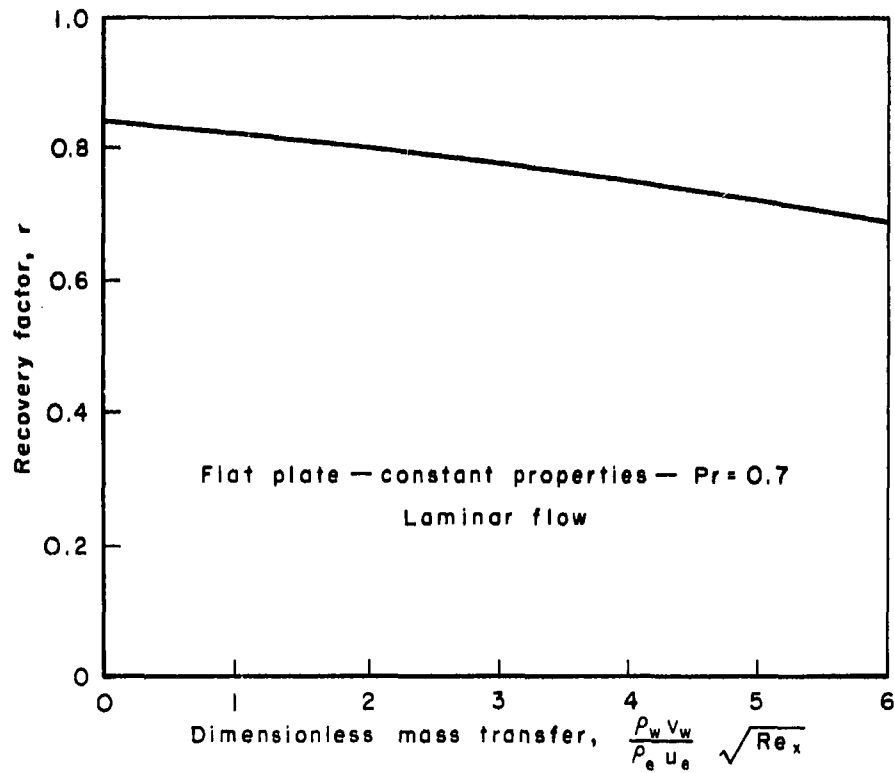


Fig. 7 — Effect of air injection on recovery factor

Thus for the situation where the coolant enters the wall at a constant temperature, T_1 , or if the surface is subliming, the resulting wall temperature must be a constant. We have, therefore, demonstrated the consistency of the assumed boundary conditions.

It may be of interest to investigate the validity of the modified Reynolds analogy (which holds for solid-wall conditions) under the new conditions when mass transfer is employed. If the analogy is valid, the parameter $(C_H Pr^{2/3}) : (C_p/2)$ would equal unity. As seen in Fig. 8, considerable departure occurs and we conclude that, at least for this constant-property laminar flow, the modified Reynolds analogy does not apply in the presence of mass transfer.

ANALYSIS OF BARON^(2, 3)

Baron was successful in introducing the influence of variable physical properties on mass-transfer cooling, while at the same time keeping the number of independent parameters at a minimum. To accomplish this, he adopted an approach similar to that used earlier by Chapman and Rubesin⁽¹³⁾ for the solid flat plate. Baron introduces the so-called Chapman-Rubesin constant, C , for the product of the density and viscosity of the air only. He notes:

$$\frac{\rho \mu}{\rho_e \mu_e} = \left(\frac{\rho_2 \mu_2}{\rho_e \mu_e} \right) \left(\frac{\rho \mu}{\rho_2 \mu_2} \right) = C \lambda \quad (17)$$

where

$$C = (\rho_2 \mu_2) / (\rho_e \mu_e) = \text{Chapman-Rubesin constant for } \underline{\text{air}} \text{ only}$$

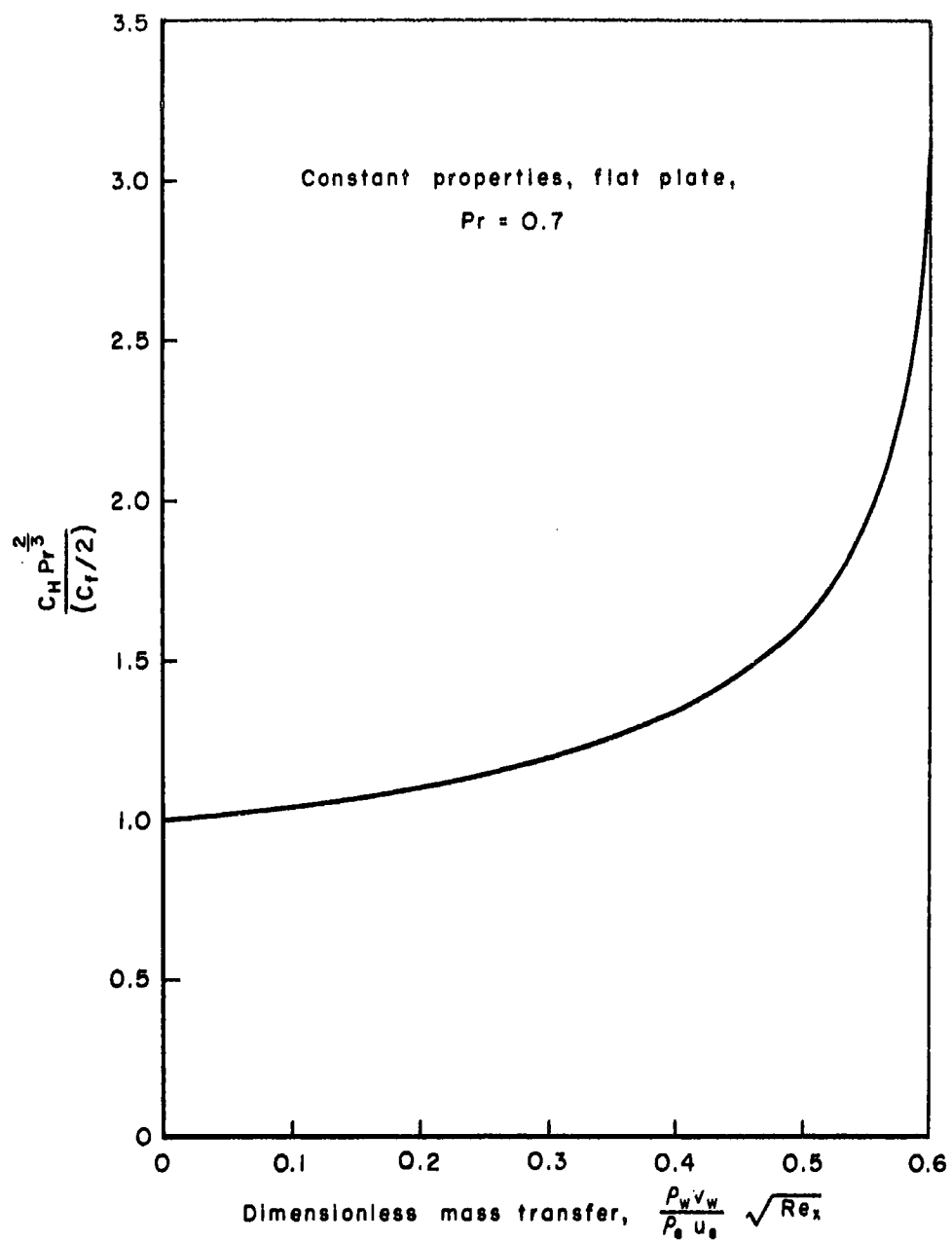


Fig. 8 — Effect of mass transfer
on modified Reynolds analogy

$$\lambda = \frac{\rho \mu}{\rho_2 \mu_2} = \frac{\mu}{\mu_2} \left[1 + \left(\frac{m_2}{m_1} - 1 \right) Y \right]^{-1}$$

The factor, C , is independent of the concentration, while the other factor, λ , is a function of both temperature (through μ/μ_2) and concentration. However, for helium and carbon dioxide, the gases considered by Baron, the viscosity term μ/μ_2 is relatively insensitive to temperature and is primarily dependent on the concentration*. Consequently, Baron assumes that λ is a function only of concentration.

Using this assumption, Baron presents two approaches:

Approach 1

Baron introduces

$$\begin{aligned} u &= \frac{\rho_e}{\rho} \frac{\partial \psi}{\partial y}, & v &= -\frac{\rho_e}{\rho} \frac{\partial \psi}{\partial x} \\ \eta &= \frac{1}{2} \sqrt{\frac{u_e}{\nu_e x C}} \int_0^y \frac{\rho}{\rho_e} dy & (18) \\ \psi &= \sqrt{\nu_e x u_e C} f(\eta) \end{aligned}$$

Using these transformations along with the additional assumption that the Schmidt number is a function only of concentration (an independent check shows this to be a realistic assumption), Baron obtains a set of three ordinary differential equations, similar in form but more complex than Eqs. (12) - (16). The net result of these substitutions is that none of

*This assumption is valid for hydrogen as well.

the terms appearing in the momentum and diffusion equations are dependent on temperature and consequently these two equations may be solved simultaneously, but independently of the energy equation. Using this approach Baron obtains the velocity profiles, the concentration profiles and the skin-friction parameter, $c_f \sqrt{u_e x / \nu_e C}$, as a function only of the mass-transfer parameter $(\rho_w v_w) / (\rho_e u_e) \sqrt{u_e x / \nu_e C}$. Any temperature effect is completely contained in the constant C .

The energy equation remains to be solved, and Baron reports that all the coefficients appearing in this equation were only mildly affected by temperature, allowing the assumption that all coefficients are functions only of concentration. This is a considerable simplification for now the energy equation is linear in temperature, since all coefficients are known functions of the dimensionless parameter, η , by virtue of the previously obtained solutions of the momentum and diffusion equations.* As in the constant-property situation, the resulting energy equation, being linear, may be solved by first treating the non-dissipative case and then adding the adiabatic-wall solution. It follows that the low-speed non-dissipative heat-transfer coefficients may be used for the high-speed case if the adiabatic-wall temperature replaces the free-stream temperature in the definition of the heat-

*There appears to be an error in Baron's final energy equation in Ref. 2. This results when he replaces u_e^2 by $(\gamma_e - 1) c_{p2} M_e^2$ rather than the correct expression $(\gamma_e - 1) c_{pe} M_e^2$. Consequently, the left hand side of Baron's energy equation 6.15 should be multiplied through by c_{p2}/c_{pe} to get the correct form.

transfer coefficient

$$q = h(T_r - T_w) \quad (19)$$

The recovery temperature, T_r , determined from the adiabatic-wall solution, is reported in terms of a recovery factor, r , which for a given injected gas is a function only of the mass-transfer parameter $(\rho_w v_w / \rho_e u_e) \sqrt{u_e x / \nu_e C}$. In addition to the recovery factor, Baron also presents dimensionless heat-transfer coefficients for two binary systems, helium-air and carbon dioxide-air mixtures.

The second approach used by Baron is not as realistic as the above and will be mentioned only briefly. In this case he assumed that λ is a constant to be evaluated at wall condition and the following transformations are then applied to Eqs. (2) - (8):

Approach 2

$$\begin{aligned} u &= \frac{\rho_e}{\rho} \frac{\partial \psi}{\partial y} & v &= - \frac{\rho_e}{\rho} \frac{\partial \psi}{\partial x} \\ \eta &= \frac{1}{2} \sqrt{\frac{u_e}{\nu_e x C \lambda_w}} \int_0^y \frac{\rho}{\rho_e} dy & (20) \\ \psi &= \sqrt{\nu_e x u_e C \lambda_w} f(\eta) \end{aligned}$$

Baron obtained some representative solutions for this simplified case and compared them with the more realistic case outlined above. This comparison is shown for helium injection in Fig. 9 and the agreement is only fair.

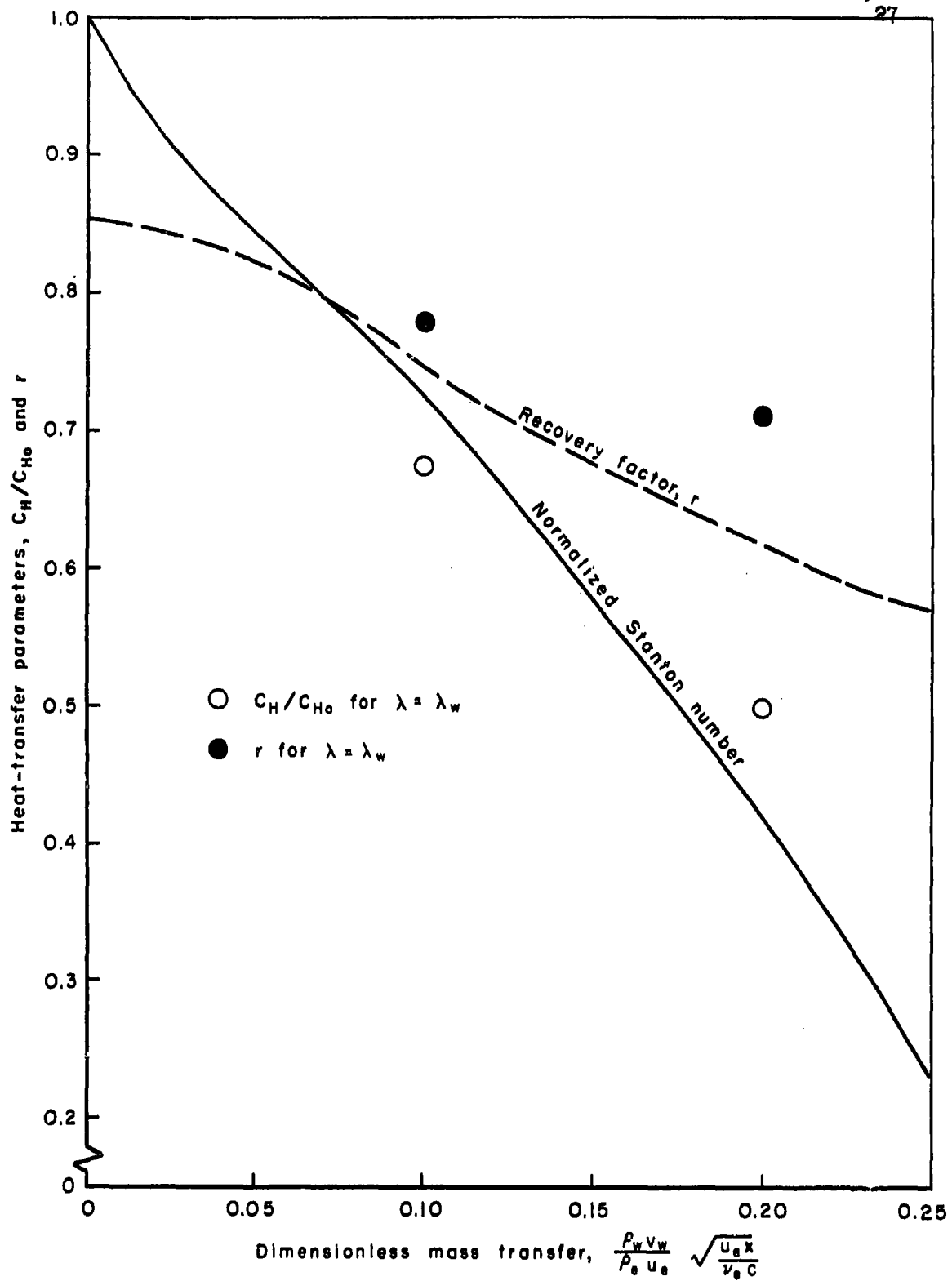


Fig. 9 — Helium results of Baron

In a later publication⁽⁵⁾ Baron generalizes his analysis to include the influence of pressure gradients. In addition, he presents a summary of his flat-plate results.*

ANALYSIS OF ECKERT AND CO-WORKERS^(4, 5, 6)

Before attempting the complete binary problem including heat transfer, Eckert and Schneider first solved the isothermal case with hydrogen as the injected gas. The physical properties were allowed to vary with concentration and the methods outlined in Ref. 14 were used to calculate the variation. The resulting velocity distributions and skin friction are compared to the constant property results in Figs. 9 and 10. This comparison reveals that unstable S-shaped velocity profiles occur at relatively low values of the dimensionless mass transfer when compared with the constant property situation. The greater influence of a light gas on skin friction is obvious in Fig. 11, where at the same values of dimensionless mass transfer considerably lower skin friction occurs for the hydrogen injection. We, therefore, conclude that the light gas is more effective in reducing skin friction but on the other hand is more de-stabilizing to a laminar boundary layer. This will be demonstrated in a later section.

In the analysis of the binary system including heat transfer, again using hydrogen as the mass-transfer medium, Eckert and his colleagues used the following transformation in dealing with Eqs. (2) - (8):

*Care should be taken in using this reference since there is some confusion in nomenclature. The mathematical development utilizes a somewhat different transformation from that used by Baron in Ref. 2, although the figures are all shown in terms of the original variables of Ref. 2.

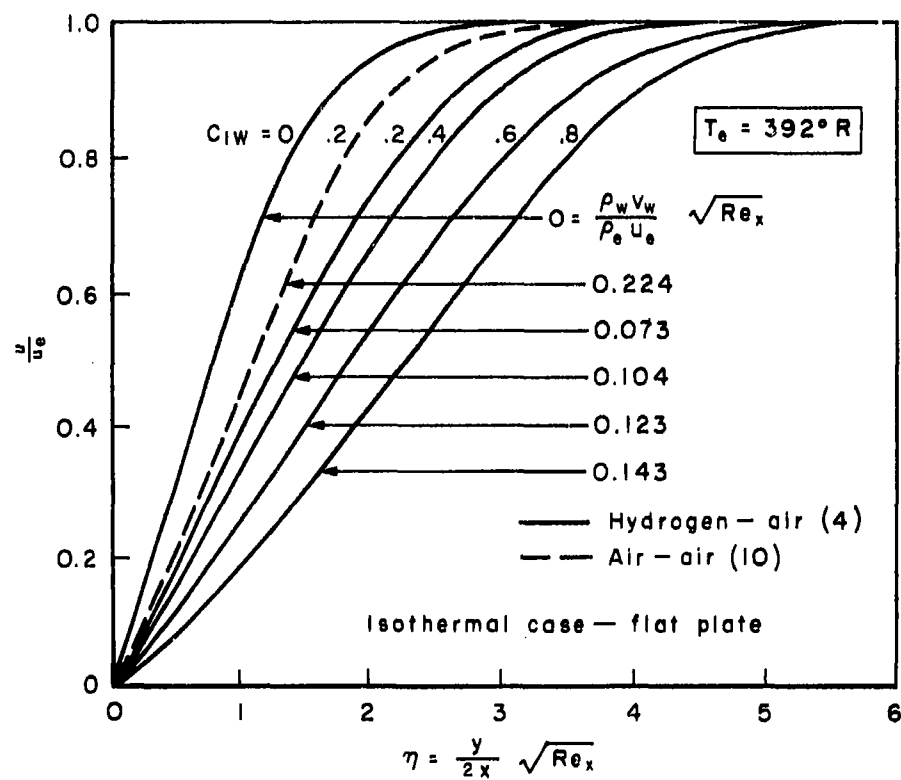


Fig. 10—Effect of light gas injection
on laminar velocity profiles

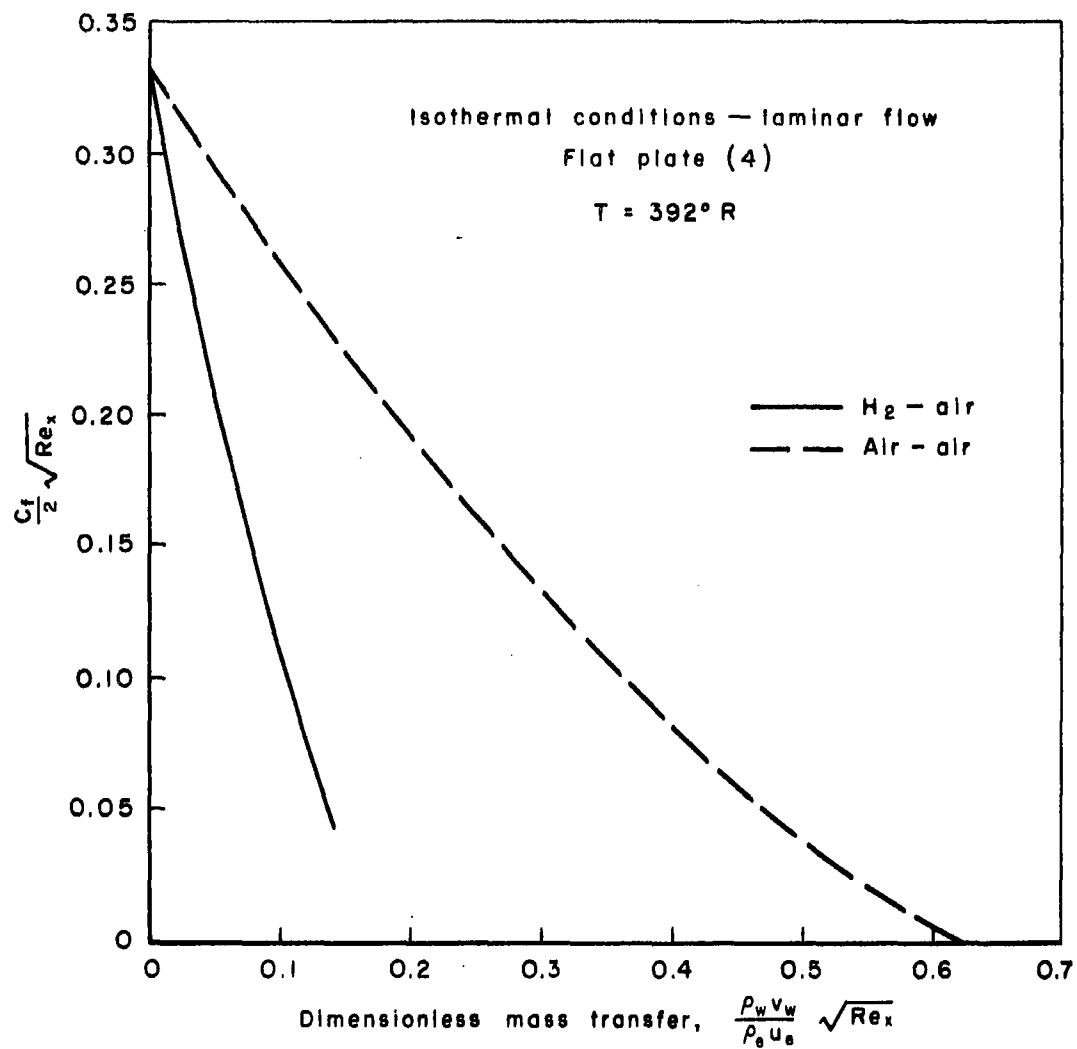


Fig. 11 — Effect of light gas injection on skin friction

$$u = \frac{\rho_e}{\rho} \frac{\partial \psi}{\partial y}, \quad v = - \frac{\rho_e}{\rho} \frac{\partial \psi}{\partial x}$$

$$\eta = \sqrt{\frac{1}{2} \frac{u_e}{v_e x}} \int_0^y \frac{\mu_e}{\mu} dy \quad (21)$$

$$\psi = \sqrt{x u_e v_e} f(\eta)$$

The transformed equations were then solved using the best available property information for hydrogen-air mixtures. These exact solutions, which were obtained using an iterative procedure on an ERA 1103 electronic computer, are valid only for the specific conditions selected. (See Figs. 2 and 3.) An example of these results is shown in Fig. 12 where the dimensionless heat-transfer coefficients are shown for zero Mach number for two different wall-temperature conditions with the free stream at 392°R. Additionally, for Mach 12, the Nusselt number and recovery temperature, both of which must be known to determine the heat transfer, are shown for a set of specific conditions. In every case we find a considerable reduction in the heat transfer when only small amounts of hydrogen are transferred away from the wall into the boundary layer. The effectiveness of light-gas injection in decreasing the heat transfer in a high-speed boundary layer is obvious from this figure.

ANALYSIS OF SZIKLAS AND BANAS⁽⁷⁾

Sziklas and Banas report solutions for a number of different coolants: hydrogen, helium, water vapor, and air. In arriving at the final form of the energy equation they assumed that the specific heat

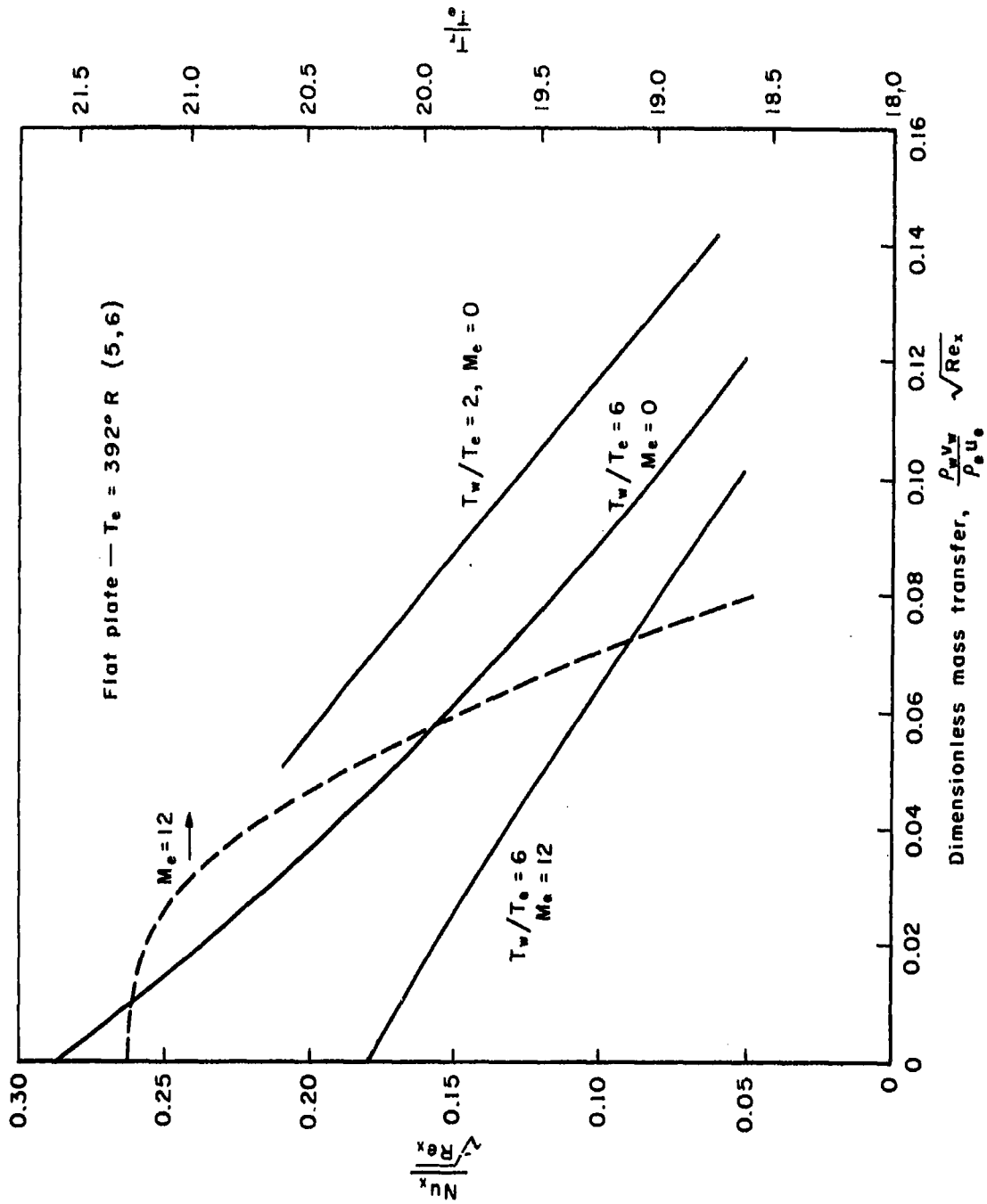


Fig. 12—Effect of hydrogen injection on laminar heat transfer

ratio, γ , is the same for the injected coolant as for the main stream gas ($\gamma_1 = \gamma_2$). They then use the standard Blasius η -transformation essentially as given in Eq. (11). In obtaining their solutions, the physical properties (including specific heat) were allowed to vary with both temperature and concentration. Methods of kinetic theory were used in the determination of these properties. As was the case with the results of Eckert, the results of Sziklas and Banas are applicable only to the specific conditions imposed in the analysis. Representative results for the helium study are given in Fig. 13, where, again, large reductions in heat transfer accompany small mass-transfer rates.

ANALYSIS OF GROSS⁽⁸⁾

The isothermal laminar binary boundary layer on a flat plate was investigated by Gross⁽⁸⁾ for three different injectant gases: hydrogen, carbon dioxide, and iodine vapor. To obtain a solution of the governing equations (Eqs. (2), (3), and (5)), Gross used the standard Blasius transformation to arrive at a system of ordinary differential equations. These were then solved using a Runge-Kutta numerical method with the aid of a high-speed electronic computer.

The resulting values of the skin-friction coefficient for the three gases investigated are shown in Fig. 14. These results demonstrate that the addition of a heavy gas such as iodine vapor (molecular weight 253.8) is much less effective in reducing the skin-friction coefficient than the addition of the lighter gases.

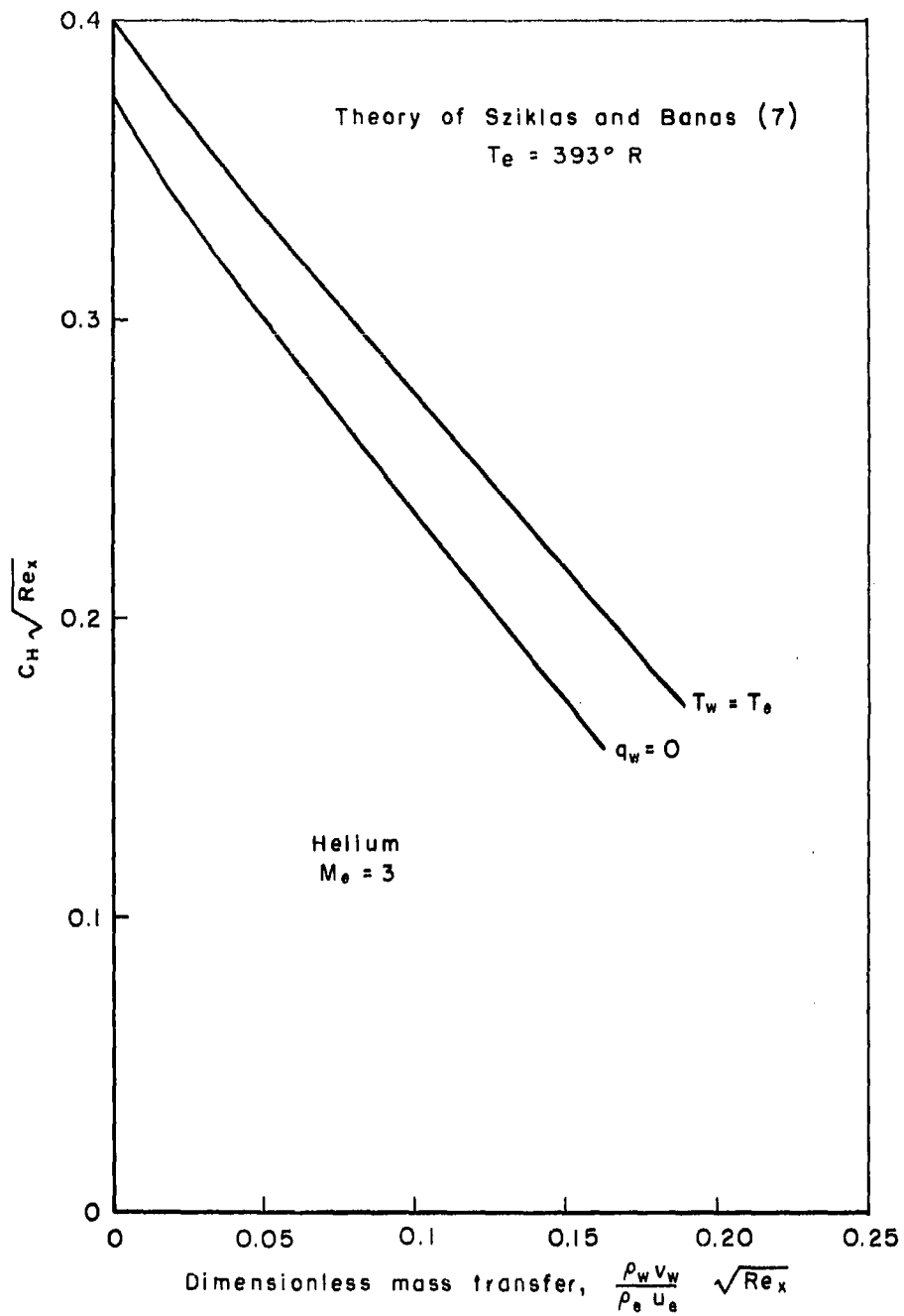


Fig. 13 — Variation of laminar heat transfer with helium injection

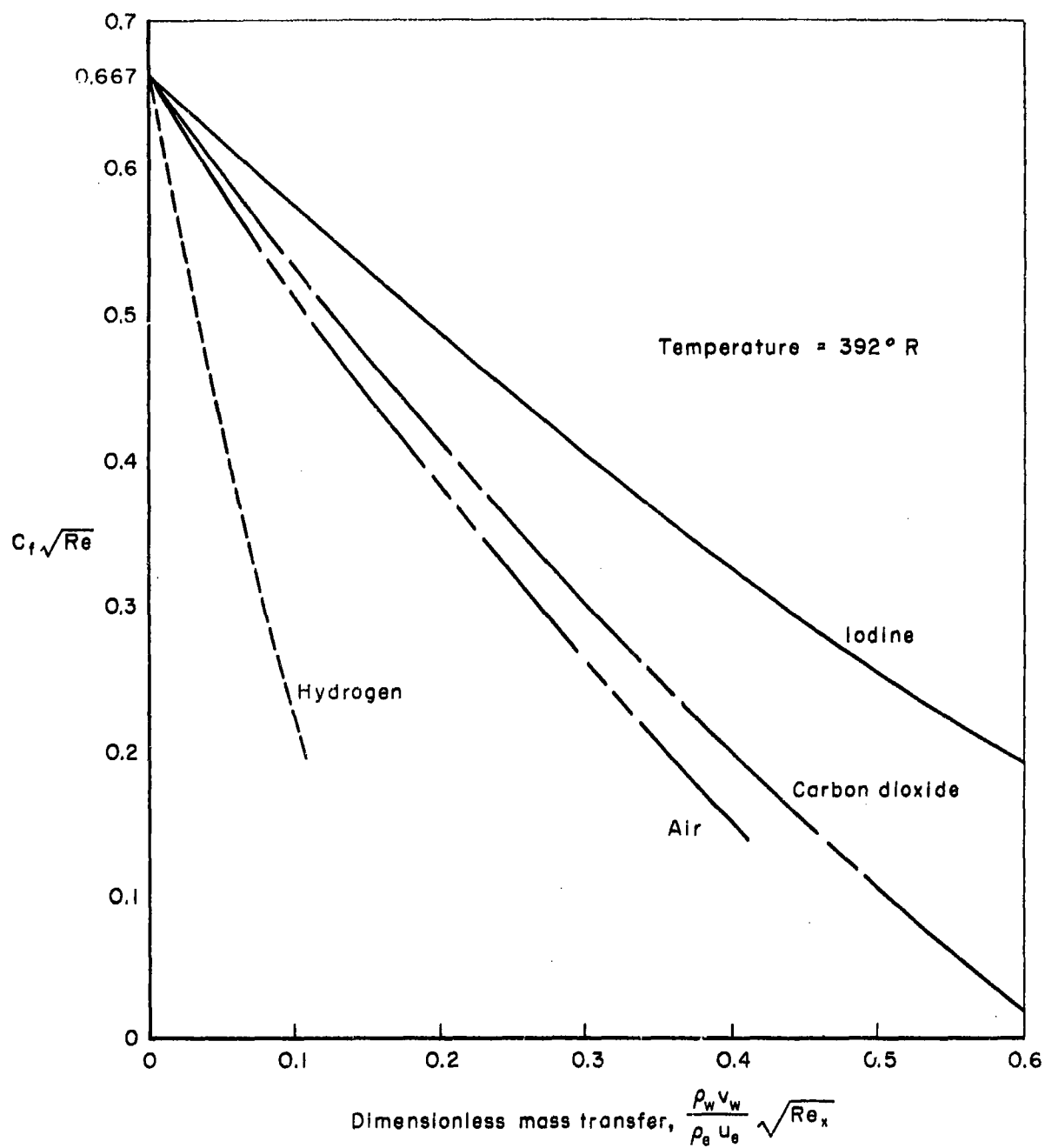


Fig. 14—Friction coefficient as a function of the blowing parameter (8)

IV. GENERALIZED PRESENTATION OF LAMINAR FLAT PLATE

BINARY BOUNDARY LAYER RESULTS

It is our goal in this section to develop a generalized presentation which may be conveniently utilized by design engineers for predicting skin friction and heat transfer in the presence of mass-transfer cooling for laminar flow over surfaces with zero pressure gradient. The available analytical solutions briefly described above are used as the basis for the generalization. Since heat transfer and skin friction for solid surfaces in the absence of mass-transfer cooling can be calculated at the present time with a measure of confidence, the approach adopted here is to present the correction factors which must be applied to such solid wall calculations to account for the effect of mass addition. Thus the normalized skin-friction coefficient and heat transfer will be given as c_f/c_{f0} , and q/q_0 , respectively, where the subscript zero implies that the quantity is to be evaluated for the same free-stream and wall-temperature conditions, neglecting the influence of mass transfer.

It was found that these normalized results for any one gas could be presented as a unique function of the mass-transfer parameter proposed by Baron, $(\rho_w v_w / \rho_e u_e) \sqrt{u_e x / \nu_e C^*}$, provided that the Chapman-Rubesin constant, C , was evaluated at the so-called reference temperature, T^* , given by Eq. (9). The success of this generalized presentation for skin friction is demonstrated in Figs. 15 and 16 which apply to hydrogen-air and helium-air binary systems, respectively. It appears that this representation is valid over a wide range of wall-temperature conditions and free-stream Mach numbers. This conclusion is true for the other binary systems as well and the reader is referred to Appendix C for

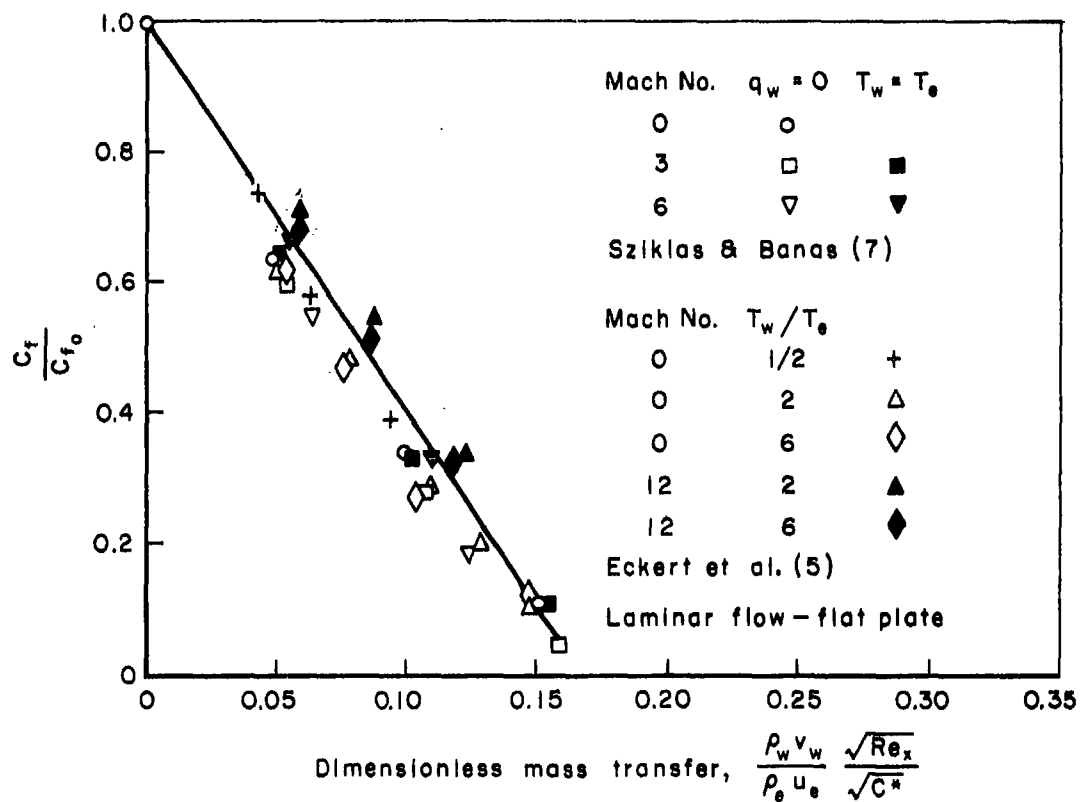


Fig. 15 — Effect of mass transfer on skin friction
Hydrogen-air

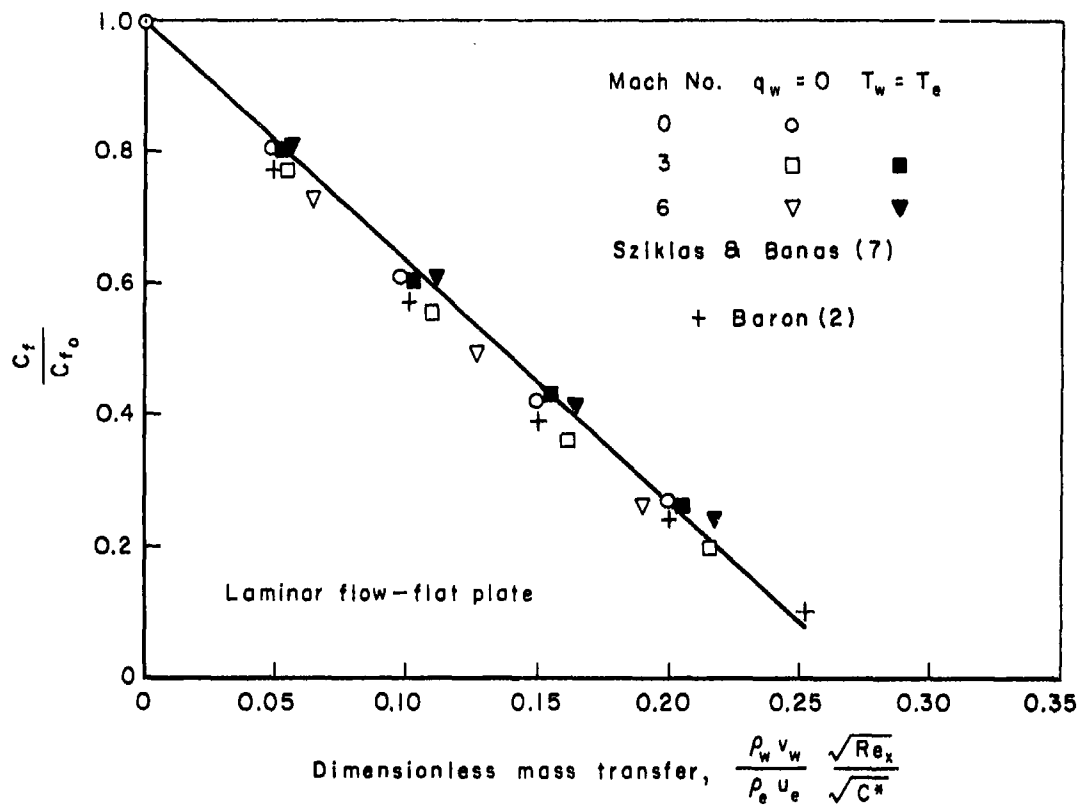


Fig. 16 — Effect of mass transfer on skin friction
Helium—air

verification of this conclusion. A summary of available skin-friction results for six gases is given in Fig. 17.

This same presentation was successful in correlating the normalized Stanton number, with the final results as shown in Fig. 18. Since the determination of the actual heat transfer requires the knowledge of the recovery factor as well as the Stanton number, the normalized recovery factor is shown in Fig. 19. It may be seen that some disagreement exists for the light-weight gases. Apparently the recovery factor is somewhat more sensitive to the different assumptions, particularly physical property variations, adopted by the various investigators. The effect on the final heat-transfer prediction of this disagreement in recovery factor is reduced if the normalized heat transfer is directly considered rather than the Stanton number. The resulting normalized heat transfer is shown in Figs. 20 through 22. It should be pointed out that some effect of the disagreement in recovery factor is still present in this presentation through the presence of C^* . However, for practical applications the wall temperature in general will be markedly lower than the recovery temperature; for this situation, inspection of the defining equation (9) for T^* reveals that any uncertainty in the recovery temperature has only a minor effect on the reference temperature itself, and consequently, only a minor effect on C^* .

It is apparent from Figs. 17 and 22 that the light gases are much more effective than the heavier gases in reducing heat transfer and skin friction. Inspection of these figures indicates that the normalized skin-friction coefficient c_f/c_{f0} and heat transfer q/q_0 vary linearly with the dimensionless mass-transfer parameter for all the gases shown.

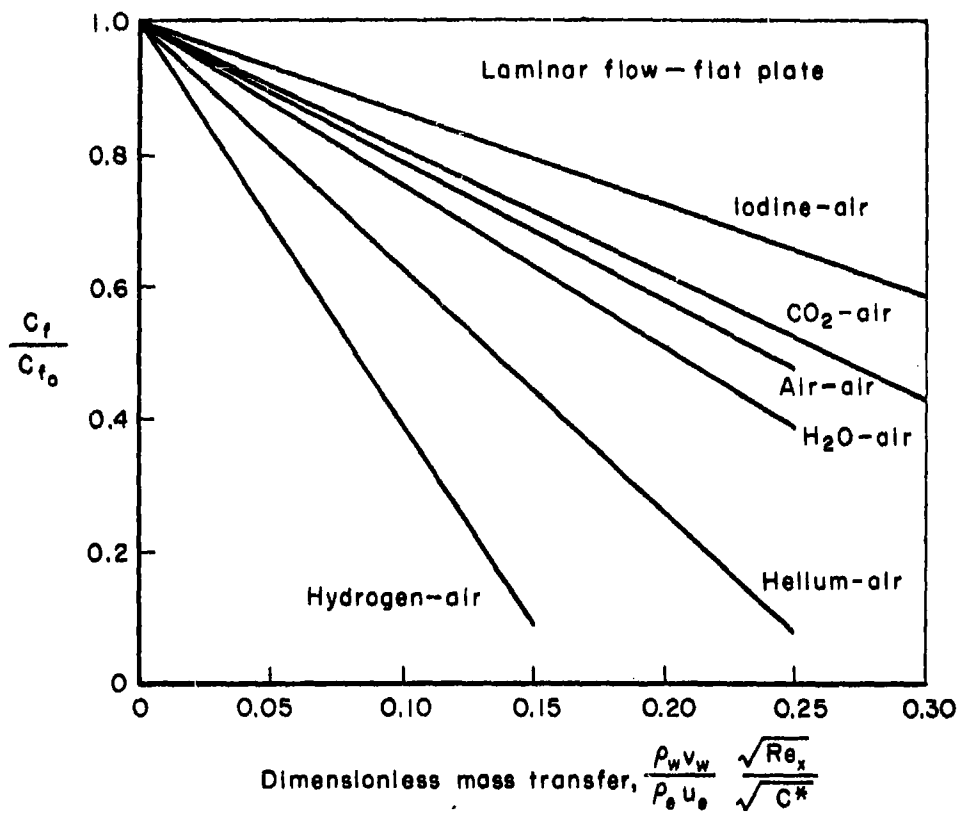


Fig. 17 — Effect of mass transfer on skin friction; summary

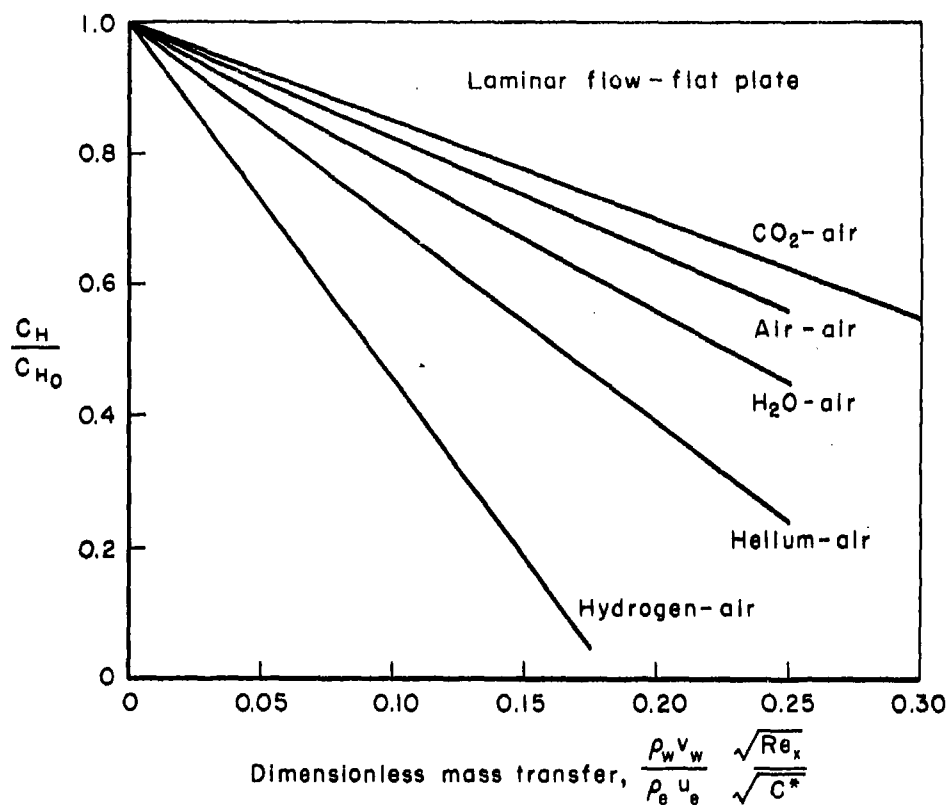


Fig. 18 — Effect of mass transfer on Stanton number

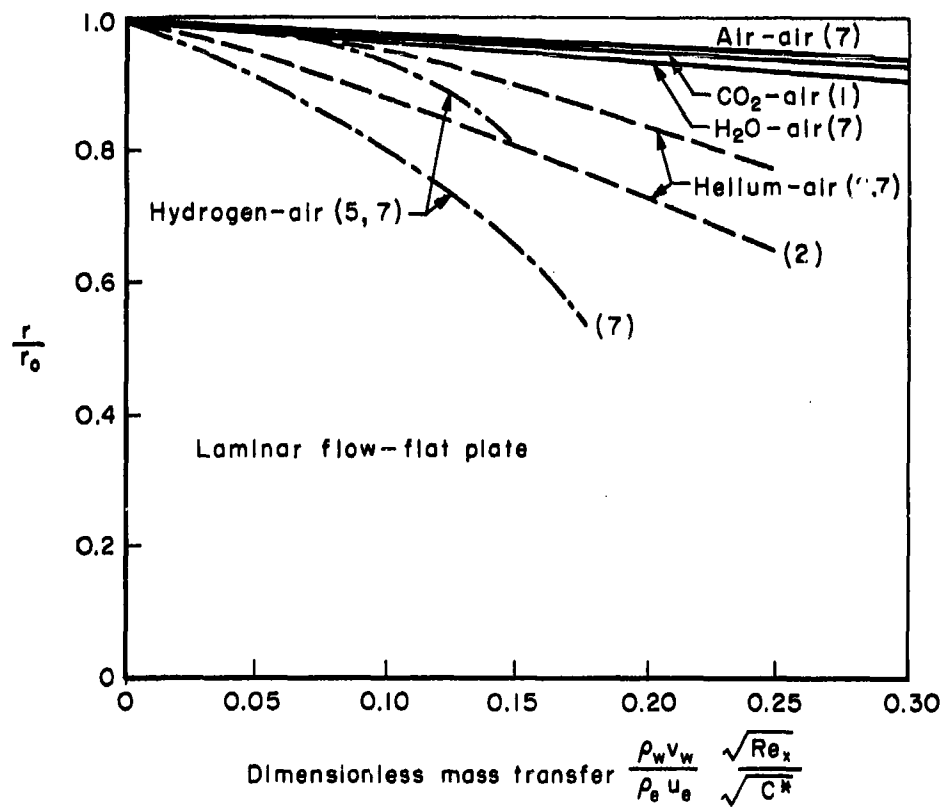


Fig. 19 — Effect of mass transfer on recovery factor

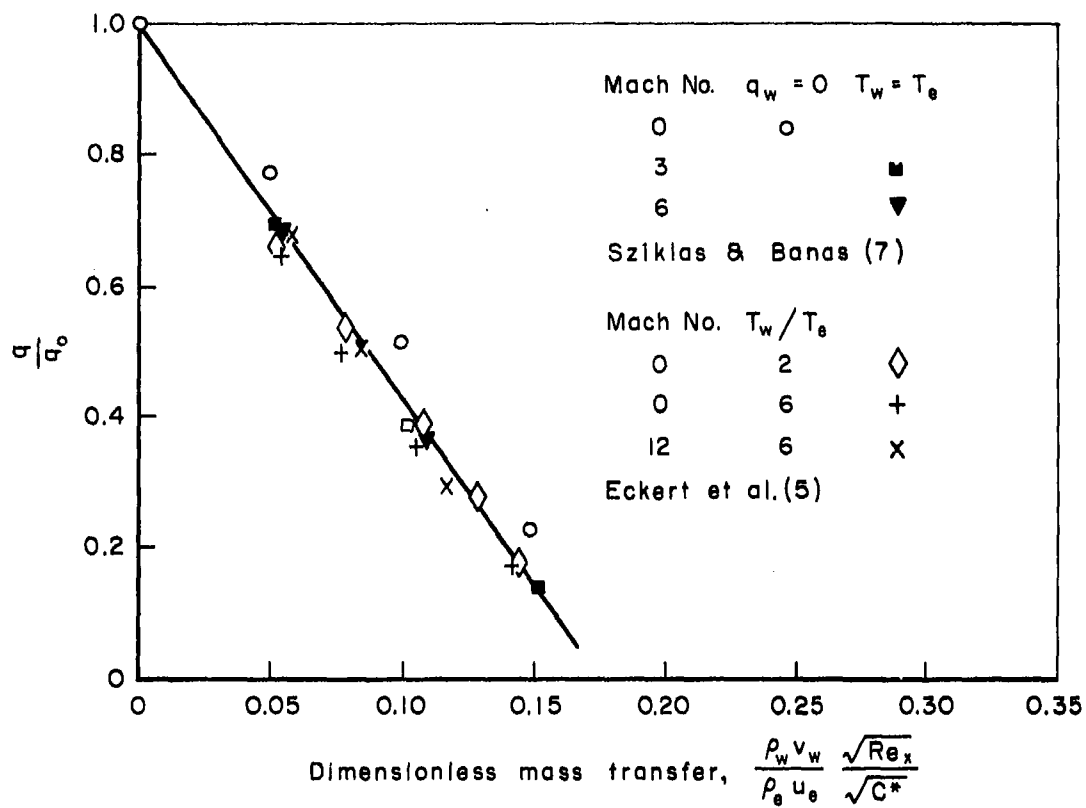


Fig. 20—Effect of mass transfer on heat transfer
Hydrogen-air

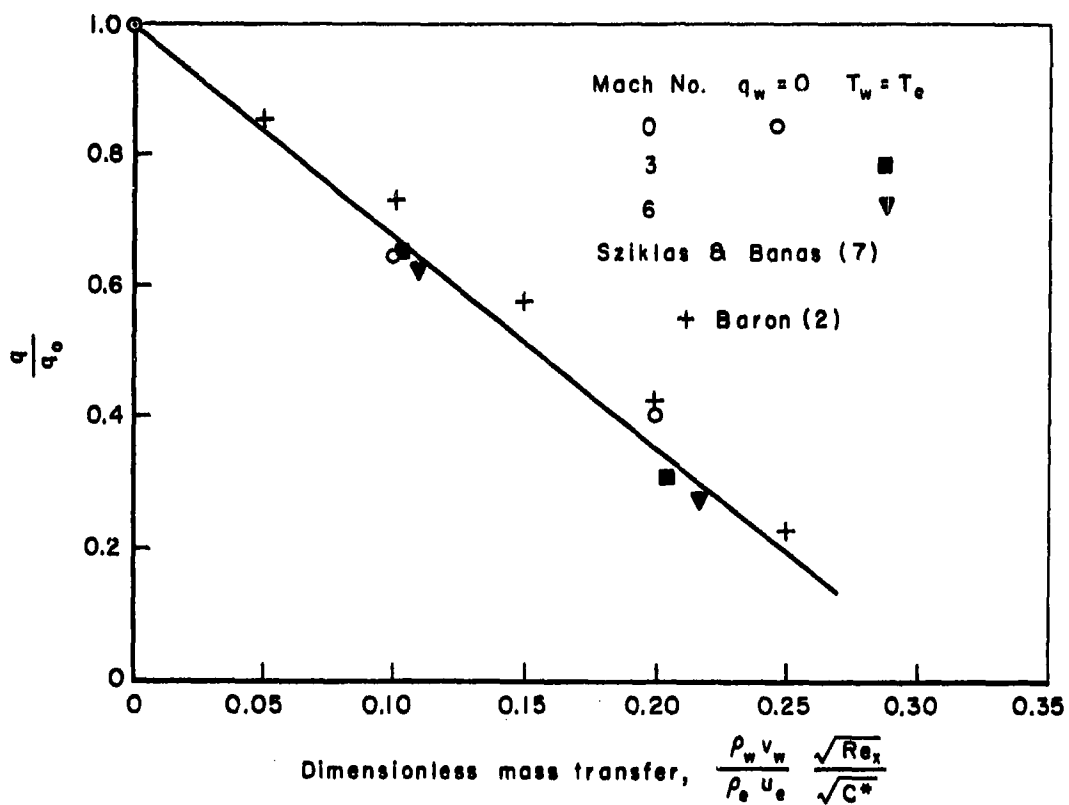


Fig. 21 — Effect of mass transfer on heat transfer
Helium-air

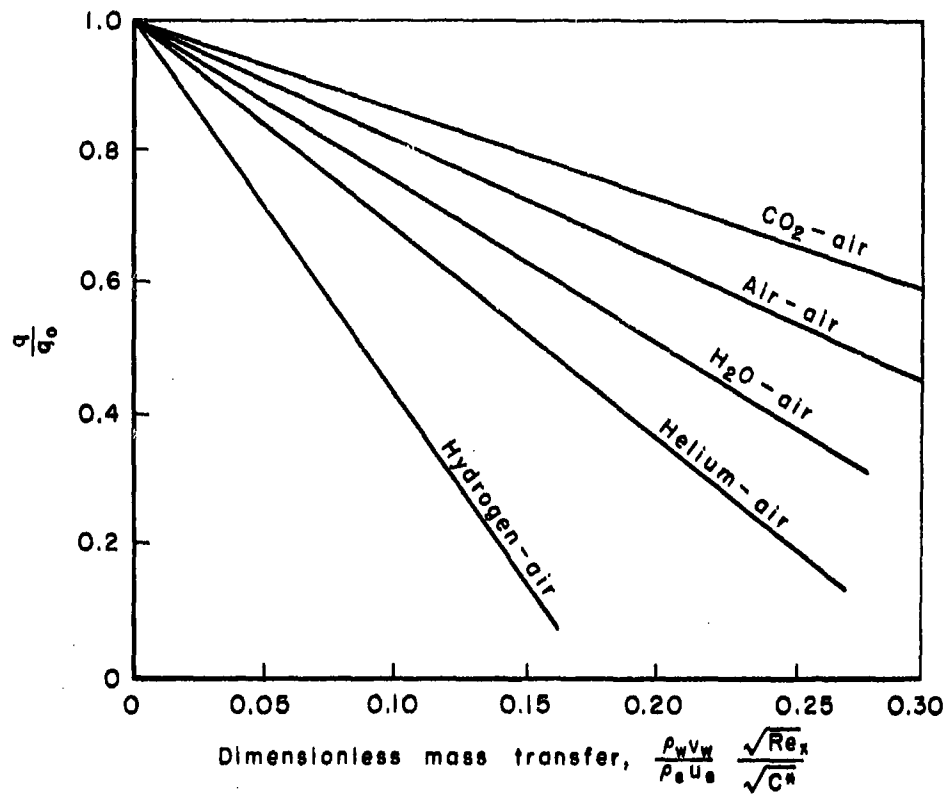


Fig. 22 — Effect of mass transfer on heat transfer
Summary

In particular, the results for air into air may be expressed by the following two equations:

$$\begin{aligned} q/q_o &= 1 - 1.82 \left\{ (\rho_w v_w / \rho_e u_e) (\sqrt{Re_x / C^*}) \right\} \\ c_f / c_{fo} &= 1 - 2.08 \left\{ (\rho_w v_w / \rho_e u_e) (\sqrt{Re_x / C^*}) \right\} \end{aligned} \quad (22)$$

It is of technical importance to determine whether the other gases can be made to agree with these equations by the simple expedient of multiplying the Baron dimensionless mass-transfer parameter by a molecular weight ratio (m_2/m_1) , raised to a constant exponent. This question can be answered by plotting the dimensionless mass transfer versus the molecular weight at a constant value of q/q_o (or c_f/c_{fo}). This is accomplished in Fig. 23 where it is seen that $1/3$ represents a fair compromise for the value of the exponent although the very light gases as well as the heavier gases such as iodine show a significant departure. Recognizing that such discrepancies do occur for the heavier and light gases, it nevertheless appears that the following equations represent the heat transfer and skin friction reasonably well.

$$\begin{aligned} q/q_o &= 1 - 1.82 \left\{ (m_2/m_1)^{1/3} (\rho_w v_w / \rho_e u_e) (\sqrt{Re_x / C^*}) \right\} \\ c_f / c_{fo} &= 1 - 2.08 \left\{ (m_2/m_1)^{1/3} (\rho_w v_w / \rho_e u_e) (\sqrt{Re_x / C^*}) \right\} \end{aligned} \quad (23)$$

It is recommended that these equations be used to predict the heat-transfer and skin-friction performance for mass-transfer cooling in a binary laminar boundary layer on a flat plate.

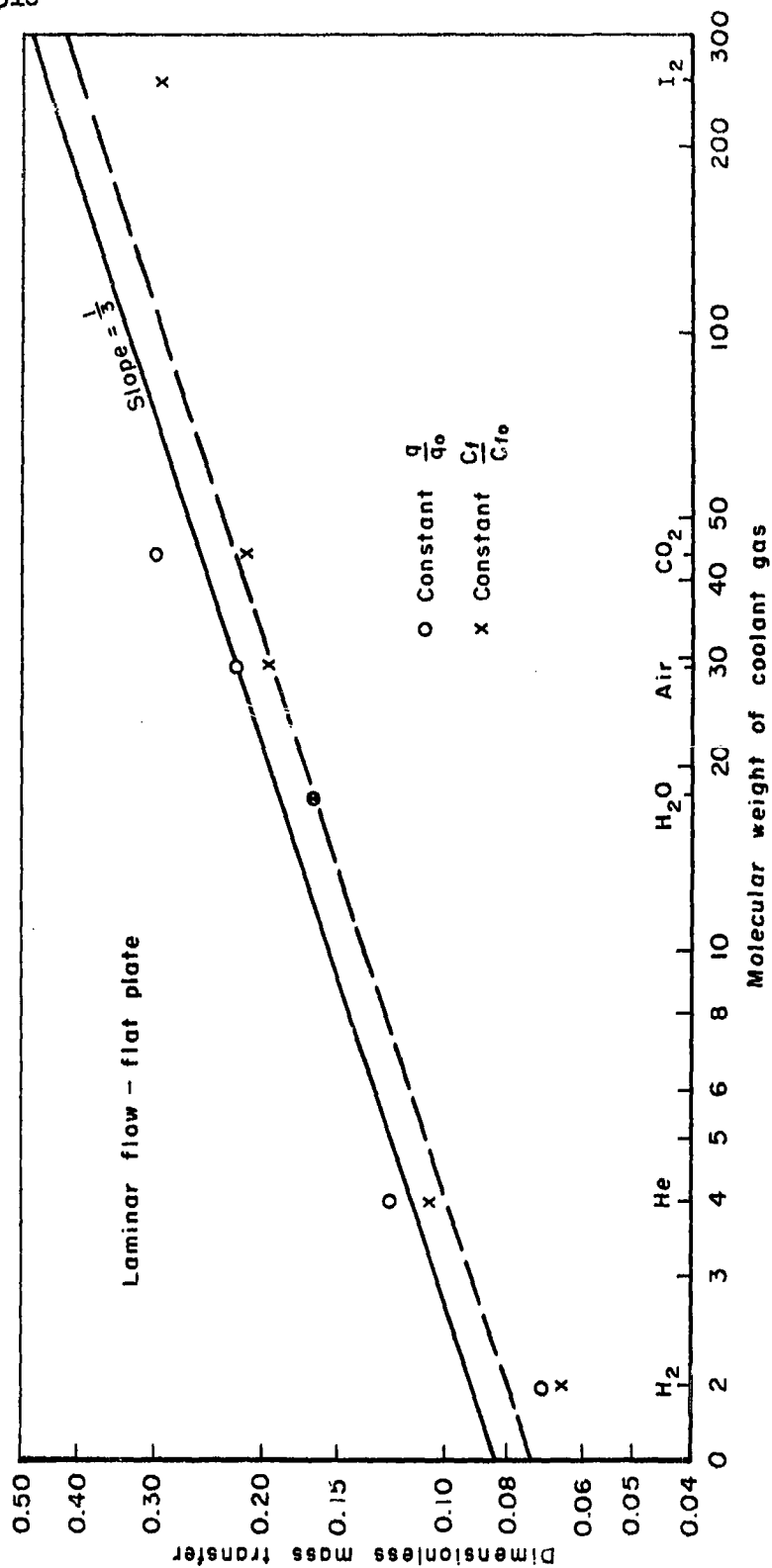


Fig. 23 — Dimensionless mass-transfer parameter
versus molecular weight of coolant gas

V. EFFECT OF PRESSURE GRADIENT ON LAMINAR
MASS-TRANSFER COOLING

Up to the present time, little effort has been directed to the solution of the binary laminar boundary layer equations with finite pressure gradients. However, a measure of the influence of a pressure gradient on mass-transfer cooling can be obtained by returning to the constant-property boundary layer model with normal injection (air-into-air) since solutions have been reported in this case for wedge-type pressure gradients (i.e., the free-stream velocity is described by $u_e = A x^m$). Examination of these solutions⁽¹⁵⁾ reveals that the presence of a favorable pressure gradient leads to more stable velocity profiles and, consequently, it appears that larger values of the dimensionless mass-transfer parameter, $(\rho_w v_w / \rho_e u_e) \sqrt{Re_x}$, may be obtained without causing transition to turbulence. Furthermore, the skin-friction coefficient remains finite in a favorable pressure gradient, with no apparent failure of the boundary layer equations even for very large mass-transfer rates. However, the heat transfer does decrease to a diminishing value, with the thermal boundary layer being displaced from the wall surface toward the free stream. An example of this skin-friction and heat-transfer behavior is given in Fig. 24 for plane stagnation flow ($m = 1$), and it may be seen that the heat transfer goes to zero at a value of the mass-transfer parameter of approximately 2 (as contrasted to 0.619 for the flat plate), while the skin friction is still approximately 40 per cent of its solid-wall value.

A direct comparison of the reduced heat flow, q/q_0 , for four

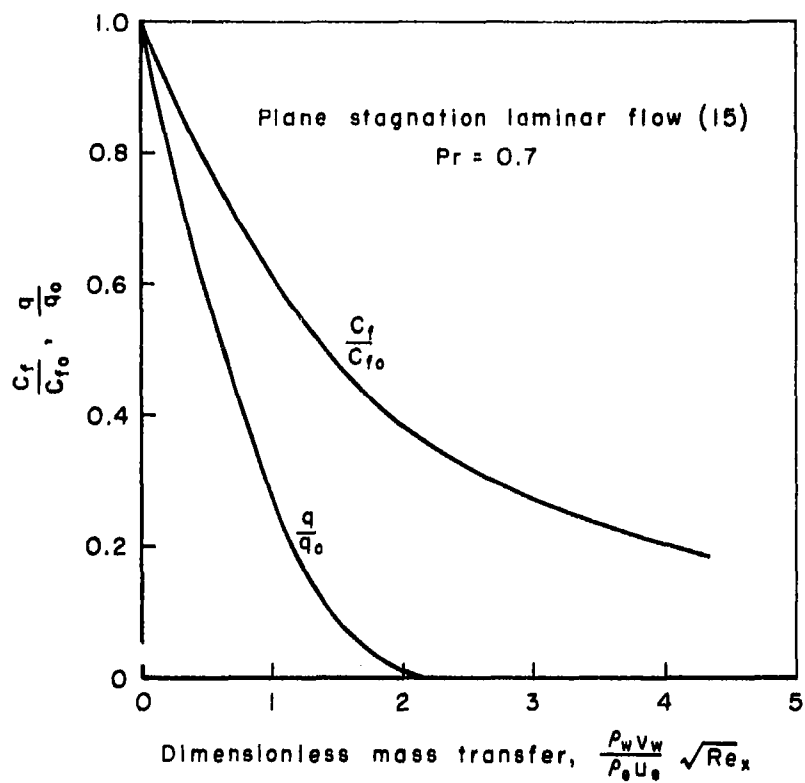


Fig. 24 — Effect of air injection on heat transfer and skin-friction coefficient

different pressure gradients ranging from the zero pressure gradient flat plate to the plane stagnation flow is given in Fig. 25. If a comparison is made at a fixed value of the dimensionless mass-transfer parameter, it is apparent that the greatest reduction in heat transfer occurs for the zero pressure gradient flat plate with the least reduction accompanying the plane stagnation flow. Therefore, to obtain a given reduction in heat flow, q/q_0 , it is necessary to go to higher values of the dimensionless mass transfer as the pressure gradient increases. Since there exists considerable interest in the three-dimensional stagnation flow, Fig. 25 also presents the reduced heat transfer q/q_0 for air injection into such a region⁽¹⁶⁾.

It finally remains to determine whether the relative position of the various coolant gases found for the flat plate geometry is markedly influenced by the presence of a pressure gradient. A recent analysis by Hayday⁽¹⁷⁾ for hydrogen injection into a plane stagnation flow leads to the results shown in Fig. 26 and close inspection suggests that the molecular weight parameter found for the flat plate, i.e. $(m_2/m_1)^{1/3}$, is approximately valid for the plane stagnation flow.

As a result, it is suggested that air-into-air results be used to predict the effect of pressure gradient on laminar mass-transfer cooling; if a coolant other than air is transferred into the boundary layer the relative effectiveness of the various coolants is to be estimated from the flat-plate results. This is simply accomplished by using Fig. 25, changing the abscissa to read $\left[(\rho_w v_w / \rho_e u_e) (\sqrt{Re_x / G^*}) (m_2/m_1)^{1/3} \right]$.

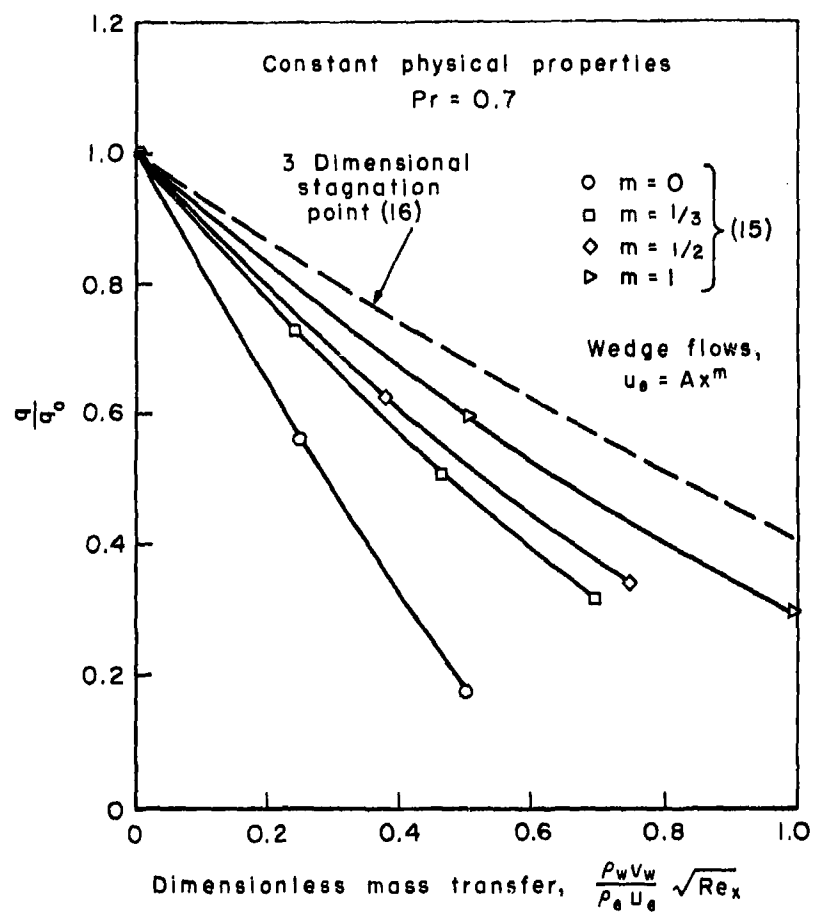


Fig. 25 — Effect of pressure gradient on mass-transfer cooling

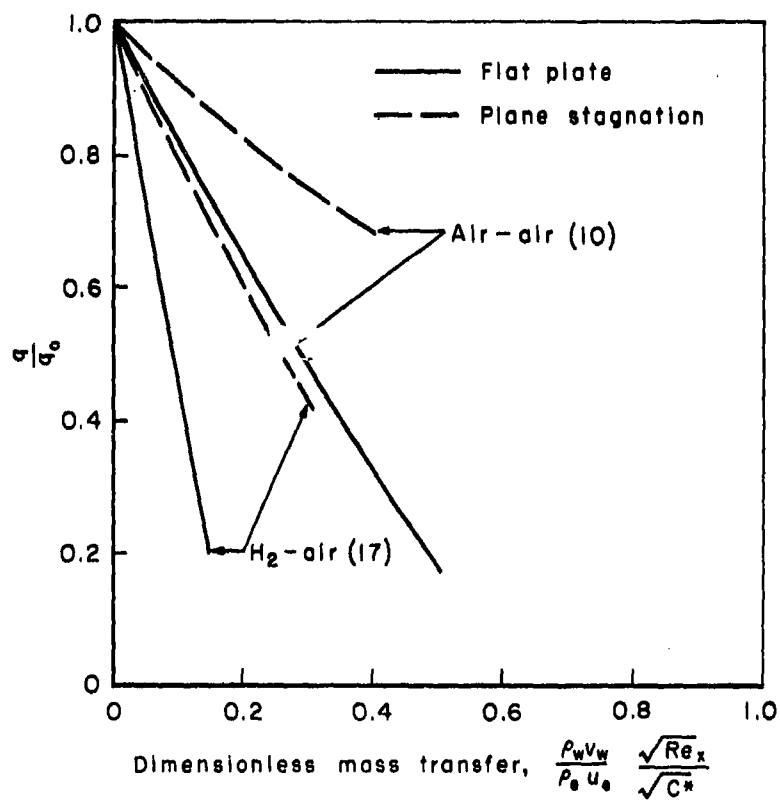


Fig. 26 — Effect of pressure gradient
on mass-transfer cooling

VI. STABILITY OF THE LAMINAR BINARY BOUNDARY LAYER

THEORETICAL STUDIES

The Tollmien-Schlichting theory of small disturbances has been widely used to investigate the stability characteristics of laminar boundary layers on solid surfaces and recently has been applied to binary boundary layers. Essentially, this theory is a perturbation analysis of the Navier-Stokes equations. Secular relationships between the coefficients of the linearized perturbation equations define a region in which disturbances of a given wave length are damped or excited. A damped disturbance suggests that eventually turbulence will occur.

Lin and Lees⁽¹⁸⁾ have presented a stability analysis for a single-component, compressible, boundary layer flow over a flat plate. The computational effort required to define the coefficient relationships is rather formidable. Consequently, some approximations have been suggested by Lin⁽¹⁹⁾ for the incompressible flow case and by Lees⁽²⁰⁾ for the compressible flow case which will be adequate to predict the minimum critical Reynolds number below which the Tollmien-Schlichting disturbances of all wave lengths are damped; hence, the flow should be stable for Reynolds numbers below this value.

The simplified Lin approach yields the following criterion for determining the minimum critical Reynolds number:

$$\left[Re_{min} \right]_{\delta^*} = 25 \frac{d(u/u_e)}{d(y/\delta^*)} \left(\frac{u_e}{u_1} \right)^4 \quad (24)$$

where

$$\delta^* = \int_0^{\infty} \left(1 - \frac{\rho u}{\rho_e u_e}\right) dy$$

where u_1 is determined by examining the specific laminar velocity profile which applies to the conditions under investigation; u_1 is that local velocity existing at the position, y , such that the following equation is satisfied:

$$0.58 = \pi \left(\frac{du}{dy}\right)_w \left[\frac{2(du/dy)_w y_1}{u(y_1)} - 3 \right] \left[\frac{u(y_1) (d^2u/dy^2)_{y_1}}{(du/dy)_{y_1}^3} \right] \quad (25)$$

Recently Gross has suggested that the Lin equations (24) and (25) be utilized as a first approximation for predicting instability in a binary laminar boundary layer.⁽⁸⁾ A comparison of the predicted minimum Reynolds number for relative destabilizing effect should indicate direction insofar as the different injection materials are concerned. In the application of Lin's single component approximation to a binary system, an isothermal boundary layer was assumed. Furthermore, the amount of the injected material was considered to be so small that (a) the boundary layer assumptions were not invalidated, and (b) the effects of the injected material would influence the solution only in the variation of the property parameters. Essentially, this means that the disturbance equations for the velocity and concentration are independent. The velocity and density profiles found by solving the momentum and diffusion equations were substituted into Eqs. (24) and (25) yielding the results shown in Fig. 27. It is apparent that in an isothermal binary boundary layer, injection of any material will be destabilizing,

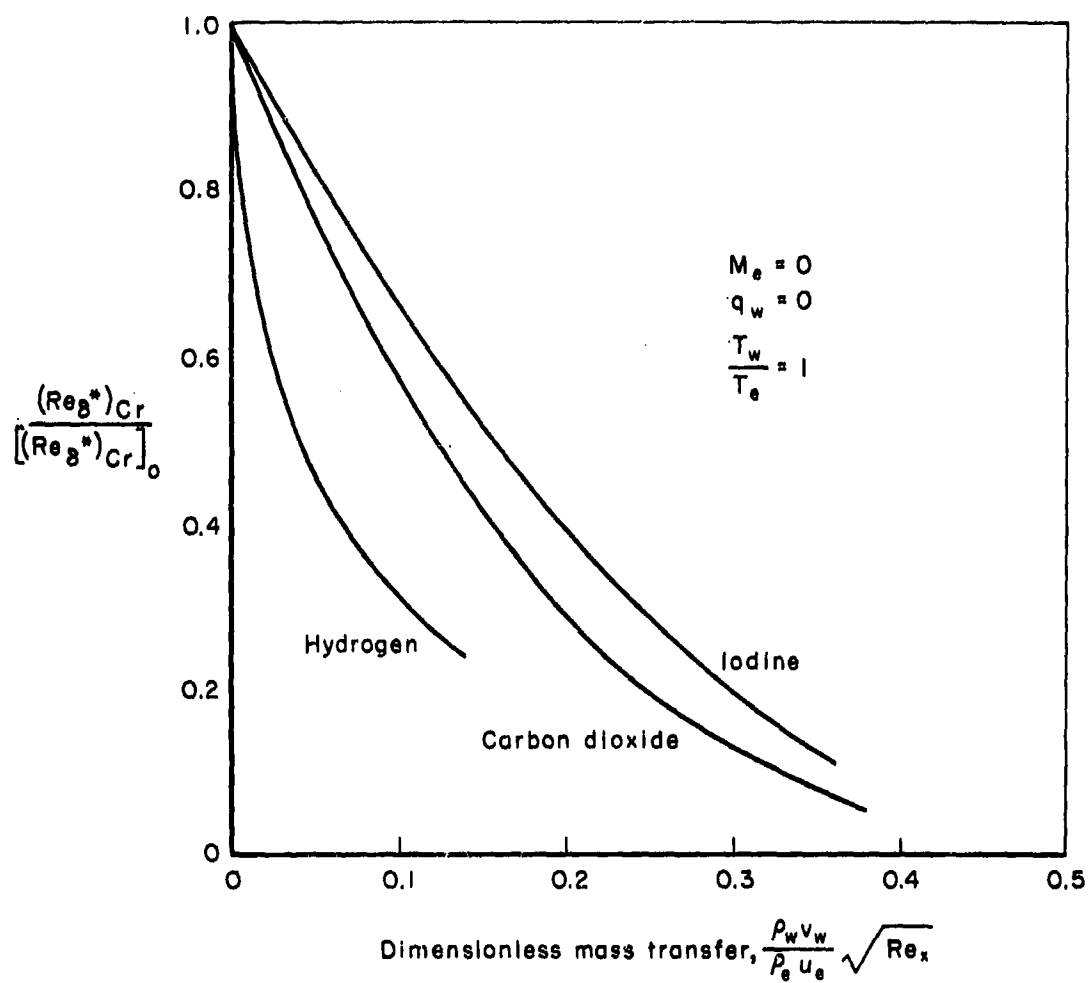


Fig. 27—Effect of mass transfer on the minimum critical Reynolds number

but this effect tends to decrease as the molecular weight of the material increases. The hydrogen, then, appears to be more destabilizing than the heavier gases, carbon dioxide and iodine. This is the result primarily of the higher velocity necessary to supply the low density gas in sufficient amounts to satisfy the blowing parameter relationship. The injection of hydrogen at the wall is somewhat analagous to heat transfer from the wall in that it reduces the density in the neighborhood of the wall. This density reduction encourages a corresponding decrease in the skin-friction coefficient. It has been shown in earlier sections that hydrogen is the most effective agent for mass-transfer reduction of heat transfer and skin friction. It is, however, also the most destabilizing. Iodine vapor and carbon dioxide, which are less efficient in reducing heat transfer and skin friction, show much less destabilizing action. As the first approximation, Fig. 27 may be used in conjunction with Fig. 22 to determine the optimum injectant to effect a given wall temperature condition while maintaining a maximum stability. A study is now under way to obtain some very accurate compressible multi-component boundary layer information which will be acceptable for a more rigorous stability analysis.

The more complex problem of the compressible, binary, boundary layer flow has been treated by E. E. Covert⁽²¹⁾ using a Tollmien-Schlichting perturbation analysis. He showed that the perturbation equations may be solved in exactly the same manner as for a single component gas except for the implicit effects of the foreign gas on the local flow properties, thereby justifying the approach of Gross.⁽⁸⁾ This procedure holds for relatively small injection rates, where the boundary layer assumptions are still valid. Covert found that the stability

characteristics could be calculated for an n-component boundary layer using the steady-state velocity and density profiles. For a given range of Mach number, one may establish a boundary layer completely stable to two-dimensional subsonic disturbances simply by cooling the surface. Covert calculated values of the wall temperature required for complete stability over a range of Mach numbers with the mass-transfer rate as another parameter (see Fig. 28). It should be noted that his calculations are based on the solution of the inviscid disturbance equations. Helium, carbon dioxide, and air injection were considered.

In general, it may be noted for all three injectants that an increase in the injection rate normally results in lower surface temperatures at the re-entry speeds of present day interest. This decrease in the surface temperature tends to stabilize the laminar boundary layer. This should be particularly true for the injection of heavy molecules since these will result in the same effect as cooling on a solid wall, namely increasing the density near the surface. However, it is obvious that the act of injection introduces a disturbance in the boundary layer by decelerating the flow. This will certainly be destabilizing at high injection rates. Therefore, we may expect a counterbalancing of stabilizing and destabilizing effects. The net result will depend upon the efficiency of the injected material in cooling the boundary layer. Figure 29 shows the minimum temperature ratio for the injection of helium as a function of Mach number with the dimensionless mass transfer rate as a parameter as determined by Covert. It is indeed so that for a Mach number below 3.5, the injection of this light gas reduces the stability character of a single component layer.

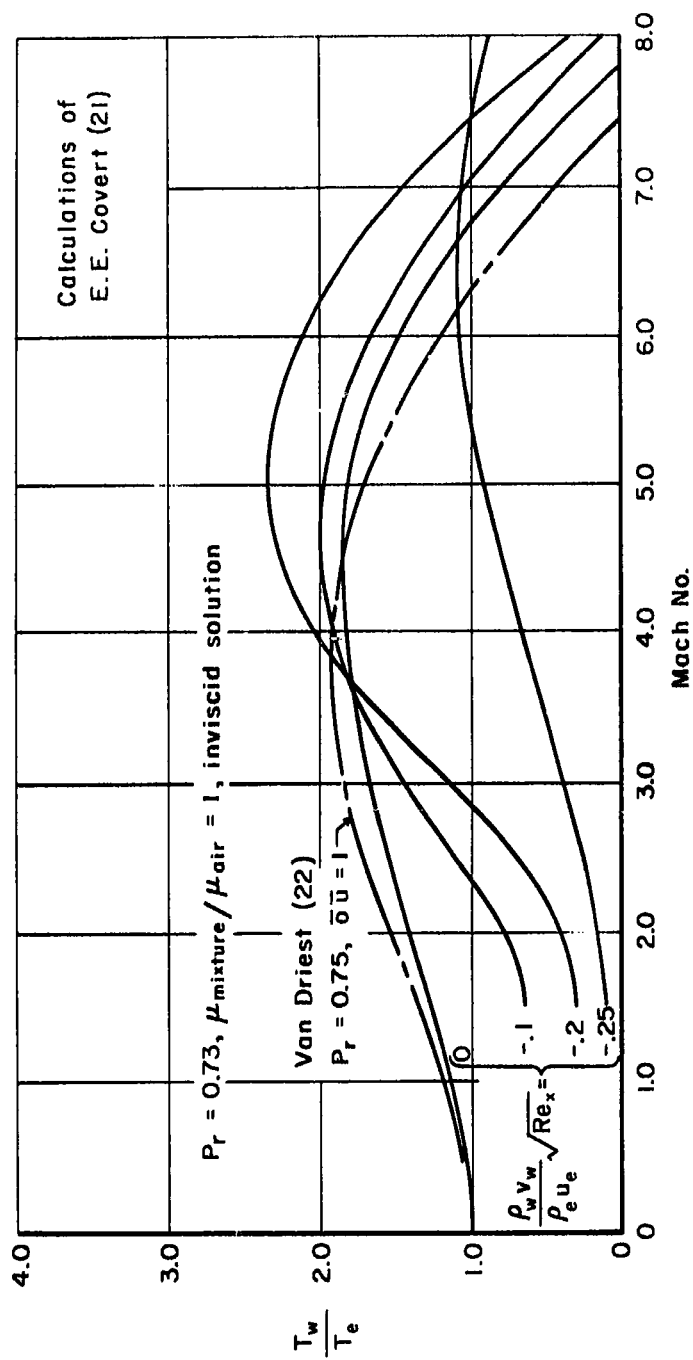


Fig. 28—Effect of helium injection on cooling required for complete boundary layer stability

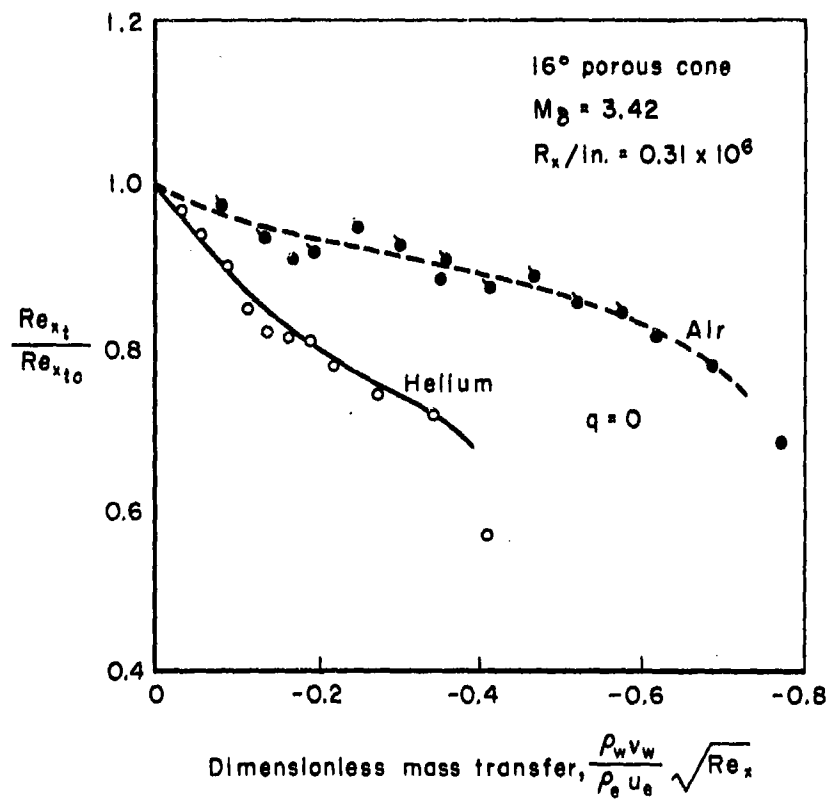


Fig. 29—Effect of mass transfer on boundary layer transition⁽²⁴⁾

However, as the Mach number increases, the adiabatic wall temperature rises very rapidly causing a high enthalpy region near the wall. The helium with its high specific heat injected into the hot boundary layer acts as a coolant decreasing the enthalpy near the wall, and the overall effect is to increase the minimum wall temperature ratio. An interesting conclusion of Covert is that no amount of air or carbon dioxide injection will increase the minimum temperature ratio. This agrees with the result shown previously by the isothermal Reynolds number calculations.

EXPERIMENTAL STUDIES

Sziklas and Banas⁽⁷⁾ have reported results of experimental work with a 7-inch 17-deg apex angle porous cone operating at Mach 2.6. The injected coolants were helium and air. Velocity profiles at various injection rates are given. The helium data for $(\rho_w v_w / \rho_e u_e) \sqrt{Re_x} \leq 0.08$ indicated profiles which agreed with theoretical calculations, but at a value of 0.14 this agreement was no longer true and the profile was transitional. The corresponding case for air showed agreement up to $(\rho_w v_w / \rho_e u_e) \sqrt{Re_x} = 0.02$, but the last injection rate again gave a transitional profile. These results indicate that mass injection rates of sufficient magnitude to produce significant cooling effects do not show a pronounced tendency toward turbulence.

Leadon, Scott, and Anderson⁽²³⁾ used a 20-deg angle cone at a Mach number of 5. The injectants were helium and air. The non-ideal permeability (and consequent use of a modified blowing parameter) of the model and large scatter in the data make interpretation difficult. Nevertheless, it was shown that the heat-transfer results of the porous

model (zero blowing) were quite similar to those for a smooth model. The transition Reynolds number with zero blowing ($\sim 2.5 \times 10^6$) on the porous model was about half as large as that for a similar smooth model. Finally, the authors point out that the boundary layer was quite stable to air and helium injection.

Scott, Anderson, and Elgin⁽²⁴⁾ have made measurements on the effects of helium and air injection on boundary layer transition on a 16-deg porous cone model at a Mach number of 3.7. They determined transition position with the use of shadowgraph photographs. The dimensionless transition Reynolds number was plotted against the corresponding value of the injection parameter, as shown in Fig. 29. The percentage decrease of Re_t/Re_{t0} is not large for injection rates which produce significant cooling effects. In addition, the order of the mass-transfer rates and the rate of decrease between helium and air is similar to the isothermal theoretical results obtained earlier.⁽⁸⁾

VII. MASS-TRANSFER COOLING IN A TURBULENT BOUNDARY LAYER

Unlike laminar flow, it is not possible to solve rigorously the governing equations for turbulent binary boundary layer flow in a direct manner. Rather, a variety of indirect approaches have been suggested ranging from the simple film theory to more complex mixing length analyses. The simple film theory or Couette flow model conceptually replaces the actual boundary layer by a film of constant thickness, neglecting any variations in the flow direction as compared with those across the film.^(25, 26) Although this approach does not yield all details of the flow, it does predict the over-all effect of mass transfer on skin friction and heat transfer quite well. More detailed mixing length analyses which require empirical data to accomplish a final solution have been advanced for air injection by Dorrance and Dore,⁽²⁷⁾ Rubesin,⁽²⁸⁾ and van Driest.⁽²⁹⁾ The first two references are applicable to the flat plate geometry, with Dorrance and Dore restricting their analysis to a Prandtl number of unity and assuming the turbulent boundary layer extends down to the surface. The analyses of Rubesin apply to a Prandtl number of 0.7, consider viscous dissipation, and allow for a laminar sublayer and a turbulent core. The incompressible analysis of van Driest considers the laminar sublayer and turbulent core using somewhat different assumptions than those of Rubesin for the flat-plate geometry, but in addition, van Driest extends the analysis to apply to air injection into a turbulent boundary layer in the region of either a two-dimensional or three-dimensional stagnation point. The results of Rubesin and van Driest are essentially in agreement with each other for the flat-plate

geometry and are somewhat higher than the prediction of Dorrance and Dore.*

A number of experimental results are reported for air injection into a turbulent boundary layer on zero pressure gradient surfaces, (26, 31-35) thereby providing a check on the above predictions. Figure 30 compares the available heat-transfer results in the form of Stanton numbers with the several analyses. It may be seen that the three analyses do not differ very markedly although Dorrance and Dore are somewhat lower. The experimental data covering a range of Mach numbers from 0 to 3 show considerable scatter but nevertheless the trend is correctly predicted by all three analyses. Similar results for skin friction are shown in Fig. 31 and the bulk of the data tend to agree with the prediction of Rubesin and van Driest. The only conflicting evidence is the experimental data of Mickley and Davis (35) which show skin-friction values much lower than the other investigators -- even lower than predicted by the film theory. Since the majority of the experimental data favor Rubesin and van Driest, it appears at the present time that this represents the more realistic and certainly the more conservative estimate of skin friction and heat transfer in the presence of air injection.

The effect of pressure gradient on heat transfer and skin friction in the presence of mass transfer in turbulent flow is apparently minimized when the results are presented in the coordinates shown in Figs. 30 and 31. The analysis of van Driest indicates that the same

*Dorrance discusses this discrepancy which arises from the form he assumes for his velocity distribution. (30)

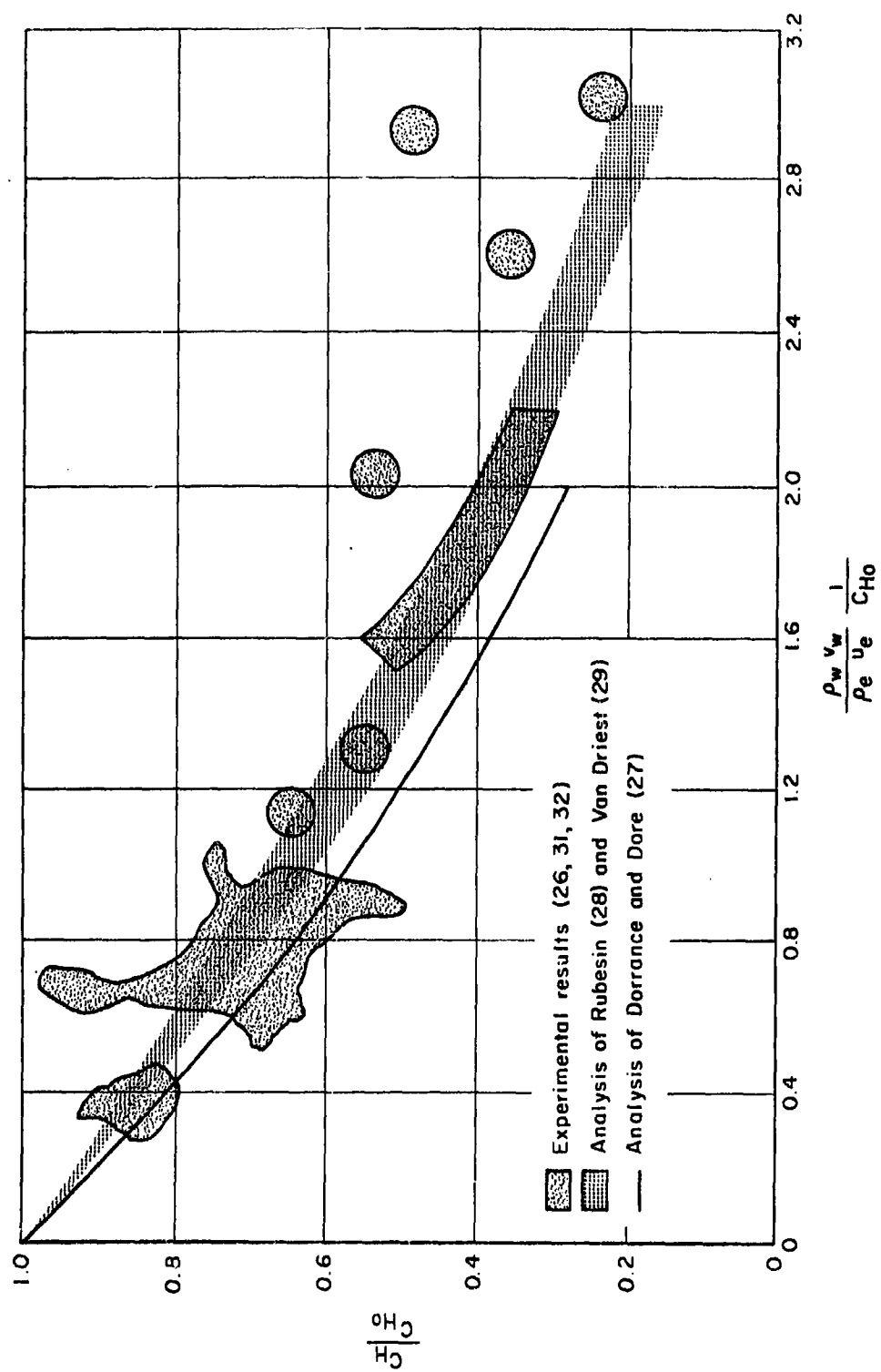


Fig. 30 — Effect of mass transfer on heat transfer, turbulent flow

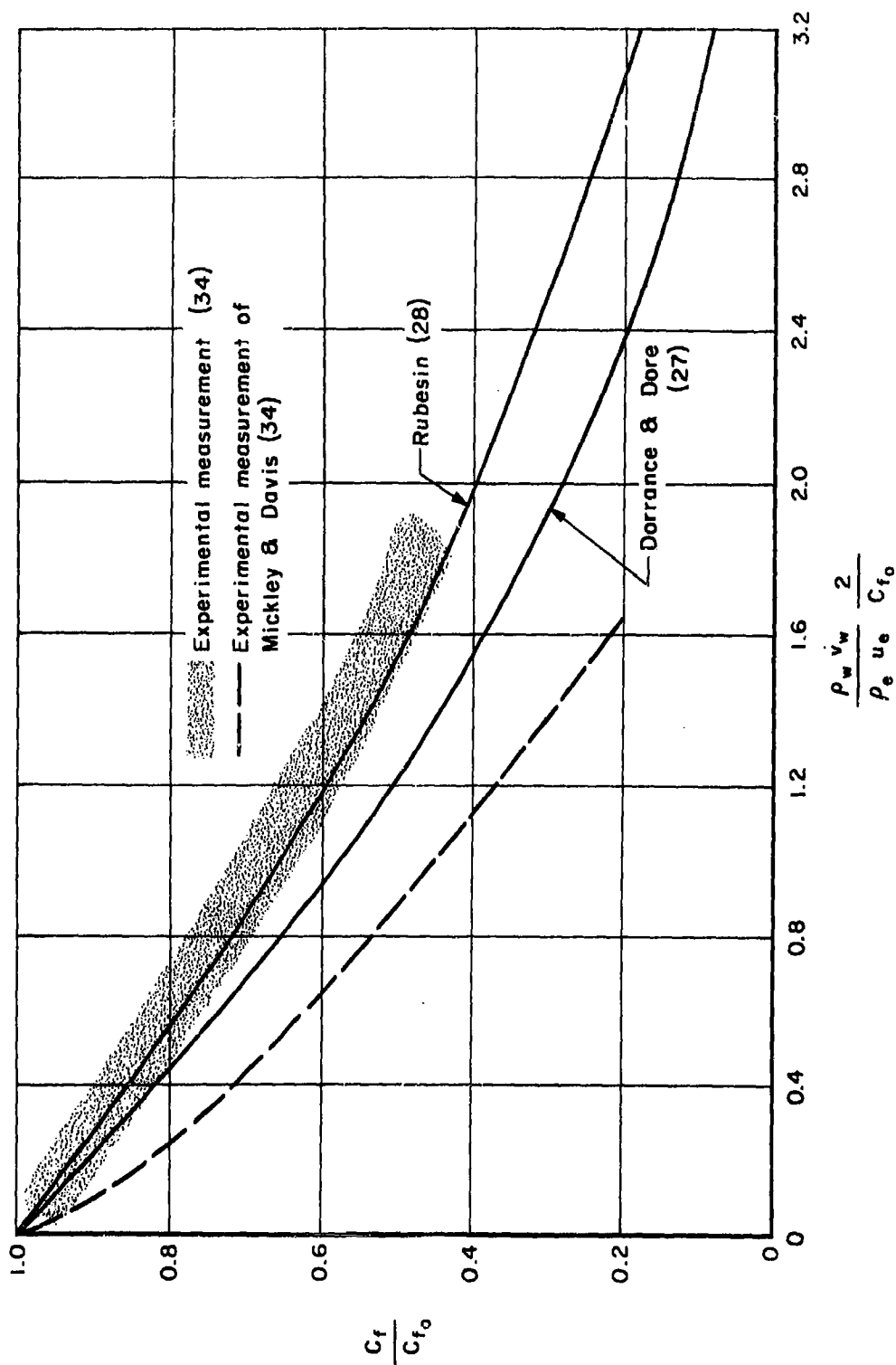


Fig. 31—Predicted and measured skin friction for air injection into a turbulent boundary layer on a flat plate

curve shown for the flat plate may also be used for turbulent flow in the region of two- and three-dimensional stagnation points.

The calculation of heat transfer requires the knowledge of the recovery factor in addition to the above-cited Stanton number. The theory of Rubesin predicts that there is no effect of air injection on the recovery factor for turbulent flow. However, this is in disagreement with experimental evidence.^(31, 32, 33) Since some of the assumptions used in the analysis of Rubesin have not been confirmed, greater weight must be given to the experimental results. These are summarized in Fig. 32 and the curve drawn through the data may be used as a guide in predicting the recovery factor for air injection into a turbulent boundary layer.

For foreign gas addition to a turbulent boundary layer on a flat plate, the skin-friction results of Pappas⁽³⁶⁾ and Ward and Harmon* are available and are represented in Fig. 33. These predictions, valid for low Mach numbers, demonstrate the advantage of the lightweight gases, helium and hydrogen, in reducing skin friction. The heavier gases, freon and teflon, are obviously less effective in reducing skin friction, but surprisingly their performance is not appreciably poorer than that of air.

For heat transfer, the mixing length analysis of Rubesin and Pappas⁽³⁷⁾ predicts the performance shown in Fig. 34 for light-gas injection into a turbulent air boundary layer on a flat plate. The limited available experimental data for helium-air^(31, 38) suggest an even greater reduction than predicted by the analysis. The predicted recovery factor shows no change from the solid wall value when light

*T. E. Ward and D. B. Harmon, personal communication, March 1959.

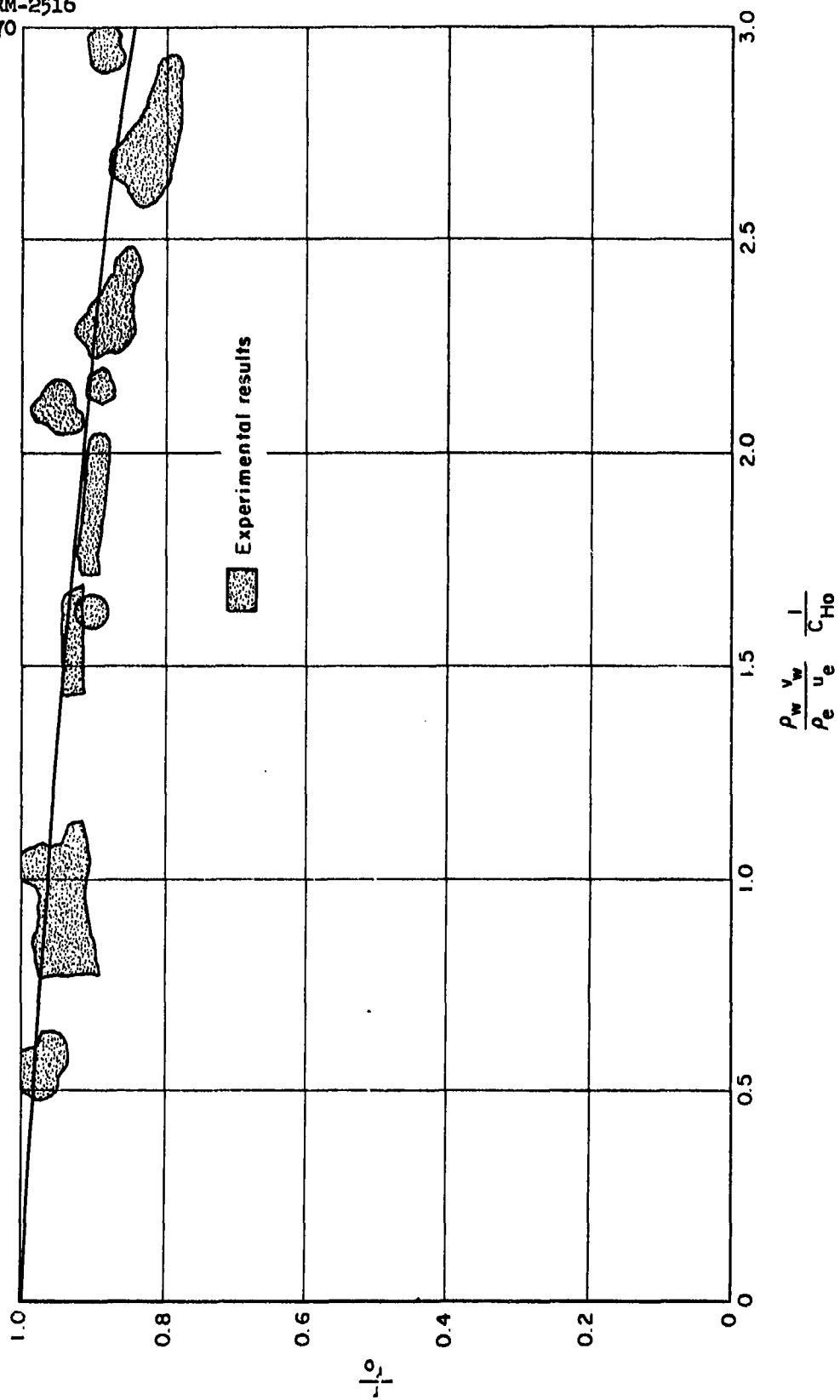


Fig. 32 — Recovery factor for air injection into turbulent boundary layer on a flat plate (31, 33)

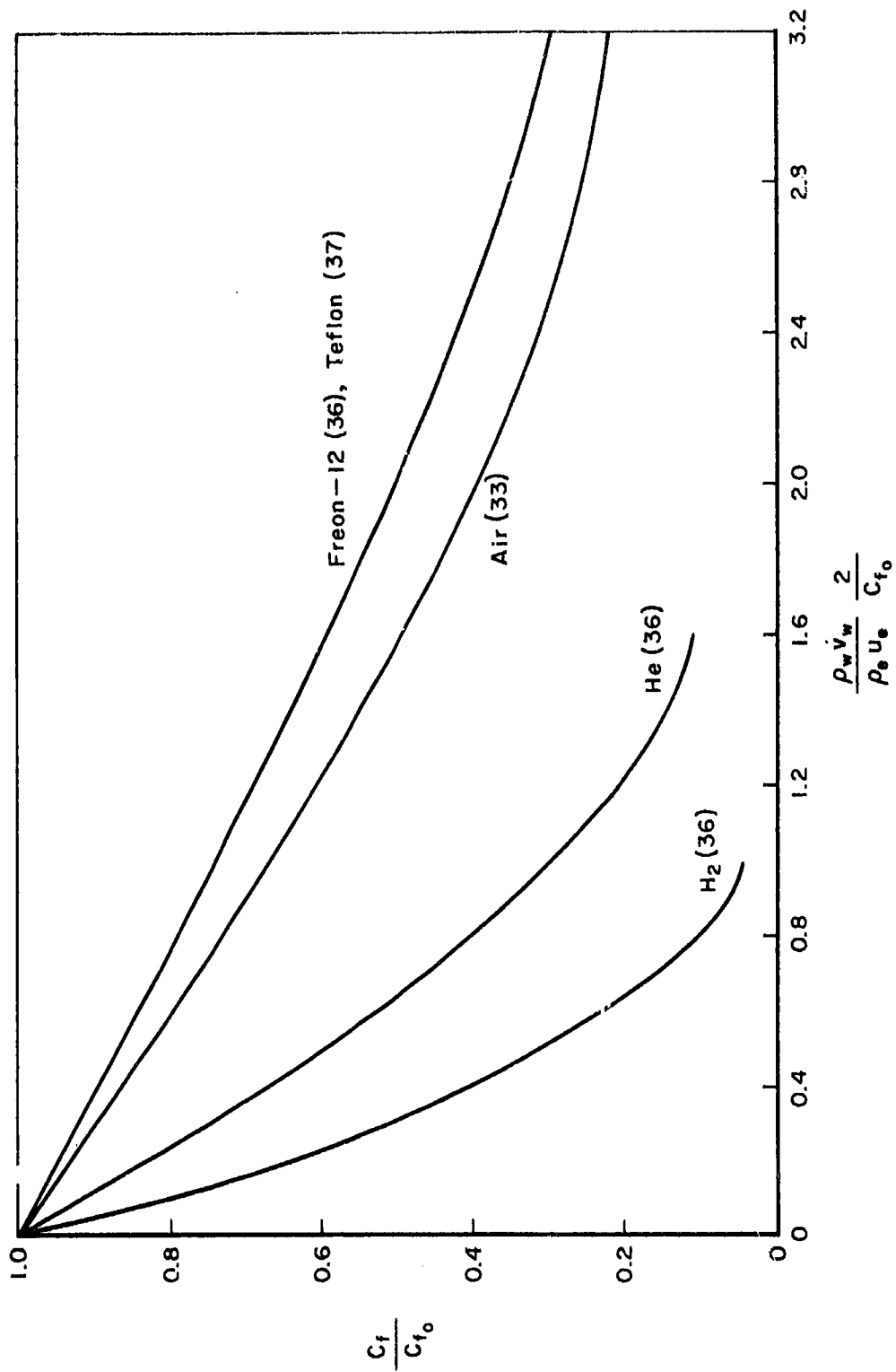


Fig. 33— Prediction of skin friction for foreign gas injection into a turbulent air boundary layer on a flat plate

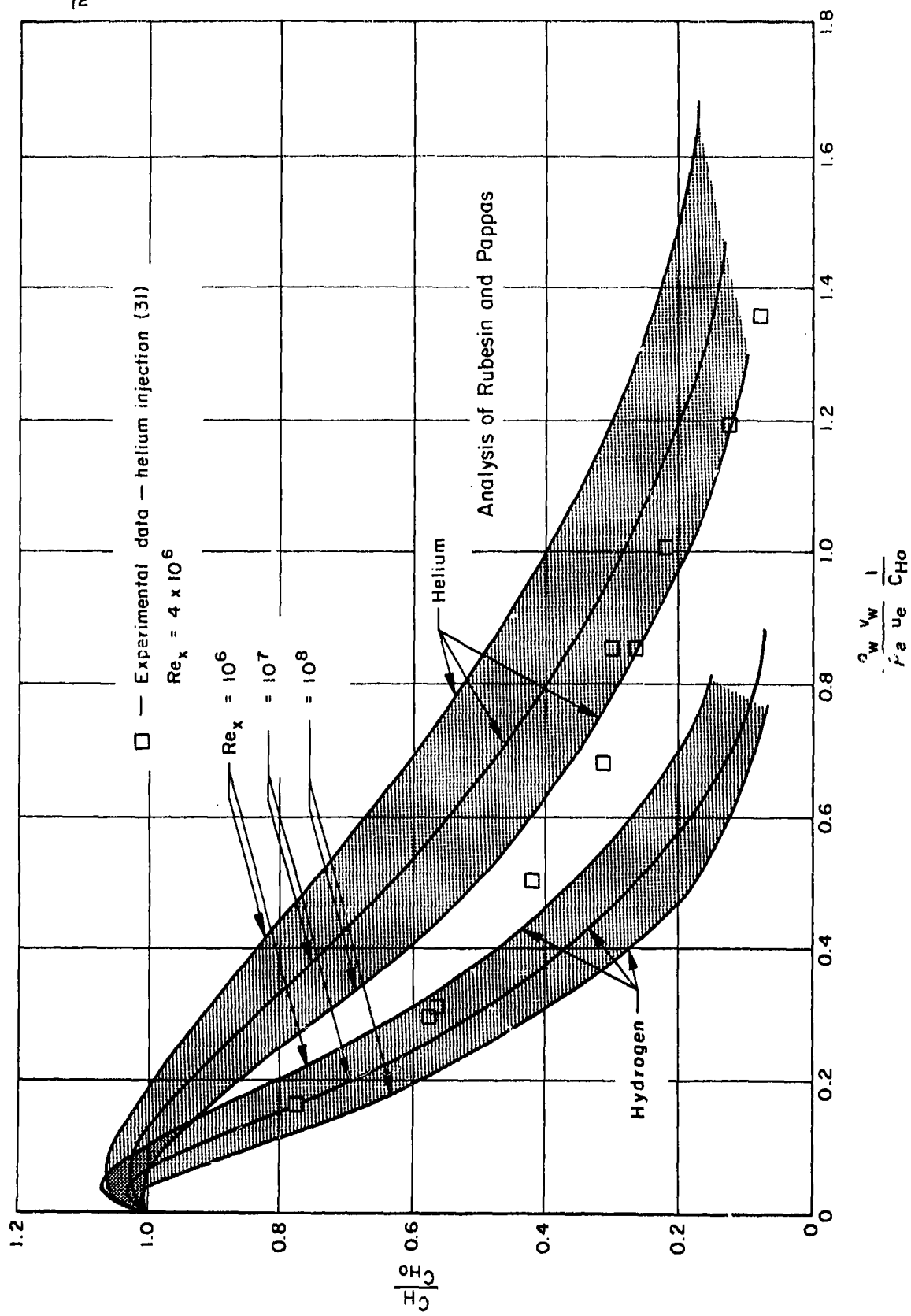


Fig. 34 — Effect of mass transfer on heat transfer, turbulent flow

gases are injected into a turbulent boundary layer, and at the present time the experimental data are insufficient to justify any definite conclusion.

To determine the influence of molecular weight of the coolant gas on the heat transfer and skin friction, the mass-transfer parameter was plotted against the molecular weight at a constant value of the reduced parameter, c_f/c_{f0} and q_H/C_{H_0} of 0.5. The results are shown in Fig. 35 where it is seen that the molecular weight appears to play a more sensitive role for the light gas, while the heavier gases are less sensitive to this property. An estimate of the reduced skin-friction coefficient and Stanton numbers for other coolants may be obtained from the presentation in Fig. 35.

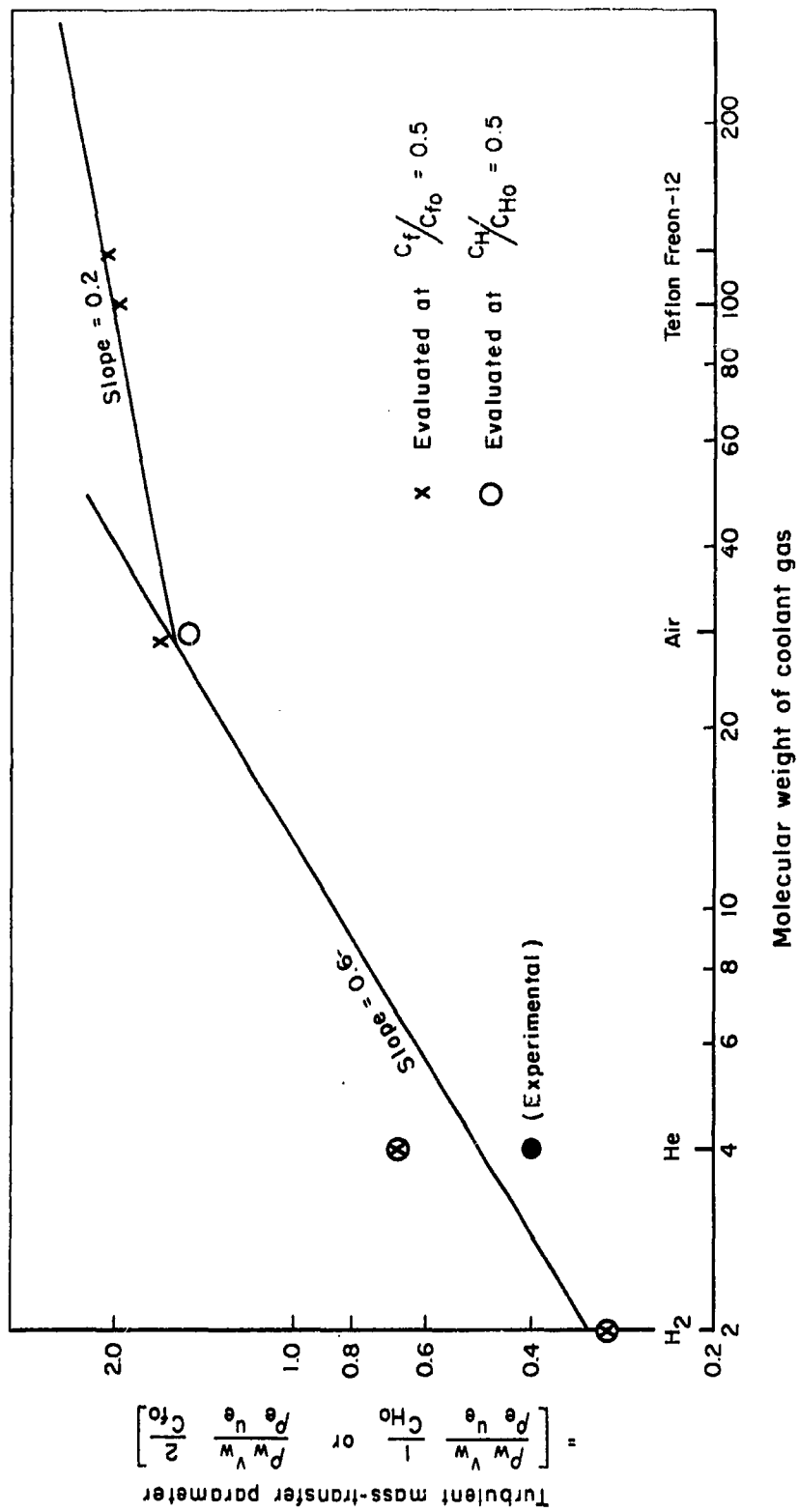
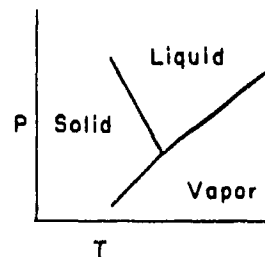


Fig. 35 — Turbulent mass-transfer parameter versus molecular weight of coolant gas

VIII. SUBLIMATION COOLING

Sublimation is defined as the physical change encountered by a substance in passing from the solid to the gaseous phase. It is characterized by the absence of any intermediate liquid phase. Reference to a pressure-temperature phase diagram makes it apparent that sublimation processes occur at relatively low pressures and temperatures. The temperature at which the vapor pressure of the solid equals the total pressure of the gas phase in contact with it is defined as the sublimation point. The snow point is defined as that temperature at which the vapor pressure of the solid is equal to the partial pressure of the substance in the gaseous phase. It is clear then that our interest lies in the snow point and not in the sublimation point. A foreign gas concentration of unity at the surface (i.e., surface at the sublimation point) would imply a blowing rate high enough to blow the boundary layer from the surface. In general, the vapor pressure of the solid material will be a function only of its temperature for equilibrium conditions.



The sublimation-cooling system has already been described briefly in the Introduction. The phase change occurring at the wall imposes an additional restraint on the boundary layer equations in the form of another boundary condition which relates the wall temperature to the concentration of foreign material by the Clausius-Clapeyron equation

$$\frac{Y_w}{\bar{m} - (\bar{m} - 1) Y_w} = \frac{B}{P_e} \exp \left(- \Delta H_s / RT_w \right) \quad (26)$$

Y_w = concentration of sublimating material at the wall

\bar{m} = m_1/m_2

B = constant of integration

P_e = pressure at the edge of boundary layer

ΔH_s = heat of sublimation per mole

R = universal gas constant

The introduction of this boundary condition implies that a set of unique values of the boundary layer functions exist once the external pressure, temperature, Mach number, and the surface material have been specified. Changing the external conditions then automatically defines a new set of functions. Consequently we may regard the subliming systems as self-regulating since the conditions at the wall respond automatically and uniquely to changes in free-stream conditions. The variation of q/q_0 with the mass-transfer parameter for a CO_2 -air mixture is shown in Fig. 22. If we specify that solid carbon dioxide is subliming into a laminar boundary layer with fixed external flow conditions, then only one point on the curve will satisfy all the boundary conditions. Since Baron's parameter correlates the Mach number and wall-temperature effects on the heat transfer, it is possible to approximate the variation of the normalized heat transfer, q/q_0 , with the mass-transfer parameter by a straight-line relationship. This fact coupled with linear approximation to the mass-transfer parameter-wall concentration (see Appendix B) relation and the Clausius-Clapeyron equation will generate a simple

algebraic representation between the wall temperature of a subliming material and the external conditions.

This equation was derived⁽³⁹⁾ and applied to systems in which ice, carbon dioxide, and ferrous chloride are subliming. The results are shown in Fig. 36. The wall temperature is quite insensitive to Mach number. On the other hand, variation in altitude (external pressure) brings about marked changes in the temperature at the surface. The external pressure is in the denominator of the Clausius-Clapyron equation and is quite important in determining the level of the wall temperature. The increased heat load brought about by larger Mach numbers is absorbed by the greater mass-transfer parameter (increased surface sublimation) rather than by large temperature increases. This accounts for the insensitivity to Mach number variation.

Our equations are, of course, dependent on the condition of equilibrium. As the external pressure decreases, the sublimation pressure is reached very quickly and at extremely low wall concentrations. This implies that only very high blowing rates are possible at extreme altitudes. This is not true because different conditions are applicable at high altitudes. As the pressure is reduced, the surface molecules see fewer and fewer air molecules. Consequently, the region over the surface becomes less crowded until a situation is reached where essentially all the molecules which leave the surface escape. In this case the sublimation rate will no longer be limited by diffusion, but will tend toward the absolute rate of sublimation.⁽⁴⁰⁾

$$\dot{m}_x = \alpha p_1 \frac{g_c m_1}{2\pi RT_w} \quad (27)$$

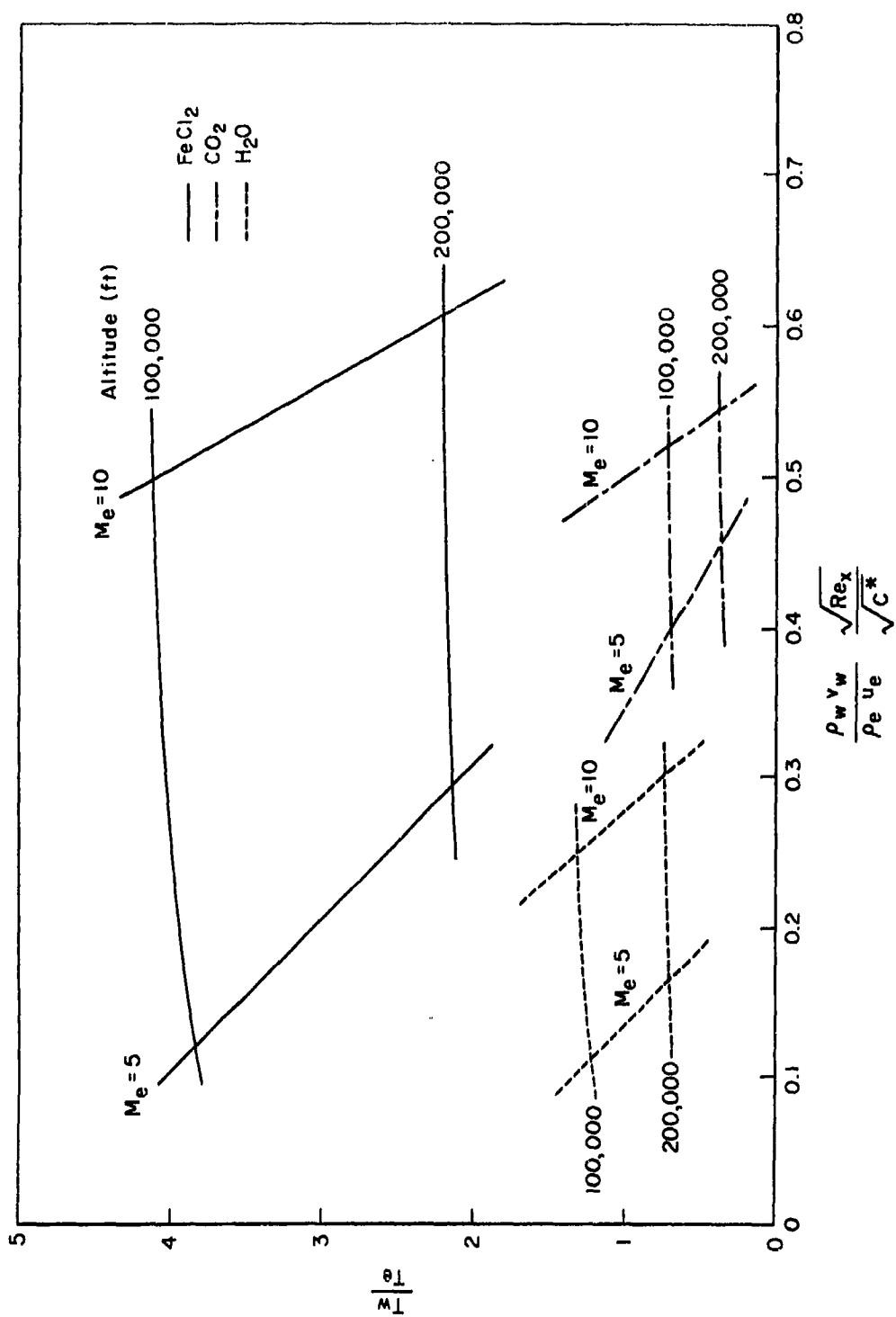


Fig. 36 — Subliming systems: wall temperature versus mass-transfer parameter

g_c = gravitational constant
 α = condensation coefficient

All the quantities here may be calculated with the exception of α , the condensation coefficient. This is usually determined experimentally and it has been found that it is relatively small in the case of polar compounds and close to unity for non-polar materials. The absolute temperature of the surface will also be an important factor for it will determine if a truly "clean" surface exists. For $T = 1000^\circ\text{K}$ we may assume that the absorbed layer is no longer present at extremely low pressures. Therefore the maximum blowing rate we may expect is:

$$\frac{-c_{p1}}{u_e} \sqrt{\frac{g_c m_1 Re_x}{2\pi RT_w}} = \frac{\rho_v W}{\rho_e u_e} \sqrt{Re_x} \quad (28)$$

However, in this case of rarefied flow, the heating rate is no longer affected by the efflux of vapor from the surface. That is, the heating rate is independent of the sublimation rate. The surface temperature and consequently the sublimation rate, however, adjust themselves so as to balance the heat input by heat absorption through sublimation. That is:

$$q = \dot{m}_x \Delta H_s \quad (29)$$

where q is determined by flight velocity and altitude and vehicle geometry.

Appendix A

ADDITIONAL VERIFICATION OF THE DIMENSIONLESS PRESENTATIONS

In this section the reduced skin friction c_f/c_{f0} and heat transfer q/q_0 are plotted as functions of the mass-transfer parameter for all of the injected materials. (Figs. 37,38.) It may be seen that the summary curve given in the main body of the report accurately represents the calculated performance.

Furthermore, the Stanton number and recovery factors are given in detail. (Figs. 39-42.) In the latter case, it is apparent that discrepancies exist in the case of hydrogen-air and helium-air, probably due to the uncertainty in the physical property values under such extreme temperature conditions.

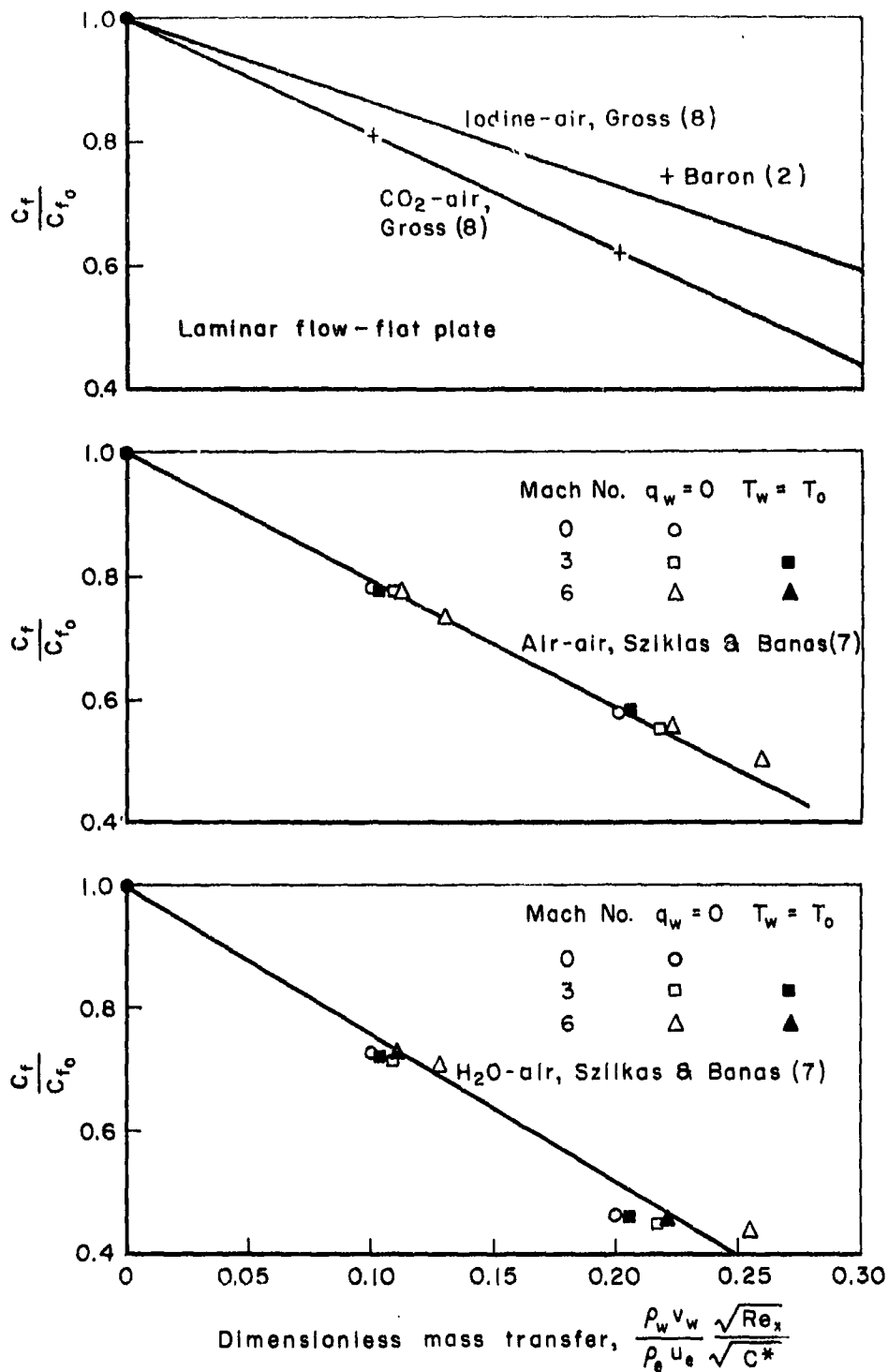


Fig. 37—Effect of mass transfer on skin friction

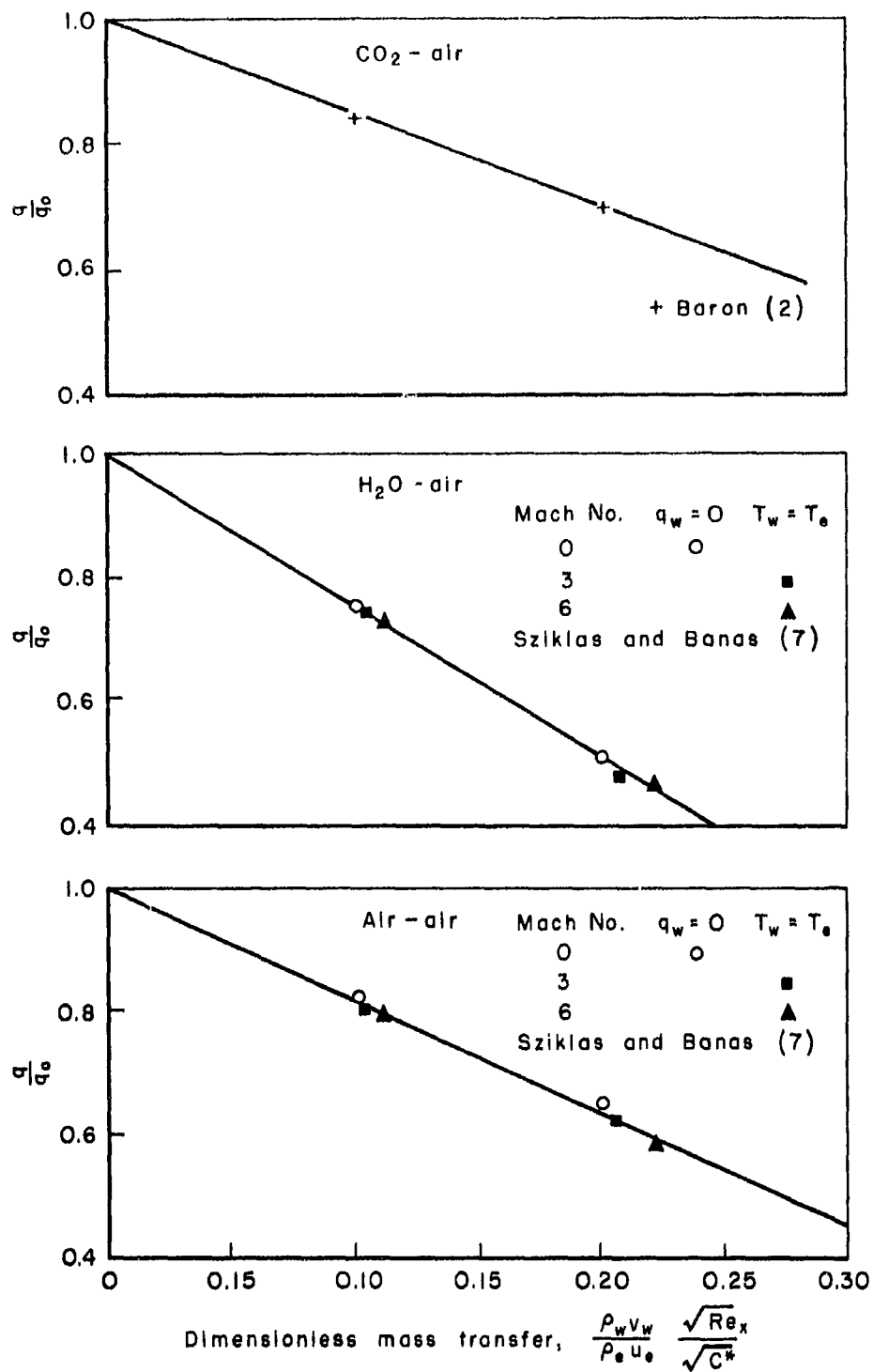


Fig. 38 — Effect of mass transfer on heat transfer

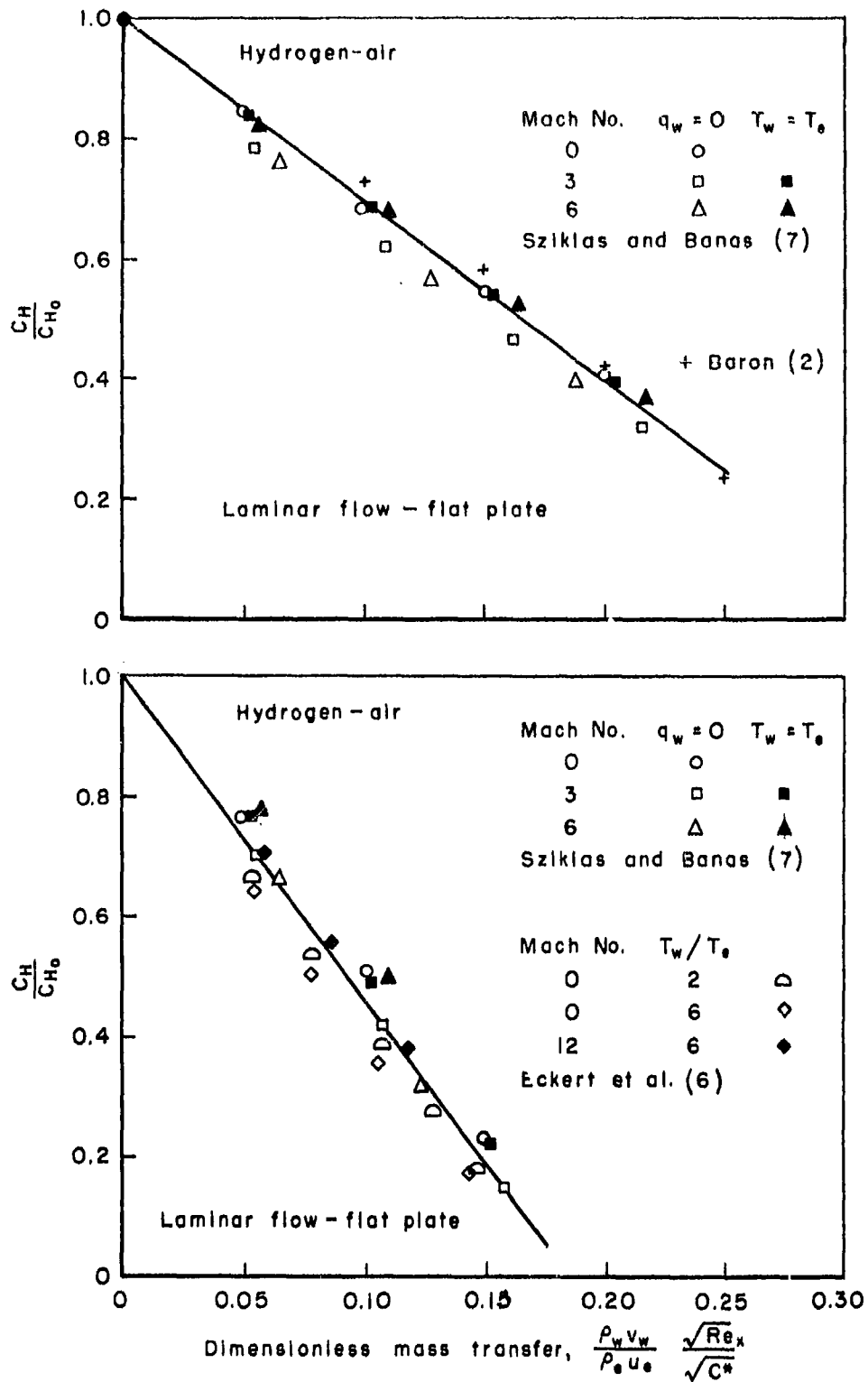


Fig. 39—Effect of mass transfer on Stanton number

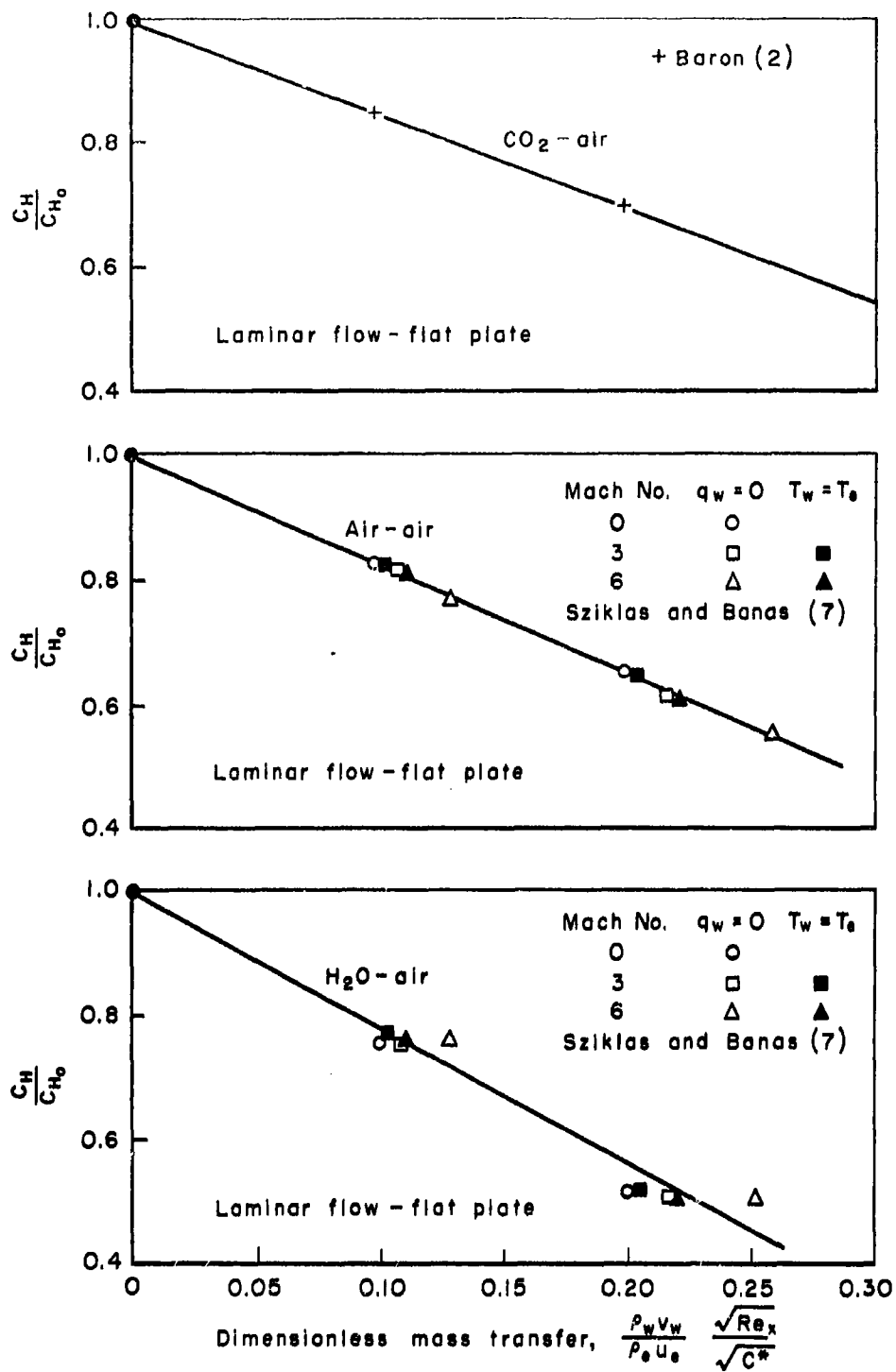


Fig. 40—Effect of mass transfer on Stanton number

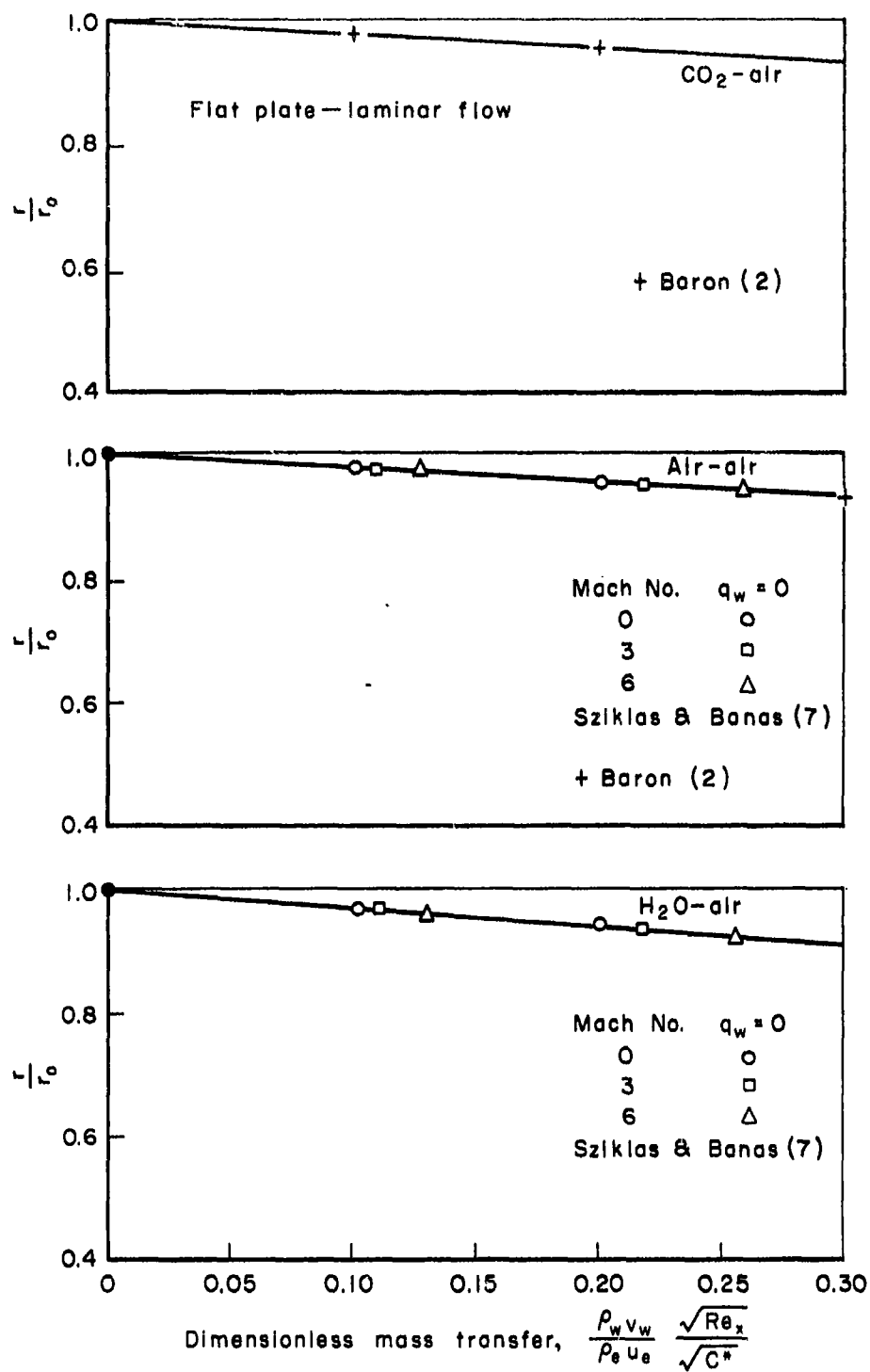


Fig. 41 — Effect of mass transfer on recovery factor

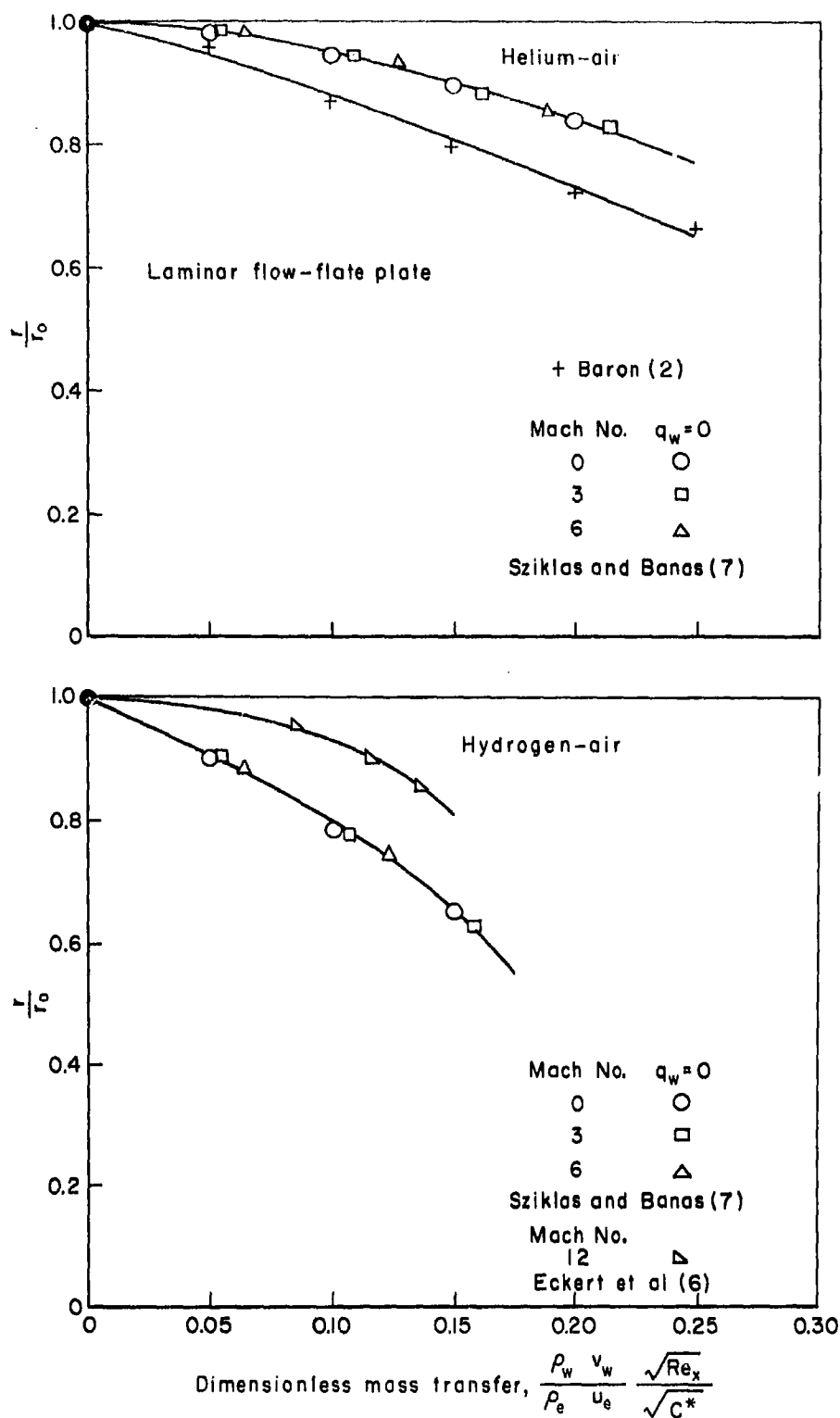


Fig. 42—Effect of mass transfer on recovery factor

Appendix B

RELATION BETWEEN WALL CONCENTRATION AND MASS-TRANSFER PARAMETER

In the treatment of a subliming surface, it is important to know the relationship between the wall mass fraction and the dimensionless mass-transfer rate. A generalized presentation of the wall mass fraction for each gas appears possible with the aid of the Baron variable $(\rho_w v_w / \rho_e u_e) \sqrt{Re_x / C^*}$ and these are shown for some five gases in Figs. 43-46. A summarizing curve is also available in Fig. 46.

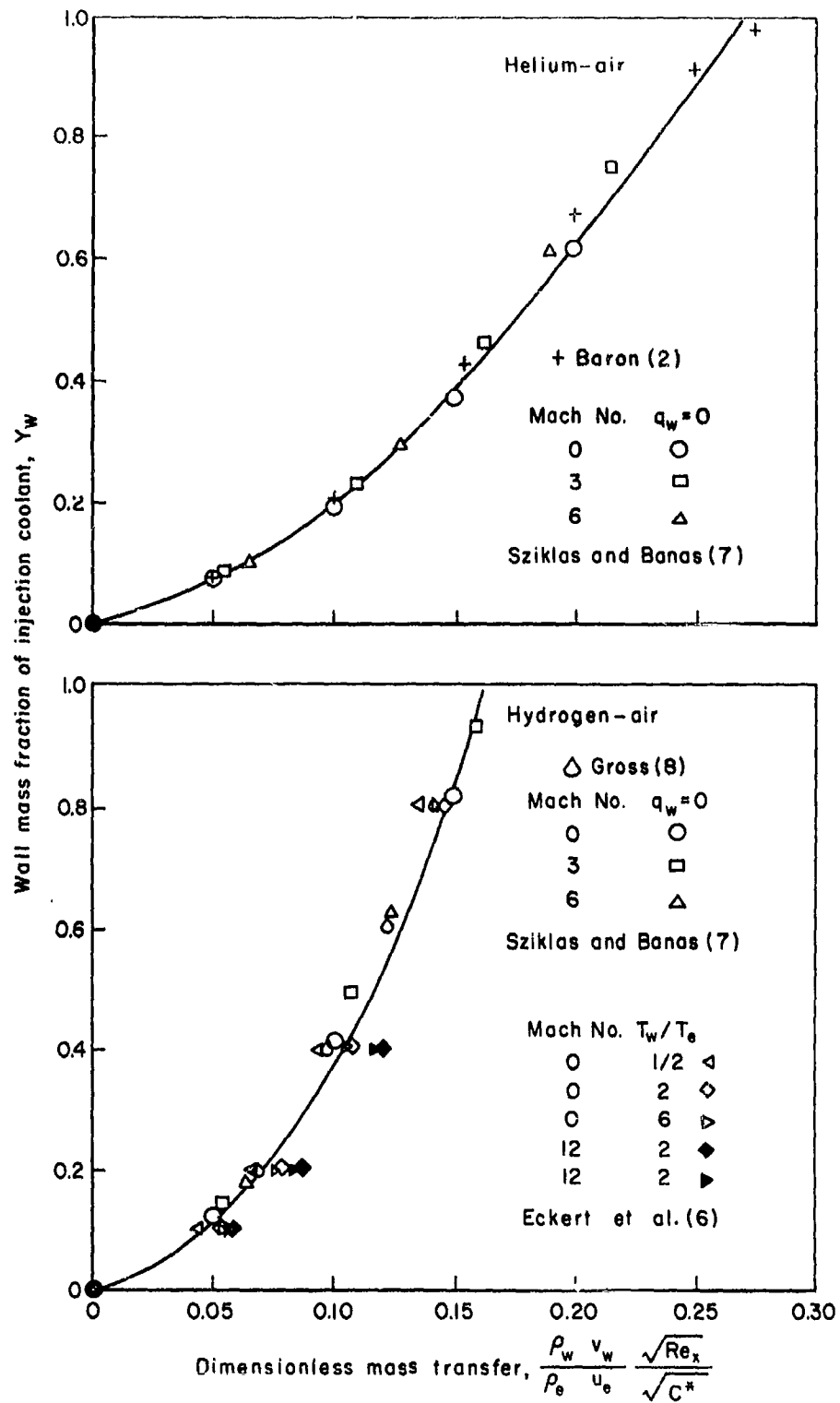


Fig. 43 - Wall mass fraction versus dimensionless mass transfer

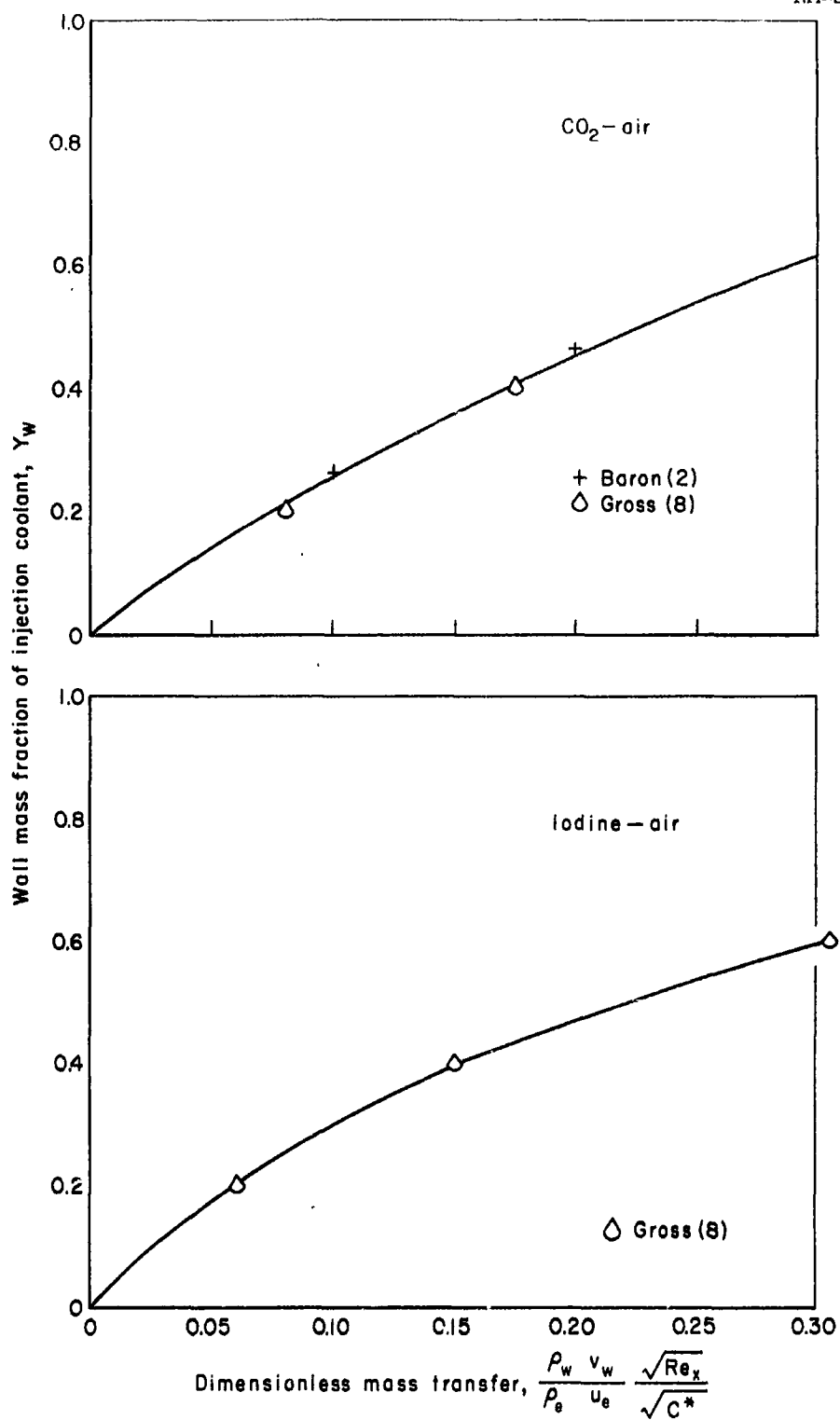


Fig. 44 - Wall mass fraction versus dimensionless mass transfer

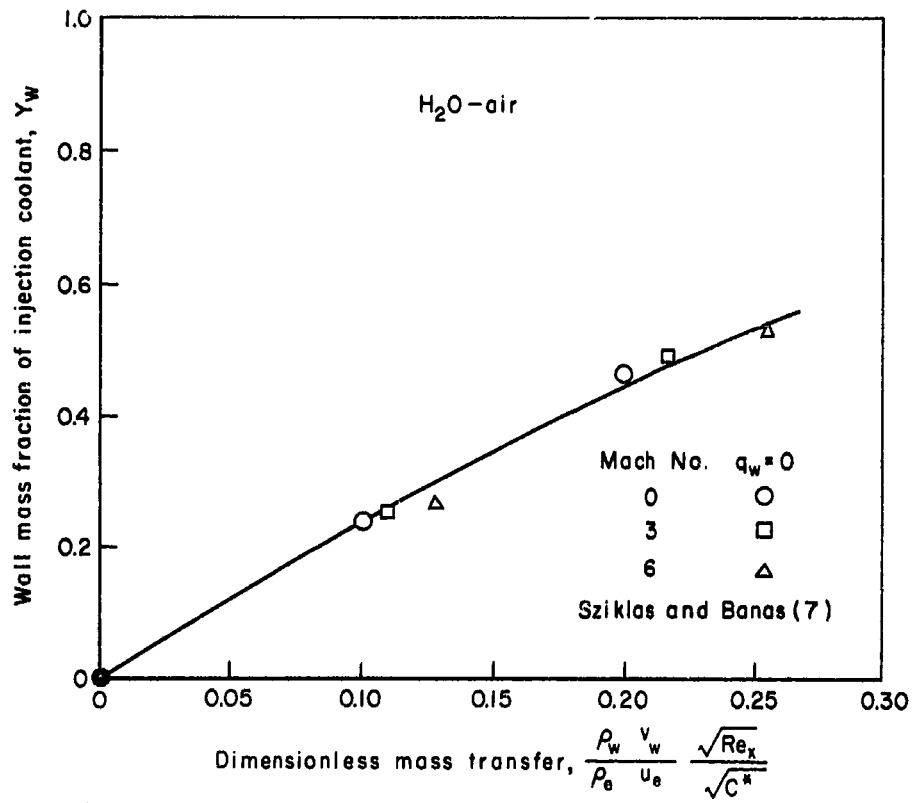


Fig. 45—Wall mass fraction versus
dimensionless mass transfer

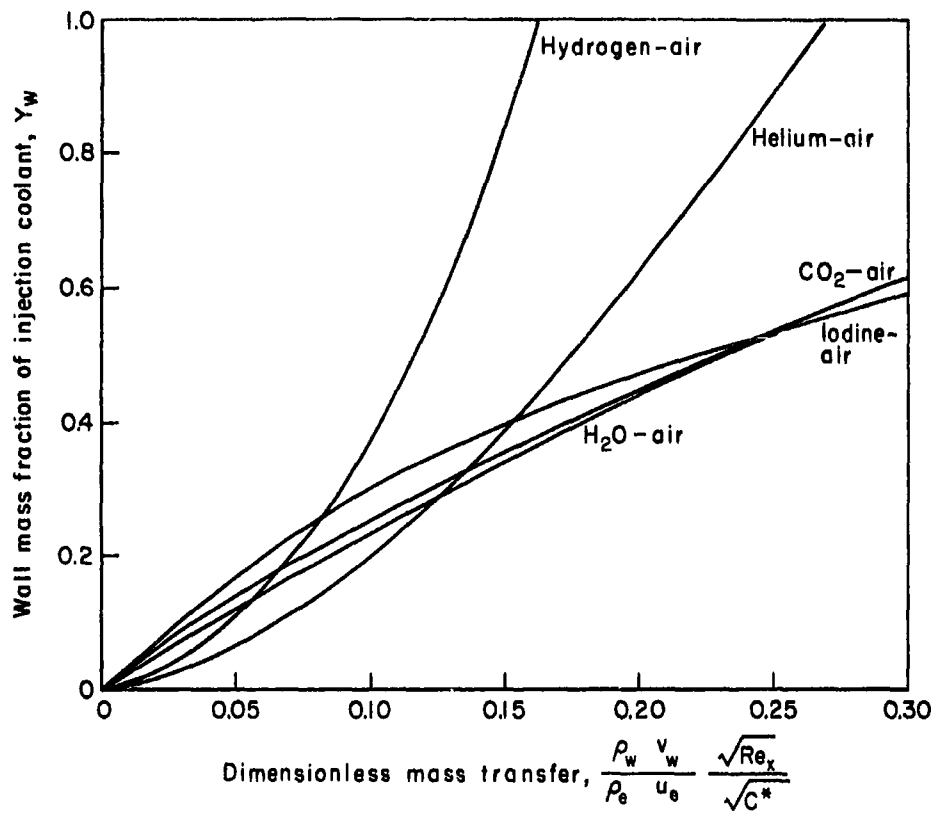


Fig. 46 — Wall mass fraction versus dimensionless mass transfer

Summary

Appendix C

ON THE USE OF MASS-TRANSFER RESULTS FOR PREDICTION OF HEAT TRANSFER

It is rather common practice to obtain experimentally mass-transfer Stanton numbers, C_M , using materials which sublime or evaporate, such as naphthalene or water, and to interpret these results directly as solid wall heat-transfer Stanton number, C_{Ho} (in some instances a correction factor involving the Lewis number is applied). However, considerable caution must be exercised in this procedure as is obvious from a comparison of Fig. 47 with Fig. 18 of the main text. Figure 18 shows the heat-transfer Stanton numbers in the form of C_H/C_{Ho} , where C_H is the heat-transfer Stanton number in the presence of mass transfer, while C_{Ho} is the Stanton number for a solid wall exposed to the same free stream conditions (i.e., C_{Ho} is the limiting value of C_H as the mass-transfer rate goes to zero). Figure 47 is a similar curve for the mass-transfer Stanton number, C_M , again normalized with respect to the value at the zero mass-transfer condition. For water vapor-air and CO_2 -air mixtures the limiting Stanton values, C_{Ho} and C_{Mo} , are in good agreement (i.e., $C_{Ho} = C_{Mo}$) and since C_M/C_{Mo} does not depart appreciably from unity over a range of mass-transfer rates, it would appear that the measured mass-transfer Stanton number, C_M , for these two systems could indeed be interpreted as solid wall heat-transfer Stanton number, C_{Ho} . However, for the other gas mixtures, it must be concluded that considerable error would arise in the use of this procedure.

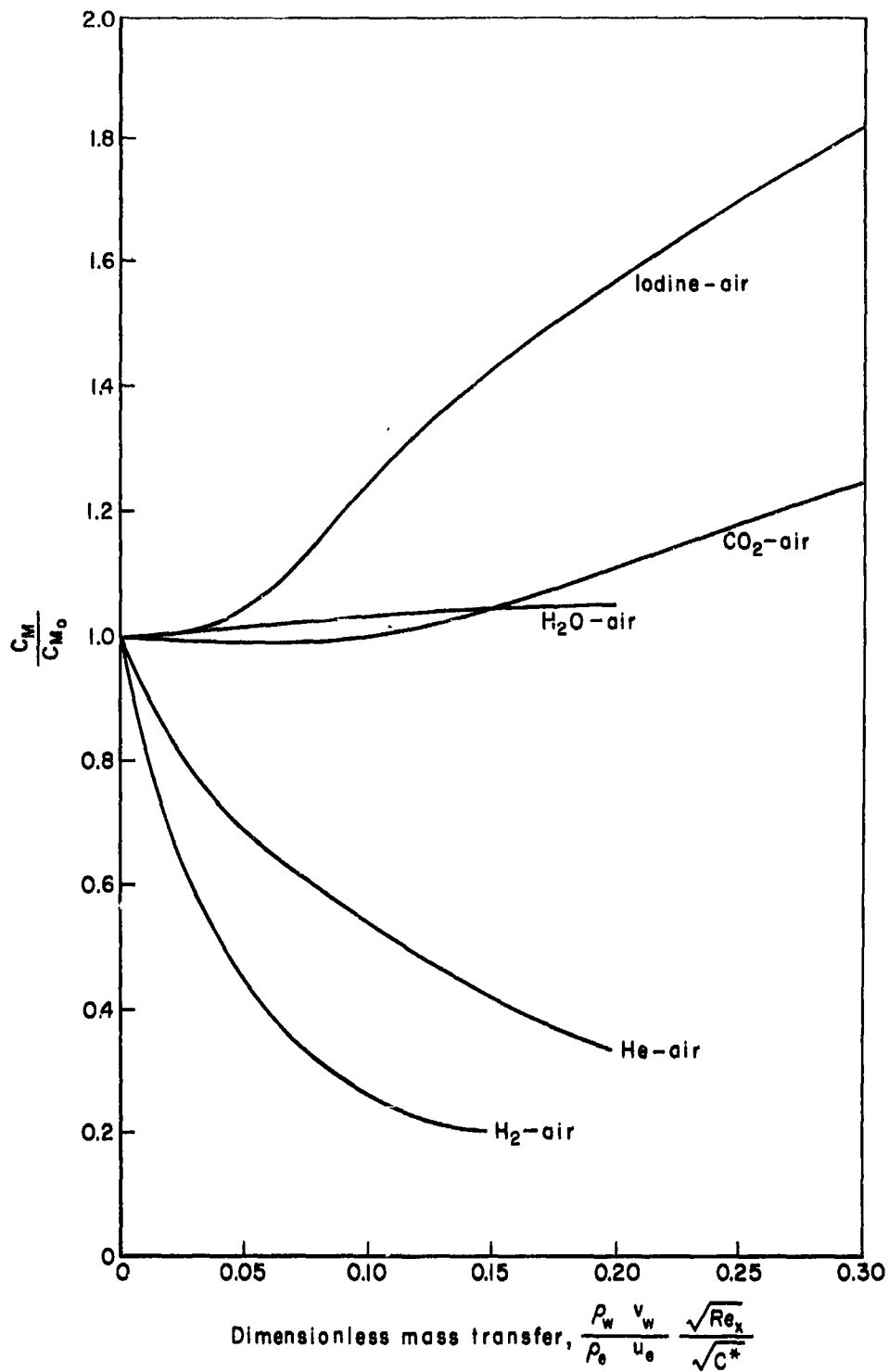


Fig. 47— Effect of mass-transfer rate on the mass-transfer Stanton number

REFERENCES

1. Eckert, E. R. G., "Mass Transfer Cooling, a Means to Protect High Speed Aircraft," presented at the First International Congress of Aeronautical Sciences, Madrid, Spain, September 1958.
2. Baron, J. R., The Binary Boundary Layer Associated with Mass Transfer Cooling at High Speed, Naval Supersonic Lab. Report 160, Massachusetts Institute of Technology, 1956.
3. Baron, J. R., "The Heterogeneous, Laminar, Boundary Layer," in D. J. Masson (comp.), Mass-Transfer Cooling for Hypersonic Flight, The RAND Corporation, Classified Paper S-51, June 24, 1957, (Secret).
4. Eckert, E. R. G. and P. J. Schneider, Diffusion Effects in an Isothermal Binary Boundary Layer, Heat Transfer Lab. Technical Report No. 5, University of Minnesota, November 1955.
5. Eckert, E. R. G., et al., "Mass-Transfer Cooling of a Laminar Air Boundary Layer by Injection of a Light-Weight Gas," in D. J. Masson (comp.), Mass-Transfer Cooling for Hypersonic Flight, The RAND Corporation, Classified Paper S-51, June 24, 1957 (Secret).
6. Eckert, E. R. G., et al., "Cooling of a Laminar Boundary Layer by Injection of a Light-Weight Foreign Gas," Jet Propulsion, Vol. 28, 1958, p. 34.
7. Sziklas, E. A. and C. M. Banas, "Mass-Transfer Cooling in Compressible Laminar Flow," in D. J. Masson (comp.), Mass-Transfer Cooling for Hypersonic Flight, The RAND Corporation, Classified Paper S-51, June 24, 1957 (Secret).
8. Gross, J. F., The Laminar Binary Boundary Layer, The RAND Corporation, Research Memorandum RM-1915, September 1, 1956 (to be published).
9. Hall, N. A., Flow Equations for Multicomponent Fluid Systems, Heat Transfer Lab. Technical Report No. 2, University of Minnesota, August 1955.
10. Hartnett, J. P. and E. R. G. Eckert, "Mass Transfer Cooling in a Laminar Boundary Layer with Constant Fluid Properties," Trans. Amer. Soc. Mech. Engrs., Vol. 79, 1957, p. 247.
11. Eckert, E. R. G., "Engineering Relations for Heat Transfer and Skin Friction in High-Velocity Laminar and Turbulent Boundary Layer Flow over Surfaces with Constant Pressure and Temperature," Trans. Amer. Soc. Mech. Engrs., Vol. 78, 1956, p. 1273.
12. Romig, M., "Stagnation Point Heat Transfer for Hypersonic Flow," Jet Propulsion, Vol. 26, 1956, p. 1098.

13. Chapman, D. R. and M. W. Rubesin, "Temperature and Velocity Profiles in the Compressible Laminar Boundary Layer with Arbitrary Distribution of Surface Temperature," J. Aero. Sci., Vol. 19, 1947, p. 341.
14. Carlson, W. O. and P. J. Schneider, Transport Properties for Binary Gas Mixtures, Heat Transfer Lab. Technical Report No. 7, University of Minnesota, January 1956.
15. Brown, W. B. and P. L. Donoughs, Tables of Exact Laminar Boundary-Layer Solutions when the Wall is Porous and Fluid Properties are Variable, NACA TN 2479, September 1951.
16. Reshotko, E. and C. B. Cohon, Heat Transfer at the Forward Stagnation Point of Blunt Bodies, NACA TN 3513, July 1955.
17. Hayday, A. A., Mass Transfer Cooling in a Laminar Boundary Layer in Steady Two-Dimensional Stagnation Flow, Heat Transfer Lab. Technical Report No. 19, University of Minnesota, April 1958.
18. Lees, L. and C. C. Lin, Investigation of the Stability of the Laminar Boundary Layer in a Compressible Fluid, NACA TN 1115, September 1946.
19. Lin, C. C., "Stability of Parallel Flows," Quart. of App. Math., Vol. III, No. 4, 1946, p. 286.
20. Lees, L., The Stability of the Laminar Boundary Layer in a Compressible Fluid, NACA TN 1360, July 1947, p. 125.
21. Covert, E. E., Stability of Binary Boundary Layers, Naval Supersonic Lab. Technical Report 217, Massachusetts Institute of Technology, June 1957.
22. van Driest, E. R., Calculations of the Stability of the Laminar Boundary Layer in a Compressible Fluid on a Flat Plate with Heat Transfer, North American Aviation Aerophysics Lab. Report AL-1334, September 1951.
23. Leadon, B. M., C. J. Scott, and G. E. Anderson, "Transpiration Cooling of a 20° Porous Cone at $M = 5$," in D. J. Masson (comp.), Mass-Transfer Cooling for Hypersonic Flight, The RAND Corporation, Classified Paper 8-51, June 24, 1957 (Secret).
24. Scott, C. J., G. E. Anderson, and D. R. Elgin, Mass Transfer Cooling at Supersonic Speeds, Rosemount Aeronautical Lab., University of Minnesota, Progress Report 13, July 1958.
25. Rannie, W. D., A Simplified Theory of Porous Wall Cooling, Progress Report 4-50, Power Plant Lab. Project MX801, California Institute of Technology, Jet Propulsion Lab. November 24, 1957.

26. Mickley, H. S., et al., Heat, Mass and Momentum Transfer for Flow over a Flat Plate with Blowing on Suction, Massachusetts Institute of Technology, Cambridge, Mass., September 1952.
27. Dorrance, W. H. and F. J. Dore, "The Effects of Mass Transfer on Compressible Turbulent Boundary-Layer Skin-Friction and Heat Transfer," J. of the Aero. Sci., Vol. 21, No. 6, June 1954, pp. 404-410.
28. Rubesin, M. W., An Analytical Estimation of the Effect of Transpiration Cooling on the Heat Transfer and Skin-Friction Characteristics of a Compressible, Turbulent Boundary Layer, NACA TN 3341, 1954.
29. van Driest, E. R., "On Mass Transfer Near the Stagnation Point," in D. J. Masson (comp.), Mass-Transfer Cooling for Hypersonic Flight, The RAND Corporation, Classified Paper S-51, June 24, 1957 (Secret).
30. Dorrance, W. H., "The Effect of Mass Addition on the Compressible Turbulent Boundary-Layer Skin Friction and Heat Transfer - An Addendum," J. of the Aero. Sci., Vol. 23, No. 3, March 1956, pp. 283-284.
31. Leadon, B. M. and C. J. Scott, Measurement of Recovery Factors and Heat Transfer Coefficients with Transpiration Cooling in a Turbulent Boundary Layer at $M = 3$ Using Air and Helium as Coolants, Rosemount Aeronautical Lab., University of Minnesota, Technical Report 126, February 1956.
32. Rubesin, M. W., C. C. Pappas, and A. F. Okuno, The Effect of Fluid Injection on the Compressible Turbulent Boundary Layer - Preliminary Tests on Transpiration Cooling of a Flat Plate at $M = 2.7$ with Air as the Injected Gas, NACA RM A55119, December 21, 1955.
33. Rubesin, M. W., The Influence of Surface Injection on Heat Transfer and Skin Friction Associated with the High-Speed Turbulent Boundary Layer, NACA RM A55113, February 1956.
34. Tendeland, T. and A. F. Okuno, The Effect of Fluid Injection on the Compressible Turbulent Boundary Layer - The Effect on Skin Friction of Air Injected into the Boundary Layer of a Cone at $M = 2.7$, NACA RM A56D05, June 1956.
35. Mickley, H. S. and R. S. Davis, Momentum Transfer for Flow over a Flat Plate with Blowing, NACA TN 4017, November 1957.
36. Pappas, C. C., Effect of Injection of Foreign Gases on the Skin Friction and Heat Transfer of the Turbulent Boundary Layer, Institute of the Aeronautical Sciences, IAS Paper 59-78, January 1959.
37. Rubesin, M. W. and C. C. Pappas, An Analysis of the Turbulent Boundary-Layer Characteristics on a Flat Plate with Distributed Light-Gas Injection, NACA TN 4149, February 1958.

38. Chauvin, L. T. and H. S. Carter, Exploratory Tests of Transpiration Cooling on a Porous 8° Cone at $M = 2.05$ Using Nitrogen Gas, Helium Gas, and Water as the Coolants, NACA RM L55C29, June 3, 1955.
39. Gress, J. F., D. J. Masson, and Carl Gazley, Jr., General Characteristics of Binary Boundary Layers with Applications to Sublimation Cooling, The RAND Corporation, Paper P-1371, May 8, 1958.
40. Balekjian, G. and D. L. Keltz, "Heat Transfer from Superheated Vapors to a Horizontal Tube," Amer. Inst. Chem. Engr. J., March 1958.

This information is furnished upon the condition that it will not be released to another nation without specific authority of the Department of Defense of the United States, that it will be used for governmental purposes only, that individual or corporate rights originating in the information, whether patented or not, will be respected, and that the information be provided substantially the same degree of protection afforded it by the Department of Defense of the United States.